STUDIES OF CA^{2+}-SIGNALING AND CL^{-}-CONDUCTANCE CHANGES IN RESPONSE TO ABSCISIC ACID, VOLTAGE CHANGES AND COLD, IN THE PLASMA MEMBRANE OF GUARD CELLS

Dissertation zur Erlangung des

naturwissenschaftlichen Doktorgrades

der Bayerischen Julius-Maximilians-Universität Würzburg

Vorgelegt von

VICTOR LEVCHENKO

aus

PRUZHANY

(REPUBLIC OF BELARUS)

Würzburg 2009

Eingereicht am: …………………………………………...

Mitglieder des Promotionskommission:

Vorsitzender: …………………………………………...

Erstgutachter: Prof. Dr. Rainer Hedrich

Zweitgutachter: Prof. Dr. rer. nat. Erhard Wischmeyer

Tag des Promotionskolloquiums: …………..…………..…..

Doktorurkunde ausgehändigt am: ………………………….

CONTENTS

SUMMARY

Land plants must control the transpiration water stream and balance it with carbon dioxide uptake for optimal photosynthesis. A highly specialized type of plant cell called guard cells have evolutionary appeared which are suited for this complicated purpose. Guard cells are located by pairs on aerated plant surface and form stomata – structural units, which represent highly regulated "watergate" (Roelfsema and Hedrich, 2005). Guard cells sense many environmental and internal plant-derived stimuli and by changing degree of their swelling tightly regulate diffusion of water vapor and other gases.

Cell processes taking place in stomata during their movements had been a subject of intensive investigation for more than three decades (Schroeder et al., 2001; Assmann and Shimazaki, 1999). With use of electrophysiological technique the basic processes underlying stomatal movements were described (Thiel et al., 1992; Dietrich et. al., 2001; Roelfsema and Hedrich, 2005). Another set of questions arised between plant biologists is how the signals affecting stomatal aperture are transduced in guard cells starting from perception by receptor structures and ending on the osmodynamic motor components. Introduction of fluorescent microspectroscopy technique allowed to characterize some Ca^{2+} and H^+-based signaling events, taking place in the cytoplasm during stomata function.

Most of the processes, taking place in stomata were characterized in guard cell preparations, such as strips of isolated leaf epidermis or guard cell protoplasts, - cells with enzymaticaly digested cell walls. Some experimental observations although point that reactions of guard cells located in their natural environment, leaves of intact plants can differ from those could be registered in preparations. These deviations might be explained by the modulation of guard cell function by apoplastic factors originating from surrounding tissues like mesophyll or leaf epidermis (Roelfsema and Hedrich, 2002). On the other hand registration of physiological responses in prepared tissues may also contain possible artifacts, related to the preparation procedures.

The aim of the experimental work presented here was to investigate the cell signaling events, taking place in guard cells upon plant stress hormone abscisic acid (ABA) and some other stimuli action. Abscisic acid is a compound that synthesized in plant roots upon drought and closes stomata in the leaf to prevent the plant organism from excessive water loss. Previous studies on guard cell of isolated epidermis and guard cell protoplasts showed, that ABA induces stomatal closure via activation of plasma membrane anion channels (Grabov et al., 1997; Pei et al, 1997). Anion channels are known to be activated by elevated

concentrations of cytoplasmic Ca^{2+} $[Ca^{2+}]_{cyt}$ (Schroeder and Hagiwara, 1989; Hedrich et al., 1990). Application of Ca^{2+}-sensitive fluorescent probes revealed $[Ca^{2+}]_{cyt}$ increases in guard cells upon ABA action (McAinsh et al., 1990). This observation led to suggestion that $[Ca^{2+}]_{cyt}$ directly participate in the transduction of ABA signal in guard cells. Although no direct evidences for co-occurrence of $[Ca^{2+}]_{cyt}$ rises and following activation of anion channels upon ABA action was not presented until yet.

Results of experimental work performed on intact *Vicia faba*, *Commelina communis* and *Nicotiana plumbagnifolia* plants showed that guard cells of intact plant leaves respond with transient activation of plasma membrane anion channels upon perception of ABA. Kinetics of the response is highly reproducible and seemed to be conserved between species. Although despite clear generation of anion current transients, no $[Ca^{2+}]_{cyt}$ increases could be recorded with using fluorescent probe Fura-2 microinjected into the cytoplasm. Together with results of later study on intact *Nicotiana tabacum* guard cells, reported obligatory $[Ca^{2+}]_{cyt}$ increases which were desynchronized with anion current transients (Marten et al., 2007b) this, may indicate that $[Ca^{2+}]_{cyt}$ increases are not necessary component of ABA signal transduction pathway. Together with absence of the effect of cytoplasm-delivered Ca^{2+}-mobilizing agents IP_3, IP_6 and NAADP on anion currents these data may suppose that role of $[Ca^{2+}]_{cyt}$ in ABA signaling must be reassessed.

Further interest represented characterization of $[Ca^{2+}]_{cyt}$ signaling and homeostasis in intact guard cells comparing with those in prepared cells. Experiments revealed strong deviations in $[Ca^{2+}]_{cyt}$ behavior between different measuring systems. While guard cells of intact plants were able to strictly maintain $[Ca^{2+}]_{cyt}$ level upon experimental shifting of $[Ca^{2+}]_{cyt}$ level in either direction of elevation or decrease, cells of isolated epidermis showed complete absence of such ability. Guard cell protoplasts showed even weaker $[Ca^{2+}]_{cyt}$ regulation ability and were capable of low physiological $[Ca^{2+}]_{cyt}$ levels maintaining only at depolarized membrane potentials. Apart to these differences, prepared guard cells showed also for-time less activation of anion currents by experimentally imposed $[Ca^{2+}]_{cyt}$ increases.

These data strongly suggest that registered in guard cell preparations $[Ca^{2+}]_{cyt}$ signals may contain significant part of artifacts and must be carefully used for the building of models of guard cells signaling. Further experimental investigations are strongly required for understanding guard cell functioning, especially with relation of vacuoles participation.

The experimental work was done by the author in the period from october 2001 until november 2004 under supervision of Professor Dr. Rainer Hedrich in laboratory of molecular plant physiology and biophysics at Julius-Maximillians University of Würzburg, Würz-

burg, Federal Republic of Germany. Scientific coordinator of the Ph. D. project is Dr. Max Robert Gustaaf Roelfsema, University of Würzburg. Most of experimental results, presented here (chapter III) are also published elsewhere (Roelfsema et al., 2004; Langer et al., 2004; Levchenko et al., 2005, 2008).

Chapter I intend to shortly introduce the reader into the field of guard cell research and point out the current level of understanding regarding this branch of plant research. Special attention is given to description of guard cell ion channels, their function and regulation, including the mechanisms of Ca^{2+}-, H^+- and phosphorylation-based signaling. This section is preceded by a short history of guard cell research and explains the actuality of presented work.

In chapter II experimental techniques, methods and data processing approaches, used in the presented work are described. Technique used for electrophysiological registrations on intact plant leaves were used before and described in more details by Roelfsema et al. (2001). Fluorescent microspectroscopy technique was for the first time applied to intact plant leaves in this work and described in more details including calibration of Fura-2 based measurements. Chapter III presents the major results of the experimental work. In chapter IV the experimental results are discussed and put into context with current knowledge of guard cell function knowledge. Finally, remarks on perspectives of guard cell signaling research are drawn.

Victor I. Levchenko,
Minsk, Republic of Belarus, 2009

ZUSAMMENFASSUNG

Landpflanzen sind in der Lage ihren Transpirationsfluss durch das Xylem zu regulieren und so den Wasserverlust mit dem Kohlendioxidbedarf der Photosynthese abzugleichen. Zu diesem Zweck haben sich im Laufe der Evolution Schließzellen entwickelt, welche in der Lage sind, diese komplizierte Aufgabe zu erfüllen. Schließzellen befinden sich auf Oberflächen oberirdischer Pflanzenorgane, wo sie als Paar eine Pore, dem sogenannten Stoma bilden. Schließzellen sind in der Lage mehrere Signale aus der Umwelt und von benachbarten Pflanzen wahrzunehmen. Anhand dieser Signale wird die Porenöffnung durch Änderungen des Schwellungsgrads der beiden Schließzellen genau reguliert.

Die intrazellulären Prozesse die während der Stomabewegungen in den Schließzellen stattfinden sind bereits seit Jahrhunderten ein intensiv bearbeitetes Forschungsgebiet. Mit Hilfe elektrophysiologischer Techniken konnten bereits einige für die Stomabewegung grundlegende Prozesse beschrieben worden. Trotzdem sind immer noch viele Fragen offen. Dazu zählen vor allem die Mechanismen, die zur Wahrnehmung verschiedener Signale der Regulierung des osmotischen Motors in Schließzellen führt.

Die meisten Studien zur Signalweiterleitung wurden mit isolierten Schließzellpräparationen durchgeführt, wie z.B. Epidermisstreifen oder Schließzellprotoplasten. Obwohl einige Schließzell-spezifische Eigenschaften in diesen Präparationen erhalten bleiben, deuteten kürzlich experimentelle Ergebnisse auf Unterschiede zwischen Antworten isolierter Schließzellen und denen intakter Pflanzen hin. Diese Unterschiede könnten durch die von Mesophyll- oder Epidermiszellen freigesetzte apoplastische Faktoren bedingt sein.

Das Ziel der experimentellen Arbeiten dieser Dissertation war die Charakterisierung des Schließzellsignalweges ausgehend vom pflanzlichen Stresshormon Abscisinsäure (ABA). ABA wird in der Wurzel bei Trockenstress synthetisiert und bewirkt den Stomaschluss, um übermäßigen Wasserverlust zu unterbinden. Bisherige Studien mit isolierten Schließzellen ergaben, dass ABA die Aktivität der Plasmamembran-ständigen Anionenkanäle erhöht. In diesem Zusammenhang wurde postuliert, dass eine Aktivierung des ABA-abhängigen Anionenkanals durch eine Erhöhung der zytosolischen Ca^{2+} Konzentration ($[Ca^{2+}]_{zyt}$) ausgelöst wird. Anionkanäle werden durch Ca^{2+} stimuliert und ABA bewirkt eine Erhöhung der $[Ca^{2+}]_{zyt}$.

Die Resultate dieser Arbeit mit *Vicia faba*, *Commelina communis* und *Nicotiana plumbagnifolia* haben gezeigt, dass Schließzellen in intakten Blättern mit einer transienten Aktivierung der Plasmamembran-ständigen Anionenkanäle auf ABA reagieren. Die sehr typische

Aktivierungskinetik dieser ABA-Antwort scheint evolutionär gut konserviert zu sein. Obwohl ABA große Anionenströme in *Vicia faba* Schließzellen auslösen konnte, wurden keine Änderungen der $[Ca^{2+}]_{zyt}$ mit dem Ca^{2+}-Fluoreszenzindikator Fura-2 aufgezeichnet. Diese Resultate zeigen, dass zumindest in *Vicia faba* Schließzellen, eine Erhöhung der $[Ca^{2+}]_{zyt}$ keine essentielle Komponente des ABA-Signalweges ist. Dieses Ergebnis zeigt, dass vor allem die Rolle der $[Ca^{2+}]_{zyt}$ im ABA-Signalwege neu bewertet werden muss. Vor allem mit dem Unfähigkeit in Kombination mit den drei tierischen Ca^{2+}-mobilisierenden Signalstoffen, IP_3, IP_6 and NAADP, die Anionenkanalaktivität zu beeinflussen.

In einem weiteren Experiment, wurden Ca^{2+}-abhängige Signalmechanismen und die Ca^{2+}–Homöostase in Schließzellen zwischen isolierten Zellen mit denen in intakten Pflanzen verglichen. Schließzellen in intakten Pflanzen waren in der Lage, die $[Ca^{2+}]_{zyt}$ unabhängig von Änderungen des Plasmamembranpotentials auf ein konstantes Niveau zu halten, während Schließzellen in isolierten Epidermisstreifen diese Fähigkeit verloren hatten. In Präparationen mit Epidermisstreifen löste eine Hyperpolarisierung des Membranpotentials einen dauerhaften Anstieg der $[Ca^{2+}]_{zyt}$ aus. In Schließzellprotoplasten war das Vermögen, die $[Ca^{2+}]_{zyt}$ zu regulieren, noch stärker eingeschränkt. Diese Zellen konnten nur bei depolarisierenden Membranpotentialen eine stabile $[Ca^{2+}]_{zyt}$ halten. Darüber hinaus war auch das Vermögen von ABA, die Anionenkanalaktivität zu erhöhen bei Schließzellen in Epidermisstreifen stark begrenzt.

Die in dieser Dissertation präsentierten Ergebnisse legen nahe, dass die bisher gemessenen $[Ca^{2+}]_{zyt}$-Signale an isolierten Schließzellen mit Fehlern behaftet sind. Die Isolierungsprozedur beeinflusst die Eigenschaften der Schließzellen und Daten aus solchen Präparationen sollten deswegen sorgfältiger bei der Entwicklung von Modellen zu Schließzellsignalwegen betrachtet werden. Einer Neubewertung der Rolle des $[Ca^{2+}]_{cyt}$ wird voraussichtlich auf die Beteiligung neuartiger Komponenten des ABA Signalwegs hinweisen. Eine dieser Komponenten könnte die Vakuole der Schließzellen sein. „Tracer-Flux" Experimente mit radioaktiven Isotopen und Patch-Clamp Studien an isolierten Vakuolen deuteten bereits auf eine wichtige Rolle der Vakuole bei der Regulierung der Schließzellbewegungen hin. Zukünftige Studien an intakten Schließzellen sind notwendig um diese Funktion in weiteren Details aufzuklären

Victor I. Levchenko,

Minsk, Weissrussland, 2009

I. GUARD CELL FUNCTION AND SIGNALLING.

STOMATAL GUARD CELLS: AN IDEAL OBJECT FOR STUDYING
PLANT CELL SIGNALLING.

1.1.1 Function of stomata. Guard sells of higher plants are kidney-shaped cells, which form in pairs structural units on the aerated plant surface, called stomata. Evolutionary, stomata have enabled land plants to control transpirational water loss, which is obligatory coupled with the uptake of carbon dioxide, necessary for photosynthesis. Surface of higher plants contacting with the air, is covered by waxy cuticle layer preventing undesirable water loss. Within this layer, stomata represent highly regulated "watergates" performing the control of transpiration stream. By changing their degree of opening (stomatal aperture), stomata regulate transpiration and exchange of other gasses such as CO_2 and thus affect photosynthesis in the leaf. This way guard cells regulate and integrate important physiological processes, which allow plants to survive in changing environmental conditions.

For the performance of such complicated task guard cells possess a highly developed system of receptors, responsible for sensing changes in environmental and plant-derived internal stimuli. Every receptor is bound to a set of intracellular proteins and non-protein factors, responsible for the intracellular propagation of the signal to final targets for which the receptor is suitable for. These signal transduction pathways can interfere with each other and form a complicated network, responsible for determining the final stomatal responses. Studies of the guard cell signaling machinery therefore represent probably the most intriguing tangle of questions in modern plant physiology.

The guard cell is highly specialized type of plant cell, characterized by absence of plasmodesmata, i.e. guard cells do not have cytoplasmic contact with other cell types or with each other. Thus, the complete stomatal apparatus could be imagined as a system of autonomously reacting cells carrying sensory and motor function at the same time. This feature makes stomatal guard cells an exclusively attractive and suitable object for studying cell signaling.

Higher plant stomata respond with changes in aperture to a wide range of stimuli (section 1.5), among which are light quality and intensity, temperature, hydration status of plant tissues, CO_2 concentration, exogenous elicitors and pollutants and some hormonal signals. Under natural conditions, guard cells most of time will be faced to a set of various signals, which frequently can have opposite effects. For example, intensive CO_2 uptake for photosyn-

thetic production during hot sunny days requires wide opened stomata on the leaf surface, but sunny weather can co-occur with drought conditions, which would stimulate plant stress hormone abscisic acid production by roots and force stomata to close. For this reason guard cells have to make trade off – either they force stomatal opening for optimal photosynthesis, or closure in order to preserve the whole plant from wilting. The fine-tuning of this process is a result of many signaling chains interaction, which provides a final complicated real-time behavior of stomata of higher plant leaves in natural conditions.

The principle of stomatal movement is based on hydrodynamic swelling and shrinking of guard cells. The changes in guard cell size are inducing stomatal movements based on a specific structure of guard cell wall. Movements of stomata are driven by osmodynamic motor, providing quick and reversible changes of osmotic compounds content inside guard cell (Raschke, 1975; Roelfsema and Hedrich, 2005). The osmodynamic motor includes two components: a system of ion transport (Thiel et al., 1992; Dietrich et al., 2001) and a chain of biochemical reactions, leading to reversible starch degradation and accumulation of mono- and disaccharides and organic acids, mainly malate (Raschke, 1975).

In contrast to the set of biochemical reaction cascades which likely provides slower changes of guard cell osmotic status, ion transporting system represents the main and quicker component which supports stomatal movements. Responses of ion transporting mechanisms to some stimuli can occur in tens of seconds. The guard cell ion transport system consists of ion channels, transporters and electrogenic pumps, located both in the plasma- and vacuolar membranes. Under the control of cell signaling machinery these transport proteins provide the coordinated work on inorganic and organic ions redistribution between guard cell and the apoplastic surrounding. The dynamics of stomatal movement also depend to a great extent on the water status and the metabolic activity of surrounding tissues, namely epidermis and mesophyll (reviewed by Roelfsema and Hedrich, 2002, 2005).

1.1.2. Short history of guard cell research and the current status of knowledge. Stomata have been attracting the attention of plant biologists already for more than two hundred years, because of the easily observed reversible movements, which could be evoked by changing environmental conditions. One of the first attempts to describe the function of stomata was made in 1812, when the German scientist Moldenhauer recognized three important factors, affecting movements of stomata on plant leaves: light, humidity and time of the day (Roelfsema and Hedrich, 2005).

At the beginning of guard cell research it was believed, that movements of stomata depend on starch synthesis and degradation, leading to the accumulation of osmotically active sugars. However, recent studies on sugar transport and metabolism show that starch synthesis and sugar transport does not necessary correlate with stomatal movements (Stadler et al., 2003). Only in 1960-es it was established, that stomatal movement strongly depends on the uptake of K^+ ions by guard cells (Fischer, 1968).

A breakthrough in the investigation of mechanisms, underlying stomatal movement came in 1980-ths with introduction of electrophysiological methods in guard cell research. The patch-clamp and microelectrode techniques allowed the description of potassium- (Schroeder et al., 1987, Blatt 1988), anion-selective (Keller et al., 1989; Schroeder and Hagiwara, 1989; Hedrich et al. 1990) channels and the H^+-ATPase (Assmann et al., 1985) activity on guard cell plasma membrane. The results of these early investigations lead to development of a biophysical model of guard cell ion transport, in which voltage control at the plasma membrane plays a major role (Thiel et al., 1992). Later experimental studies with electrophysiological techniques were often more focused on guard cell signaling and brined more details on the regulation of ion transport by different cytoplasmic and external factors.

A further step forward in guard cell research was made with the introduction of fluorescent dyes and luminescent reporters that allowed measurements of $[Ca^{2+}]_{cyt}$ and $[H^+]_{cyt}$. These techniques confirmed increases of guard cells $[Ca^{2+}]_{cyt}$ in response to the plant stress hormone ABA (McAinsh et al., 1990; Gilroy et al., 1991) as well other hormones (Irving et al., 1992). On the analogy to signaling pathways in animal cells the $[Ca^{2+}]_{cyt}$ increases are discussed as important signaling events that participate in the propagation and amplification of external stimuli. In addition to the potential role of cytoplasmic Ca^{2+}, other intracellular ion concentrations may contribute to signaling pathways within guard cells. Thus, abscisic acid and other plant hormones were also showed to affect cytoplasmic pH in stomatal guard cells (Irving et al., 1992).

Overwhelming majority of the data obtained on guard cell ion transport and signaling have been obtained in experiments carried out with guard cell preparations, such as isolated epidermal strips or cell wall-free guard cell protoplasts. At the beginning of 2000-th, researchers in R. Hedrich's laboratory came up with the idea to verify the literature data concerning guard cell ion transport and signaling, with those could be registered experimentally in guard cells located in their natural environment – leaves of intact plants. The newly developed experimental approach, in which electrophysiological registrations and fluorescent spectroscopy measurements on intact plant leaves were combined, provided a lot of interest-

ing findings. Responses of single intact guard cells in intact plants could be registered, which were induced by light (Roelfsema et al., 2001), CO_2 (Roelfsema et al., 2002, Marten et al., 2007a) and ABA (Roelfsema et al., 2004, Levchenko et al., 2005, Marten et al., 2007b). The good reproducibility of these guard cell physiological reactions in intact system allowed a detailed characterization of kinetic parameters of changes in ion transport activities, most of which had not been observed in preparations with isolated guard cells. A detailed comparison of the data with measurements on isolated guard cells and guard cell protoplasts (Levchenko et al., 2008) showed significant deviation of $[Ca^{2+}]_{cyt}$ responses and ion channel regulation between isolated guard cells and their counterparts in the intact system (chapter IV).

1.3 ION TRANSPORT IN GUARD CELLS.

1.3.1 K$^+$ transport across guard cell plasma membrane. Potassium is a key osmotic component, requiring for stomatal movement. Movements of stomata depend on quick redistribution of K^+ between the guard cells and the apoplast. The main pathway for translocation of K^+ in and out of the guard cells, are potassium selective channels of the plasma membrane. There are three groups of channels, participating in K^+ translocation via guard cell plasma membrane: outward-rectifying K^+-selective channels, inward-rectifying K^+-selective channels and non-selective voltage-independent ion channels (Very and Sentenac, 2002).

Outward-rectifying K$^+$ channels. Potassium loss by guard cells during stomatal closure occurs via outward-rectifying K^+-selective (K^+_{out}) channels of the plasma membrane. A characteristic feature of outward-rectifying potassium channels is their strong voltage-dependence. Activation of K^+_{out} channels occurs at depolarized membrane potentials at guard cell plasma membrane. Stepping the membrane voltage in voltage-clamp experiments from resting value of -100 mV to more depolarized values (e.g. 0 mV) evokes activation of K^+_{out} currents with sigmoidal kinetics, which saturate approximately 1-2 s after applying voltage step (Blatt, 1988). At physiologically relevant conditions, the activation threshold for outward-rectifying channels is approximately -60 mV (Roelfsema et al., 2001).

Specific feature of K^+_{out} channel gating is dependence of channel activation threshold on external K^+ concentration. Activation of outward-rectifying K^+-selective channels normally occurs at the membrane potential values slightly more positive, than Nernst potential of K^+ ions (Blatt, 1988; Roelfsema & Prins, 1997).

The properties of outward-rectifying potassium channels were described for guard cells of number of different plant species. This comparative characterization with use of the patch-

clamp technique, however, did not reveal species-specific threshold activation potential for the K^+_{out} channels activation (Dietrich et al., 1998).

The properties of single outward-rectifying K^+ channels have been described in a number of experimental publications (Schroeder et al., 1987; Hosoi et al., 1988; Miedema and Assmann, 1996). The average conductance of a single outward-rectifying K^+ channels at a physiological range of K^+ concentrations was estimated at 15 – 25 pSm. The outward-rectifying K^+-selective channels are sensitive to changes in the cytoplasmic pH (Blatt and Armstrong, 1993). Single-channel recordings showed that this feature is a channel-intrinsic property, determined by the property of channel protein (Miediema and Assmann, 1996). An increase in pH_{cyt} during abscisic acid action is probably the main factor, which enhances the activity of outward-rectifying K^+-selective channels in guard cells of isolated epidermal strips (Blatt and Armstrong, 1993). In contrast to the sensitivity towards cytoplasmic protons, outward-rectifying K^+ channels are insensitive to changes in the cytoplasmic Ca^{2+} concentration (Schroeder and Hagiwara, 1989; Lemtiri-Chlieh and MacRobbie, 1994). Several experimental investigations point to regulation of K^+_{out} activity through protein kinase-mediated phosphorylation (Thiel and Blatt, 1994; Armstrong et., al., 1995, section 1.4.2).

The outward rectifying K^+-selective channel of guard cell plasma membrane in *Arabidopsis* is encoded by single gene only, named *GORK* (Guard Cell Outward Rectifier K^+). This gene was cloned by the research group of R. Hedrich (Ache et al., 2000). A knock-out mutant line of *Arabidopsis*, lacking a functional channel protein was also obtained later, which showed almost complete absence of outward-rectifying K^+ currents in guard cells. These loss-of-function *Arabidopsis* plants displayed also a slower stomatal closure in response to abscisic acid compared to wild-type plants (Hosy et al., 2003).

Expression of GORK increases after cold- and salt shocks treatments, upon drought stress and after perception of ABA. Interestingly, the GORK expression in guard cells (in contrast to other cell types) did not show a dependence on ABA presence, thus allowing guard cells to control their transpiration independently of the plant water status (Becker et al., 2003).

Inward-rectifying potassium channels. The uptake of K^+ ions, necessary for stomatal opening, occurs via inward rectifying K^+-selective channels in the of guard cell plasma membrane. Inward rectifying potassium channels (K^+_{in}) activate at range of hyperpolarized potentials at the plasma membrane (more negative than -100 mV at physiological conditions, Roelfsema et al., 2001, Langer et al., 2004). In contrast to K^+_{out}, gating of inward rectifying K^+ channels does not depend on the external K^+ concentration, although it does require ex-

ternal K^+ concentrations in the milimolar range (Blatt, 1992). Inward rectifying K^+ channels are characterized by a higher selectivity in range of monovalent cations compared to outward rectifying K^+ channels (Schroeder 1988). Conductance of single K^+_{in} channels was determined in range of 5 - 8 pSm (Schroeder et al., 1987, 1993; Dietrich et al., 1998; Very et al., 1995, 1998).

A specific feature of inward rectifying potassium channels is their sensitivity to the apoplastic pH (Blatt, 1992; Ilan et al., 1996). Lowering the apoplastic pH leads to a shift of the activation potential to more depolarized values and increases the number of open ion channels (Hoth et al., 1997, Hoth and Hedrich, 1999). Activation of K^+_{in} channels by apoplastic protons could serve as a mechanism that favors potassium uptake during stomatal opening. Proton pump activity, which energizes this process, together with plasma membrane hyporpolarization also acidifies apoplastic pH and thus can further enhance the activity of K^+_{in} channels (reviewed in Dietrich et al., 2001). Cytoplasmic Ca^{2+} has an opposite effect on the activity of inward rectifying K^+-channels. An increase of $[Ca^{2+}]_{cyt}$ deactivates K^+_{in} with a half-inhibition constant of ~330 nM and cooperative binding of four Ca^{2+} ions per channel protein (Grabov and Blatt, 1999).

Inward rectifying K^+-selective channels were the first ion channel type, cloned in higher plants. The *KAT1* (Anderson et al., 1992) and *AKT1* (Sentenac et al., 1992) encoded inward-rectifying K^+-selective channels of *Arabidopsis* were cloned almost at the same time. Based on the structural similarity with a group of voltage-dependent K^+-selective channels of the animal kingdom, these channels were related to so-called "Shaker-like" channels (Very and Sentenac, 2003).

In contrast to K^+_{out}, the inward rectifying potassium-selective conductance of guard cell plasma membrane is formed by several gene products. In experimental work by Szyroki et al., (2001) ionic currents were compared in guard cells between wild type and mutant *Arabidopsis* plants expressing a nonfunctional *kat1* allele (a mutation with En-transpozone insertion). In spite of the absence of the functional gene, challenged with micro electrodes mutated guard cells displayed the same magnitude of inward-rectifying potassium currents and normal kinetics of stomatal opening and potassium uptake. This pointed that KAT1 is not the only channel protein, participating in K^+ uptake by guard cells. Further search for additional K^+ uptake channels lead to the identification of *KAT2*, *AKT2/3* and *AtKC1* channels in guard cells (Véry and Sentenac, 2002).

1.3.2. Anion transport across the guard cell plasma membrane. Anions release from the guard cell to the apoplast is a central mechanism that leads to stomatal closure (Roelf-

sema et al., 2004; Schroeder et al., 2001). Efflux of anions is electroneutral process, because it happens in parallel with release of K^+. Activation of plasma membrane anion channels is a naturally occurred reason which evokes plasma membrane depolarization necessary for voltage-gated K^+_{out} channels opening. The activation of plasma membrane anion channels shifts free-running plasma membrane potential towards Cl^- reversal potential, which located in positive voltage range. Depolarization of plasma membrane in turn activates K^+ efflux via outward-rectifying K^+-channels. This sequence of events leads to stomatal closure and has been described upon several stimuli action, including the responses to darkness (Roelfsema et al., 2001), CO_2 (Brearley et al., 1997; Roelfsema et al., 2002) and ABA (Grabov et al., 1997; Raschke et al., 2003; Roelfsema et al., 2004).

The passive release of anions from guard cell occurs via plasma membrane anion channels, characterized with selectivity for a range of small anions (Hedrich and Marten, 1993; Schmidt and Schroeder, 1994). Two types of anion conductance have been described, which can coincide during patch-clamp registration in the same guard cell protoplast (Schroeder and Keller, 1992). Both channels differ with respect to their current-voltage characteristics and pharmacological properties. The channels display either slow (S-type) voltage -independent or rapid (R-type) voltage-dependent activation/deactivation kinetics.

S-type anion channels. Anion channels, characterized with weak voltage dependence and slow activation/deactivation kinetics were named S-type anion channels (Schroeder and Hagiwara, 1989) or SLAC (Linder and Raschke, 1992).

S-type anion channel gating is characterized by long opening times of 0.1 – 40 s. The average conductance of single channels has been estimated at 35 ± 7 pS (Schmidt and Schroeder, 1994), but slow anion-selective channel conductances of ~18, 36 and 52 pS, as well as lower and larger conductance were also recorded in outside-out patches of *Vicia faba* plasma membrane. The occurrence of several well-defined single-channel conductances and the observed direct transitions among different conductance states suggests that simultaneous and cooperative opening of small units gives rise to multiple conductance states (Schroeder et al., 1993). The selectivity of S-type anion channels in a row of anions revealed a relative permeability order of NO3- >> Br- > F- > Cl- > I- >> malate2-, and showed high permeability of NO3- over Cl- (~ 20 : 1) (Schmidt and Schroeder, 1994). Despite the lower (1 : 0.24) permeability of malate compared to Cl-, S-type anion channel were shown to facilitate currents that are sufficient for providing physiological rates of malate efflux from guard cells, necessary for stomatal closure (Hedrich et al., 1994). Interestingly, cytoplasmic malate^{2-} led also to slow decline in whole-cell S-type anion currents reducing by 90% within 15 min of

patch-clamp registration in whole cell mode. Such downregulation of ion channel activity could serve as a mechanism, inhibiting S-type anion channels activity during stomatal opening (Schmidt and Schroeder, 1994).

Regulation of S-type anion channels can occur through phosphorylation from cytoplasmic side by Ca^{2+}-independent protein kinases (Shwarz and Schroeder, 1998). However, an increasing cytoplasmic Ca^{2+} concentration could also directly activate S-type anion channels (Schroeder and Hagiwara, 1989).

The activity of S-type anion channels in path-clamp experiments could be inhibited by blockers that also block anion channels in animal cells. Among them are 5-nitro-2,3-phenylpropylaminobenzoic acid (NPPB), anthracene-9-carboxylic acid (9-AC), niflumic acid as well as 6,7-dichloro-2-cyclopenthyl-2,3-dihydro-2-methyl-1-oxo-1Hinden-5-yl oxyacetic acid (IAA) (Marten et al., 1992; Schroeder et al., 1993).

R-type anion channels. The second type of guard cell plasma membrane anion conductance, characterized by a strong voltage dependence, was named CGAC1, or R-type anion channels (Hedrich et al., 1990). This channel is characterized by a decrease in open probability at plasma membrane potentials negative of -50 mV (Keller et al., 1989; Kolb et al. 1995; fig. 3-5 B). Rapidly-activating anion channels are also characterized by time-dependent inactivation during prolonged stimulation at depolarized voltages with half-time of 10 – 12 s (Kolb et al., 1995).

The maximal conductance of single R-type anion channels was determined at 89 pSm, the permeability sequence in row of anions is $SCN^- > NO_3^- > Br^- > Cl^- > malate^{2-}$ (Dietrich and Hedrich, 1998). A detailed biophysical study of permeation of various anions through GCAC1, in isolated membrane patches of *Vicia faba* suggested that GCAC1 operates as a multi-ion single-file pore (Dietrich and Hedrich, 1998). Gating of R-type anion channels is also modulated by external anions. The voltage value, leading to maximal channel activity shifts to more negative membrane potentials after increasing the external anion concentration (Hedrich and Marten, 1993; Dietrich and Hedrich, 1998). Low-permeability anions such as acetate$^-$, propionate$^-$ and malate$^-$, as well as the anion channel blockers NPPB, IAA, SITS and DIDS also were able to shift the half-maximal activation potential of R-type channels (Marten et al., 1992). The inhibition constant for the various anion channel blockers was found to correlate with their ability to modulate the voltage dependence. This finding suggests coupling between anions permeation and gating in GCAC1 (Dietrich and Hedrich, 1998).

Just like S-type channels, the activity of R-type anion channels is also subject to regulation by cytoplasmic Ca^{2+} and depends on nucleotide binding from the cytoplasmic side, requiring no phosphorylation (Hedrich et al., 1990). Currents via R-type anion channels are sensitive to stilbene derivates, such as DIDS (4,4-diisothiocyanatostilbene-2,2-disulfonic acid), which are not blocking plasma membrane S-type anion channels (Marten et al., 1992).

The main organic anion, participating in guard cell metabolism is malate (Raschke et al., 1975). Malate accumulates in leaf apoplast at elevated CO_2 concentrations and after prolonged illumination (Raschke and Schnabl, 1978). Perception of malate at the extracellular side of rapidly-activating anion channels leads to a shift of voltage-dependent gating to more hyperpolarized potentials with a K_m of 0.4 mM and ΔV_{max} of 38 mV (Hedrich and Marten, 1993). Such shift in voltage dependence will increase the activity of R-type anion channels in hyperpolarized guard cells (Hedrich and Marten, 1993). This way apoplastic malate can serve in a feedback mechanism, activating anion channels at elevated CO_2 concentrations in the leaf (Hedrich et al., 1994).

Many properties of single R-type channels, including anion selectivity range and single channel conductance correspond closely with those of S-type anion channels. Based on this close correspondence, it was supposed that R- and S-type anion channels can have a similar pore structure, or even can represent different gating modes of the same channel protein (Dietrich and Hedrich, 1994).

Recently a putative gene encoding SLAC protein was identified (Saji et al., 2008). Screening of T-DNA insertion mutants of *Arabidopsis* revealed an ozone-sensitive phenotype plants *ozs1*, showed enhanced sensitivity to ozone, sulfur dioxide and desiccation. Functional characterization of the mutant revealed that phenotype is based on disrupted regulation of stomatal function. Analysis of genomic sequence revealed mutation in a gene encoding transporter-like protein of the tellurite resistance / C_4-dicarboxylate transporter family of bacteria and fungi (Saji et al., 2008). Four *OZS1*-related genes were identified in *Arabidopsis* genome. The hydrophobicity analysis predicted for OZS1 a membrane-bound protein with ten transmembrane domains. The localization of the protein was predicted at the plasma membrane. The levels of *OZS1* transcripts were high in shoots and sepals but low in seeds, roots and cultured cells (Saji et al., 2008).

Simultaneously the other working group reported identification of ethyl methanesulfonate-mutagenized *Arabidopsis* plant *cdi3* which was impared in CO_2-dependent leaf temperature changes (Negi et al., 2008). The mutation also disrupted stomatal function and was localized in *SLAC1* gene mediating CO_2 sensitivity in plant gas exchange (Negi et al., 2008).

Four structurally related to *SLAC1* genes were also identified in *Arabidopsis* genome which showed distinct tissue-specific expression pattern. Apart from disruption of stomatal function mutant plants showed also over-accumulation of osmotic ions by guard cell protoplasts. Guard cell-specific expression of SLAC1 or its family members restored wild-type stomatal responses and ion homeostasis in *Arabidopsis* plants (Negi et al., 2008). The functional characterization of slac1 plants revealed decreased guard cell responses to CO_2, abscisic acid, ozone, light/dark transitions, humidity change, calcium ions, hydrogen peroxide and nitric oxide (Vahisalu et al., 2008). Analysis of whole cell membrane currents in guard cell protoplasts revealed complete absence of S- but not R-type type anion channels activity in *slac1* mutant plants (Vahisalu et al., 2008).

1.3.3. H^+-ATPase of guard cell plasma membrane.

The guard cell plasma membrane is energized by the proton pump, which performs an ATP-dependent H^+ translocation from the guard cell cytoplasm to the apoplast. Proton translocation from the inner to the outer side of the cell creates an electrical potential difference and a pH gradient across the plasma membrane. Both the electrical- and H^+-concentration difference are utilized by guard cells for translocation of other ions, which have to be transported against their electrochemical gradients.

Guard cell plasma membrane H^+-ATPase are activated by illumination (Assmann et al., 1985; Serrano, 1988), perception of auxins (Lohse and Hedrich, 1992) and by several other exogenous factors, like the fungal toxin fusicoccin (Goh et al., 1995). Experiments revealed that blue light at 460 nm is most effective in provoking light-induced stomatal opening (Sharkley and Raschke, 1981). Later studies led to discovery of PHOT-1 and PHOT-2 light activated protein kinases and showed their involvement in guard cell blue light signaling (Kinoshita et al., 2001).

Plasma membrane H^+-ATPases have a linear current-voltage relation in membrane potentials range of -180 – +50 mV. At more negative potentials, the outward current generated by the pump decreases and reverses at a potential of approximately -230 мV (Lohse and Hedrich, 1992, Taylor and Assmann, 2001). The amplitude of the electrical currents caused by H^+-ATPases are relatively small. H^+-ATPase currents up to 3 pA were registered upon blue light stimulation in *Vicia faba* guard cell protoplasts in whole cell mode of patch clamp (Assmann et al., 1985; Taylor and Assmann, 2001). However, in a special modification of patch-clamp method, a slow whole cell mode, currents of up to 20 pA per guard cell protoplast could be recorded after blue light stimulation (Assmann, 1993; Schroeder, 1988). The amplitude of proton currents evoked by blue light in the guard cells of intact *Vicia faba*

plants was on average 17 pA (Marten et al., 2007a). The higher magnitude of whole-cell H^+-ATPase current with increasing cell integrity clearly indicates that H^+-ATPase activity strongly depends on an intact guard cell cytoplasm.

The activity of plasma membrane H^+-ATPases is characterized by dependence on the intracellular pH (Becker et al., 1993). Guard cells maintain cytoplasmic pH value of approximately around 7.4 – 7.8 (Blatt and Armstrong, 1993). An increase of cytoplasmic proton concentration leads to activation of the proton pump. In this manner, the H^+-ATPase automatically establishes a pH homeostasis in the cell.

A rise of cytoplasmic Ca^{2+} concentration reversibly inhibits the activity of isolated plasma membrane H^+-ATPases, with the half-inhibition constant of proton pumping and ATP hydrolysis of ~0.3 μM (Kinoshita et al., 1995). The activity of H^+-ATPases is mostly regulated through an autoinhibitory domain, located at C-terminus of the protein. The release of this autoinhibitory domain from the catalytic site of the ATPase occurs after phosphorylation and binding of 14-3-3 proteins (Kinoshita and Shimazaki, 1999). However, 14-3-3 proteins also can bind to an alternative site that does not require a phosphorylation step (Fuglsang et al., 2003).

1.3.4. Ca^{2+} transport across guard cell plasma membrane. Calcium ions have unique properties compared to most other ions that are transportesd across biological membranes. Their small crystal radius, together with double electrical charge, causes a high electrical field density around Ca^{2+} ions. In accordance with this feature, living systems have evolutionary developed high-affinity binding sites for Ca^{2+} ions at regulatory domains of proteins. The metabolism of living cells is based on orthophosphate exchange, which forms Ca^{2+} salts with extremely low solubility. Therefore the range of permitted concentrations of free Ca^{2+} ions in the cytoplasm of living cells (the physiological Ca^{2+} range) is lower than 10^{-6} M. In accordance to this feature cells have developed special transport mechanisms, which enable quick and precise control of the cytoplasmic Ca^{2+} concentration (Sanders et al., 2002). The Ca^{2+} homeostasis depends on Ca^{2+}-permeable channels, Ca^{2+}-pumps and Ca^{2+}/H^+ exchangers in the plasma membrane as well as endomembranes (Sanders et al., 1999, 2002).

Ca^{2+}-permeable channels of guard cell plasma membrane. Unlike Ca^{2+}-selective channels in animal cells, Ca^{2+}- channels of plant membranes are typically non-selective cation channels and therefore usually termed Ca^{2+}-permeable channels instead of Ca^{2+}-channels. The main pathway for Ca^{2+} entry from the cell wall into the cytoplasm of guard cells is opening of plasma membrane Ca^{2+}-permeable channels (Demidchik et al., 2002).

Some of these channels are voltage-dependent and activate upon membrane hyperpolarization. The existence of these channels was predicted in experiments aimed to measure H^+-ATPase activity (Lohse and Hedrich, 1992). Large inward currents at hyperpolarized potentials could be inhibited by La^{3+} addition, a known Ca^{2+} channel blocker. In later experiments, the direct relation between the plasma membrane hyperpolarization and an increase in the cytoplasmic Ca^{2+} concentration in *Vicia faba* guard cells was demonstrated using Ca^{2+}-sensitive fluorescent probe Fura-2 (Grabov and Blatt, 1998). These authors proposed also a physiological role of hyperpolarization-activated Ca^{2+}-channels in the intracellular transduction of ABA signal. A more detailed characterization of this channel type with the patch-clamp technique (Hamilton et al., 2000) revealed high channels permeability for Ca^{2+} and Ba^{2+} compared to K^+ and Cl^- (>10 : 1). These features, in combination with blockage by La^{3+} and Gd^{3+}, are also characteristic of many Ca^{2+}-selective channels of animal kingdom. The maximal single channel conductance of hyperpolarization activated Ca^{2+} permeable channels in 30 mM Ba^{2+} was estimated at 12.8 pSm. The activity of these channels increased at elevated external Ba^{2+} and Ca^{2+} concentrations in the range of 0.3 – 30 mM, but decreases at high cytoplasmic Ca^{2+} concentrations in the range of 0.2 – 2 μM. The channel gating was not affected by cytoplasmic Ba^{2+} (Hamilton et al., 2001). Ca^{2+}-permeable channels in isolated membrane patches also showed increase of the channel open probability upon ABA binding (Hamilton et al., 2000), which is well in agreement with the previously obtained data on the shift of the activation potential after ABA application (Grabov and Blatt, 1998).

During an attempt to identify chemical ligands that are able to activate R-type anion channels in protoplasts of *Arabidopsis* guard cells, Pei et al. (2000) discovered activation of Ca^{2+}-channels in response to 50 μM H_2O_2 application. Just as in *V. faba* guard cell protoplasts, these channels were activated upon hyperpolarization of the plasma membrane (Pei et al., 2000).

The hyperpolarization activated Ca^{2+}-permeable channel may provide a pathway for Ca^{2+}-entry induced by high apoplastic Ca^{2+}. Especially, since high Ca^{2+}-levels activate these channels. Nevertheless, guard cells were found to possess an alternative mechanism to respond to high external Ca^{2+} concentration, which is provided by the Ca^{2+}-sensor protein CAS. Guard cells of *Arabidopsis*, expressing an antisense sequence of *CAS* lost their ability to generate $[Ca^{2+}]_{cyt}$ oscillations in response to rise in the external Ca^{2+} concentration (Han et al., 2003, section 1.4.3).

Active transport of Ca^{2+} across the guard cell plasma membrane. Maintenance of $[Ca^{2+}]_{cyt}$ at the nanomolar physiological level requires the continuous activity of ATP-

dependent active transport mechanisms. These Ca^{2+} ATPases remove Ca^{2+} from the cytoplasm, which enters as a result of background activity of Ca^{2+} conducting pathways.

Active transport of Ca^{2+} ions is accomplished by Ca^{2+}-ATPases in the plasma membrane (Sze et al., 2000). These calcium ATPases in plant cells (ACA) belong to the P2B family of P-type ATPases and characterized by a high homology to Ca^{2+}-ATPases of mammalian plasma membranes (PMCA pumps) (Axelsen and Palmgren, 2001).

The regulation of Ca^{2+}-ATPase activity occurs through an autoinhibitory domain, located at N-terminus of the protein. This autoinhibitory domain of the ACA pumps can bind a Ca^{2+}/calmodulin complex. Elevated $[Ca^{2+}]_{cyt}$ leads to binding of the Ca^{2+}/calmodulin complex and release of the autoinhibitory domain, resulting in activation of Ca^{2+}-ATPase. This way the Ca^{2+}-pump is turned in self-regulating loop with negative feedback, where the rise in cytoplasmic Ca^{2+} concentration will lead to the automatic increase of pump activity. Apart from the regulation through Ca^{2+}/calmodulin binding, the activity of ACA pumps is also regulated by Ca^{2+}-dependent proteinkinases (CDPKs, section 1.4.2).

1.3.5. Vacuolar ion transport in guard cells. The vacuolar system of guard cells consists of several small vacuoles, mostly localized at distant ends of the cell. In most cells small vacuoles could be easily distinguished on photomicrographs of guard cells, injected with fluorescent dye Fura-2 (fig. 2-8 A). Turgescent guard cells normally have only a few large vacuoles, which fragmentize and reduce in size upon stomatal closure (Diekmann et al., 1993).

A large part of the ions, taken up by guard cells during stomatal opening accumulates in vacuoles. Ions are translocated in the opposite direction, from the vacuole to the cytoplasm and further on to the apoplast, during stomatal closure (Roelfsema et al., 2005; MacRobbie, 2006). With regard to signaling the vacuolar transport of Ca^{2+} and H^+ is of particular importance (Blatt, 2000).

Potassium transport across the vacuolar membrane of guard cells. Translocation of K^+ ions through the vacuolar membrane of guard cells can occur through three types of ion channels: slow vacuolar channels (SV-type), quick vacuolar channels (FV-channels) and vacuolar K^+-selective channels (VK-channels).

Slow vacuolar channels forms the main part of K^+ conductance of the guard cell tonoplast. Gating of SV channels is characterized by slow opening upon tonoplast depolarization (corresponds to the reduction of negative potential at the cytoplasmic side of the vacuolar membrane), providing efflux of K^+ from the vacuole. During strong tonoplast depolarization

a reversion of ionic current occur, since K^+ may flow into the vacuole through SV channels (Ivashikina and Hedrich, 2005). Quick vacuolar channels are characterized by short activation times upon tonoplast depolarization and probably also serve for K^+ efflux from the vacuole under physiological conditions.

Quick and slow vacuolar channels are characterized by an opposite Ca^{2+}-dependence. The activity of quick vacuolar channels is inhibited by cytoplasmic Ca^{2+} concentrations, exceeding 0.1μM level (Hedrich et al., 1986; Allen and Sanders, 1996), while currents via SV-channels could be registered only when Ca^{2+} concentration from the cytoplasmic side exceeds 0.5 μM (Hedrich and Neher, 1987). SV vacuolar channels also display a Ca^{2+} permeability at selected ionic conditions and the channels can be sensitized by cytoplasmic Mg^{2+}, whereas FV channels activity subjected to the reverse regulation by cytoplasmic Mg^{2+} concentrations (Carpanetto et al., 2001, Pei et al., 1999).

A third type of K^+-permeable channels in the tonoplast is the K^+-selective VK channel (Ward and Schroeder, 1994). VK-channels are characterized by absence of rectification in range of vacuolar membrane potentials -100 - +100 mV. VK-channels therefore can either serve for the uptake or release of luminal K^+ at conditions which do not lead to activation of SV- or FV-channels (Allen et al., 1998).

The molecular identity of the vacuolar potassium channels has not been clarified, yet. It is, however, likely that vacuolar channels may encode by the family of TPK and KCO3 genes. All TPK family genes encode a GYGD amino acid sequence in the pore region of the channels, suggesting a K^+-selective filter (Czempinski et al., 2002; Becker et al., 2004).

Transport of K^+ from the cytoplasm to the lumen of the vacuole occurs against the electro-chemical gradient, and therefore most likely is carried out by secondary active transport proteins. Translocation of K^+ can occurs trough H^+/K^+ exchangers (CHX) (Venema et al., 2003; Cellier et al., 2004), which are characterized by a high homology to Na^+/H^+ exchangers (NHX) of yeasts. The latter proteins are able to carry out H^+-coupled translocation of Na^+ (Gaxiola et al., 1999).

Vacuolar Ca^{2+} transport. Guard cell vacuoles are important intracellular Ca^{2+} stores, and play a role in Ca^{2+}-signalling as well as in maintaining of Ca^{2+}-homeostasis. The vacuolar Ca^{2+} concentration of guard cells has not been determined experimentally, but is supposed to be in the milimolar range according to measurements with vacuoles of *Riccia* rhizoid cells and root hair cells of *Zea mays* (Felle, 1988).

Passive efflux of Ca^{2+} from the vacuole into the cytosol of guard cells occurs by opening of Ca^{2+}-permeable tonoplast channels. Controlled activation of these channels can lead to

the generation of $[Ca^{2+}]_{cyt}$ signals, which may carry stimulus-specific information. This information has to be recognized by Ca^{2+}-sensitive proteins that transduce the signal further along signal transduction chains (Evans and Hetherington, 2001; Sanders et al., 2002). By using the patch-clamp technique on the tonoplast of plant cells several ligand-activated Ca^{2+}-permeable channels were identified. The existence of IP_3- and cADPR-gated Ca^{2+}-channels was identified on the tonoplast, derived from beet roots (Allen et al., 1995). Furthermore, the tonoplast of *Commelina communis* guard cells was shown to possess a cADPR-activated Ca^{2+} channels (Leckie at. al., 1998) as well as Ca^{2+}-permeable channels, activated by IP_6 (Lemtiri-Clieh et al., 2003). Apart from these ligand-gated Ca^{2+}-permeable channels, guard cell tonoplasts also have been shown to possess a voltage-dependent Ca^{2+}-channels (VV Ca-channels, Allen and Sanders, 1994).

The permeability of vacuolar SV-channels for Ca^{2+} has been the cause of a intensive discussion on the physiological role of these cation channel. Whereas some papers favor a role for SV-channels in Ca^{2+}-induced release of Ca^{2+} from vacuolar stores (CICR), (Ward and Schroeder, 1994; Bewell et al., 1999), others show experimental data that question the idea of SV channels participation in CICR (Potossin et al., 1997, 2002; Ivashikina and Hedrich, 2005).

Little is known about the molecular identity of Ca^{2+}-channels of plant cell vacuolar membranes. The single copy gene in *Arabidopsis* genome *AtTPC*1 (Furuchi et al., 2001), probably encodes the SV-channel (Carter et al., 2004; Peiter et al., 2005). But a role of the gene product in Ca^{2+} regulation was not unequivocally shown. Genes, homologous to rhyanodine and IP_3 receptors of animal endomembranes have not been identified in the *Arabidopsis* genome. This may suggest that the plant receptors for inositol phophates and cADPR have evolved independently or diverged significantly from their animal counterparts (Shwacke et al., 2003).

Much less data have been obtained with regard to the mechanisms, responsible for the reuptake of Ca^{2+} into the vacuoles. Refilling of the vacuolar lumen can occur because of the activity of Ca^{2+}-ATPases of the ACA family (Sze et al., 2000) and Ca^{2+}/H^+ exchangers encoded by *CAX* genes (Hirshi et al., 1996). The activity of tonoplast Ca^{2+} pumps is regulated via binding of Ca^{2+}/calmodulin, whereas the regulation of CAX transporters seems to be more complex and probably involves several CPIX proteins that tightly interact with the CAX proteins (Cheng and Hirschi, 2003).

Vacuolar anion transport. At physiological relevant conditions the tonoplast potential favors movement of anions from the cytoplasm to the vacuole. Only a single publication de-

scribes an anion channel, located in the tonoplast of guard cells (Pei et al., 1996). This channel, registered on the tonoplast of *Vicia faba* guard cells is characterized by the single channel conductance of 34 pSm and is permeable for anions. Ion channel promote Cl^- and malate^{2-} anions transport to the guard cell vacuole. The activity of the channel required both Ca^{2+} and ATP presence and showed regulation by Ca^{2+}-dependent protein kinases (Pei et al., 1996).

Vacuolar anion channels may be encoded by genes, homologous to bacterial and animal genes of ClC channels. Disruption of *AtCLC* gene in *Arabidopsis* leads to reduction of nitrate accumulation by plants growing on medium with elevated NO^{3-} support (Geelen et al., 2000) However, so far the CLC genes were found to encode H^+/Cl^- antiporters, instead of channels (De Angeli et al., 2006).

Vacuolar H^+ transport. Translocation of H^+ through guard cell tonoplast is accomplishes by two types of proton pumps – V-ATPases and pyrophosphotases (Hedrich et al., 1986, 1989; Sze et al., 1999). Besides the differences in the utilized substrates, V-ATPases are also characterized by a more complex structure, which is similar to mitochondrial F1/F0-ATPases.

The stoichiometry of the H^+ translocation by V-ATPases can vary from values of more than 3 (Davies et al., 1994) to 1 proton per hydrolyzed ATP molecule (Müller and Taiz, 2002). The low stoichiometry values are probably important for the vacuoles with low pH levels, as the steep H^+ gradient would otherwise invert the proton flux through V-type ATPases (Gambale et al., 1994). Regulation of vacuolar V-ATPase activity occurs via the balance of redox reactions and by the nucleotides binding from the cytoplasmic side of the membrane (Kluge et al., 2003).

Pyrophosphotases, or PP-ases, participate in generating a H^+ gradient across the vacuolar membrane, making use of pyrophosphat as energy source (Drozdowich and Rea, 2001). Since pyrophosphate accumulates as a by-product of biosynthesis, it is mostly available in cells of young growing tissues (Maeshima, 2000). The participation of PP-ases in vacuolar proton transport therefore probably is negligible in mature guard cells, where the rate of macromolecule biosynthesis is not so high.

1.4 CELLULAR SIGNALLING IN STOMATA.

1.4.1 Receptory system of guard cells. Stomatal movement has a large impact on metabolic activity of a plant, as well as its water relations. Optimizing the stomatal conductivity to the demands of the whole plant is an extremely complicated challenge for autono-

mously reacting cells, like guard cells. In order to fulfill this challenging function, guard cells have developed a set of receptors during evolution, which enables them to respond quickly and precisely to a wide range of external and internal factors.

Photoreception. Light is a central factor, which induces stomatal opening. Apart from the photon flux density and the photoperiod (for review see Shimazaki et al., 2007), the wavelength has also important meaning. During early studies on light reception by guard cells, researchers put their attention to the fact, that stomatal opening can be induced by lowering the CO_2 concentration in the leaf (Heath, 1959). Based on this observation a model was postulated, which proposes photosynthetic regulation of stomatal aperture via the control of the CO_2 concentration inside the leaf. This hypothesis was also confirmed by the close correspondence of the chlorophyll absorption spectra with the spectral characteristics of stomatal opening process (Kuiper, 1964). However, further investigation of the light-induced stomatal opening has shown, that blue light is much more effective in inducing stomatal opening than red light (Sharkey and Raschke, 1981). Later experiments showed that blue light stimulates stomatal opening even in the presence of saturating photon flux densities of red light. This observation suggested the existence of a separate light perception systems for blue and red light (Iino et al., 1985).

A typical response, registered upon stimulation of stomatal guard cells of epidermal strips or guard cell protoplasts with pulse of blue light is an acidification of cell surrounding. This response is linked to the activation of plasma membrane H^+-ATPase (Assmann et al., 1985, Shimazaki et al., 1986). The timecourse of the proton pump activation represents a single transient, activating with the delay of 1 min. The velocity of proton extrusion reaches it's maximum at 120 s after the stimulus onset and starts to decay slowly afterwards (Kinoshita and Shimazaki 1999; Roelfsema et al., 2001).

The perception of blue light in guard cells of *Arabidopsis* occurs via two PHOT receptors - PHOT1 and PHOT2 (Kinoshita et al., 2001; Briggs and Christie, 2002). Guard cells of the double mutant *phot1/phot2 Arabidopsis* plants were shown to have lost the ability to respond to blue light, based on lack of changes in the stomatal aperture and acidification of the external medium (Kinoshita et al., 2001).

PHOT receptors are membrane-associated kinases, containing flavin mononucleotides serving as light sensors. The flavin mononucleotides bind at two LOV-domains, located at the N-terminus, whereas C-terminal part of the protein represents serine/threonine kinase (Christie et al., 1999). Blue light reception triggers autophosphorylation of PHOT receptors, leading to consequent binding of 14-3-3 proteins, most likely stabilizing receptor molecules

in an active state (Kinoshita et al., 2003). A similar mechanism has been described for activation of the plasma membrane H^+-ATPase. Here, the autoinhibitory domain of the ATP-ase becomes phosphorylated in blue light, which leads to liberation of the C-terminus from the catalytic site of ATPase. The active state of the H^+-ATPase is also stabilized through binding of 14-3-3 proteins.

To date there is no evidence for a fact of direct phosphorylation of plasma membrane H^+-ATPase by the PHOT receptor kinases. The signal transduction pathway from PHOT receptors to the H^+-ATPase activated upon stimulation of guard cells with blue light, seems to be more complicated and depends on presence of functional RPT2 protein (Inada et al., 2004). Based on its protein sequence, the RPT2 protein may represent a factor, responsible for protein-protein interactions.

A few experimental studies point to the involvement of $[Ca^{2+}]_{cyt}$ changes in the signal transduction chain, triggered by blue light. Guard cell responses to blue light were inhibited by high concentrations of verapamil, a known blocker of Ca^{2+}-channels (Shimazaki et al., 1997) whereas high external Ca^{2+} concentrations stimulate blue light induced extracellular acidification (Roelfsema et al., 1998). In whole *Arabidopsis* seedlings, a rise in $[Ca^{2+}]_{cyt}$ was recorded after stimulation with blue light. This response was via a PHOT1-dependent signaling pathway (Baum et al., 1999). In mesophyll cells of *Arabidopsis*, the stimulation of hyperpolarization-activated Ca^{2+} channels in the plasma membrane by blue light was described. Activation of these channels was dependent on the presence of functional PHOT1 and 2- receptors (Stoelzle et al., 2003). However, the direct experimental evidences for a blue light induced rise of $[Ca^{2+}]_{cyt}$ in stomatal guard cells, is missing.

Besides the PHOT-dependent signal transduction chain, leading to stomatal opening with an effective absorption maximum at 460 nm, guard cells are also sensitive to a broad spectrum of visible light wavelengths, called photosynthetic active radiation. Perception of photosynthetic active radiation activates a different mechanism leading to stomatal opening, known as the red light-induced stomatal opening. The existence of this signaling pathway can be most obviously demonstrated with DMCU, an inhibitor of photosystem II, which abolishes stomatal opening upon red, but not blue light illumination (Sharkley and Raschke, 1981).

The photosynthetic activity is linked to stomatal movement through changes in the intracellular CO_2 concentration. Stomatal guard cells of the intact *Vicia faba* leaf did not show any response to illumination with narrow beam of red light, focused on single guard cell. However, illumination of larger leaf area, which leads to a change in the CO_2 concentration

inside the leaf, did evoke changes in the free-running membrane potential of guard cells (Roelfsema et al., 2002).

Guard cells respond to elevated CO_2 concentrations with a reversible activation of S-type anion channels. The activation of anion channels leads to plasma membrane depolarization that in turn reverses the potassium flux across the plasma membrane and thus results in an efflux of osmotic active ions and a reduction of stomatal aperture (Roelfsema et al., 2002). The involvement of intracellular Ca^{2+} changes has been proposed in signal transduction chain, which leads to the activation of S-type anion channels upon increasing CO_2 concentrations (Webb et al., 1996), whereas a role of the intracellular pH could be excluded (Brearley et al., 1997).

Thermoreception. Depending on the time scale of physiological or biochemical processes, a quick and slow (supposing the change in gene transcription) temperature effects on guard cells could be separated.

Quick responses are provoked by temperature dependent changes in the activity of ion channels and pumps. The active transport systems are characterized by a higher temperature dependence, because of the biochemical process that drives ion translocation. The temperature dependence of ion channels can vary considerably between different channels types.

The temperature dependence of outward-rectifying and inward-rectifying K^+ channels in the guard cell plasma membrane has been studied with the patch clamp technique (Ilan et al., 1995). At moderate temperatures (13 - 20° C) the conductance of both types of K^+-selective channels increases with a rise in the temperature. A further temperature increase (20 - 28° C), however, leads to a decrease of K^+_{out} channel conductance, whereas the conductance of K^+_{in} channels continues to rise. Such a divergence in the temperature dependency of outward- and inward-rectifying K^+-channels was suggested to contribute to K^+ uptake and stomatal opening at high temperatures, possibly favoring to transpirational cooling of the leaf (Ilan et al., 1995).

The effect of a "cold shock" has been studied in guard cells in isolated epidermal strips of *Nicotiana plumbagnifolia*, expressing the Ca^{2+}-sensitive luminescent protein aequorin. A short period (10 – 20 s) of cooling to 0°C caused a transient increase of $[Ca^{2+}]_{cyt}$ of up to 4 – 6 µM, which lasted for 2 min (Wood et al., 2000). The Ca^{2+} channel inhibitors La^{3+} and Ruthenium Red, as well as EGTA partially reduced the Ca^{2+} responses, suggesting the participation of extracellular as well as intracellular Ca^{2+} stores in generation of cold dependent $[Ca^{2+}]_{cyt}$ changes.

ABA reception. Guard cells display huge coordinated changes in membrane conductance after perception of abscisic acid. The activity changes of ion channels leads to a quick closure of stomata, which is one of the most typical responses of stomatal guard cells. The most apparent ABA induced response at the guard cell plasma membrane is the activation of anion channels (Thiel et al., 1992; Grabov et al., 1997; Pei et al., 1997; Raschke et al., 2003).

The activation of plasma membrane anion channels shifts the free-running potential of guard cell plasma membrane towards reversal potential of Cl^-, i.e. in the depolarizing direction. Membrane depolarization in turn opens voltage-dependent outward-rectifying K^+ channels, thus creating a pathway for passive efflux of K^+ from the cell. The loss of osmotic components leads to reduction of turgor pressure and in turn to stomatal closure. Despite of the observation that ABA directly activates K^+_{out} channels through a cytoplasmic alkalization (Blatt and Armstrong, 1993), such an upregulation will not be sufficient to drive stomatal closure. Instead, K^+ efflux requires a motive force for the efflux of K^+ from the cell, in other words, a difference between the reversal potential of K^+ ions and actual value of membrane potential (Thiel et al., 1992). This potential difference is provided by the activity of plasma membrane anion channels and not by the K^+_{out} channel themselves. Thus, activation of K^+_{out} channels can be considered as a factor that increases the potency for potassium efflux, but not as a process leading to stomatal closure.

Anion channel activation upon ABA application has been postulated to be dependent on Ca^{2+}-signalling in guard cells (Schroeder et al., 2001). A number of experimental investigations have report various patterns of $[Ca^{2+}]_{cyt}$ elevations in response to ABA application (McAinsh et al., 1990, 1992; Gilroy et al., 1991; Staxen et al., 1999; Romano et al., 2000; Marten et al., 2007b; section 1.4.3). A rise in the cytoplasmic Ca^{2+} concentration can activate anion channels in the guard cell plasma membrane (Schroeder and Hagiwara, 1989; Hedrich et al., 1990). The latter response is most likely the result of the regulation by Ca^{2+}-dependent proteinkinases (Mori et al., 2006). Even though the ABA-dependent activation of anion channels thus may be mediated though Ca^{2+} signals, this sequence of events had not been measured in guard cells at the start of the PhD-research project. Results of the experimental investigation of ABA-induced anion channels activation, combined with a parallel registration of $[Ca^{2+}]_{cyt}$ in intact guard cells, did not show any changes of $[Ca^{2+}]_{cyt}$ level in spite of significant activation of the anion current during ABA application (Levchenko et al., 2005; section 3.4.2).

A similar situation, observed for activation of an ion channels, has also been reported for the ABA-induced inhibition of plasma membrane inward-rectifying K^+ channels. The

necessity of $[Ca^{2+}]_{cyt}$ rises for the ABA-dependent inhibition of inward-rectifying K^+ channels (Schroeder and Hagiwara, 1989) could not be confirmed by patch-clamp experiments with *Vicia* guard cell protoplasts. When 5 mM BAPTA was added to patch pipette, an apparent inhibition of K^+_{in} channels was observed upon ABA application in spite of the absence of $[Ca^{2+}]_{cyt}$ elevation (Romano et al., 2000).

Even though ABA has a pronounced effect on ion transport in guard cells, the nature of the receptor, responsible for ABA binding and initiation of the cellular reactions remains obscure. Highly controversial is also a question of the subcellular localization of the ABA receptor. Analysis of the experimental data on the kinetics of ABA-induced effects in most cases points to the necessity of ABA trapping inside the cells (Ogunkanmi et al., 1973; Paterson et al., 1988; MacRobbie, 1995), thus supposing the cytoplasmic localization of the receptor.

In correspondence with the model of the simple diffusion of protonated ABA through the lipid bilayer, the extent and velocity of the stomatal closure in response to ABA application appeared to depend on extracellular pH value (Ogunkanmi et al., 1973; Paterson et al., 1988) with a more pronounced effect of ABA at low external pH levels. Similar conclusions were drawn from the analysis of the pH-dependencies of kinetic properties of the ABA-induced $^{86}Rb^+$ efflux from guard cells of epidermal strips of *Commelina* (MacRobbie, 1995) and pH-dependency of the extent to which inward-rectifying K^+ channels are inhibited by ABA (Schwartz et al., 1994). An intracellular localization of the receptor also supports the fact that stomatal closure can be induced by photorelease of a caged form of ABA, microinjected into the guard cell cytoplasm (Allan et al., 1994).

Other experimental evidences, however, suggest an extracellular perception side for the initiation of ABA-responses. In experiments directed on the inhibition of stomatal opening by ABA, cytoplasmic microinjection of ABA had no effect on the stomatal aperture (Anderson et al., 1994). Thus binding of ABA can occur both at the intracellular and extracellular sides of the plasma membrane. Authors suppose, that abscisic acid presented only at the cytoplasmic side of the membrane is not sufficient for evoking stomatal closure.

Experiments with a conjugate of ABA and biotin showed binding to the external side of the plasma membrane of *Vicia faba* guard cell protoplasts and epidermal strips (Yamazaki et al., 2003). A treatment with proteinases prevented the binding of biotinilated ABA to the external side of the plasma membrane. The perception sites of the conjugate could be visualized by binding of avidin tagged with a fluorescent probe. Perception sites showed patchy distribution over the plasma membrane with equal fluorescence, supposing assembling of

receptor proteins to a complexes. The binding of biotinilated ABA could be inhibited by ABA and it's active analogs. Conjugate binding was also shown to possess the physiological activity, promoting stomatal closure and guard cell protoplast shrinking. The constant for ABA binding to the supposed putative receptor was determined in 17 nM.

1.4.2. Phosphorylation/dephosphorylation cascades. The reversible phosphorylation of target proteins is an important cellular mechanism for the control of many processes in living cells. Phosphorylation of proteins is carried out by proteinkinases, a large group of enzymes that possess the ability to bind inorganic phosphate covalently to a residue at a certain amino acid residue, representing a phosphorylation side. The amino acid residues serin, threonine and tyrosine can serve as acceptors on the target proteins. The opposite process, removal of the Pi-group from target proteins, is dependent on the activity of other proteins, called phosphatases.

Substrate phosphorylation. Plants possess four different classes of proteinkinases, among which are Ca^{2+}-dependent proteinkinases (CDPK), Ca^{2+}-independent proteinkinases (CIPK), Ca^{2+}/calmoduline-activated kinases (CaMK) and mitogen-activated (MAPK) proteinkinases, which are different in terms of their structure and regulation.

Big number of cells functions, regulated by phosphorylation in plant cells fulfilled by CDPKs, which include 34 genes found in *Arabidopsis* genome. Presence of calmodulin-like domain, serving for Ca^{2+} binding, combined with the kinase domain in one functional protein is a characteristic feature of Ca^{2+}-dependent proteinkinases. Calcium-dependent proteinkinases are unique class of kinases, found only in plants and several protozoa and completely absent in fungi, animal and human genomes (Sheng et al., 2002). The phylogenetic analysis supposes that plant CDPKs evolutionally appeared as a result of genes fusion of Ca^{2+}-calmodulin-activated proteinkinases and Ca^{2+}-binding protein calmodulin (Harmon et al., 2000). Besides the activation by Ca^{2+} binding, Ca^{2+}-dependent proteinkinases are also regulated by phosphorylation, binding of 14-3-3 proteins and phospholipids (reviewed by Sheng et al., 2002).

Many processes, related to regulation of ion transport in guard cells are subjected to regulation by proteinkinases and phosphatases (Pei et al., 1998).

From *Vicia faba* guard cells a 53 kDa proteinkinase were purified, able to phosphorylate inward-rectifying K^+ channels KAT1 *in vitro* in a Ca^{2+}-dependent manner. Phosphorylation showed necessity of the membrane phospholipid components presence, indicating possible occurrence of the phosphorylation process *in vivo* (Li et al., 1998). Co-expression of

KAT1 gene and the Ca^{2+}-dependent proteinkinase (...) gene from soybean in *Xenopus* oocytes led to the reduction of inward K^+-selective currents in comparison to the amplitude of currents in the oocytes, expressing KAT1 along. This fact can tell about the direct involvement of Ca^{2+}-dependent proteinkinase in the regulation of inward-rectifying K^+ channels activity in plants (Berkowitz et al., 2000).

Vacuolar anion-selective channels of *Vicia faba* guard cells, participating in the process of Cl^- uptake during stomatal opening showed strong regulation by Ca^{2+}-dependent proteinkinase AtCPK1. A product of AtCPK1 gene expression induced also stimulation of malate uptake by isolated guard cell vacuoles of *Vicia* and uptake of Cl^- by vacuoles of red beet root cells (Pei et al., 1996). Calcium-dependent proteinkinase (isoform CPK1) lead to the inhibition of Ca^{2+} uptake by the membrane vesicles suspension, containing Ca^{2+}-pump ACA2. The protein kinase lead to inhibition of both basal and calmodulin-stimulated activity of Ca^{2+}-pump, targeting to endoplasmic reticulum of plants (Hwang et al., 2000).

Function of CIPKs was shown for the signal transduction chain, leading to the activation of guard cell plasma membrane S-type anion channels upon ABA perception (Shwarz and Schroeder, 1998). Biochemical approaches lead to the isolation of Ca^{2+}-independent proteinkinase, upregulated by ABA at the expression level. The kinase was named AAPK (<u>A</u>BA <u>a</u>ctivated serine/threonine <u>p</u>rotein<u>k</u>inase) (Li and Assmann, 1996) or ABR (<u>Ab</u>scisic Acid <u>R</u>egulated protein kinase) (Mori and Muto, 1997). The kinase gene *AAPK* was cloned and characterized latter (Li et al., 2000). Transient expression of negative dominant allele, suppressing the kinase activity in guard cells of isolated epidermal strips of *Vicia faba* leads to disruption of ABA-induced activation of plasma membrane anion channels and stomatal closure (Li et al., 2000). In patch-clamp registration on guard cells protoplasts of *Vicia faba* were confirmed, that the final step in ABA-induced phosphorylation of S-type anion channels has a Ca^{2+}-independent character, as the activation of S-type anion channels took place with buffered $[Ca^{2+}]_{cyt}$ upon high cytoplasmic ATP concentrations (Schwarz and Schroeder, 1998).

Use of infrared thermal imaging for scanning of *Arabidopsis* mutants with disrupted water regulation lead to isolation of *ost1* (<u>O</u>PEN <u>ST</u>OMATA 1) mutant, characterized with reduced ability to react by stomatal closure in response to induction of drought conditions (Merlot et al., 2002). Phenotypical analysis of the mutants revealed that plants, carrying recessive mutant allele *ost1* characterize with normal stomatal responses to increasing CO_2 concentration and illumination by blue light, but were impaired in sensitivity to ABA. Further analysis of *ost1* locus showed, that the product of OST1 gene expression represents a

Ca^{2+}-independent proteinkinase with molecular weight 41 kDa, which includes 362 amino-acid residues. Gene of OST1 kinase showed 79 % identity with Ca^{2+}-independent proteinkinase AAPK (ABR), cloned from *Vicia*. Protein extracts, purified from roots and guard cell protoplasts demonstrated Ca^{2+}-independent kinase activity *in vitro*. Like AAPK kinase from *Vicia faba*, the expression of OST1 in *Arabidopsis* cells was stimulated by ABA. Recombinant expression of OST1 in *Esherichia coli* produced an inactive gene product, showing no kinase activity *in vitro*, most likely supposing involvement of ABA-induced signaling components for the protein activation.

Participation of OST1 in ABA-induced signal transduction chain likely associated with production of reactive oxygen species (ROS), as *Arabidopsis* plants, expressing *ost1* allele demonstrated reduced ROS production. At the same time external H$_2$O$_2$ or Ca^{2+} application evoked the same degree of stomatal closure in mutant line and wild type plants (Mustili et al., 2002).

Substrate dephosphorylation. Reverse to the phosphorylation process of orthophosphate residues removal from phosphorylation sites of target proteins occurs via the activity of enzymes, named proteinphosphatases. The first identified ABA-signalling mutants were a phosphatase mutants, carrying mutation in proteinphosphatase genes *abi1* and *abi2* (Korneeff et al., 1984).

Biochemical and genetic approaches identified presence of 2B (Ca^{2+}-dependent), 2C and 1/2A types of proteinphosphatases in guard cells. The identity of phosphatases, performing the regulation of defined separate functions often remains unclear excepting the pharmacological evidences of the dephosphorylation process. Regulation related to 2B phosphatases involvement has been shown for outward-rectifying K$^+$ channels of guard cell plasma membrane. Cyclosporine A, an inhibitor of animal 2B-type phosphatases, inhibits stomatal closure and reduces the degree of ABA-induced inhibition of stomatal opening in *Pisum* (Hey et al., 1997), supposing the role of 2B phosphatases as negative regulators of stomatal opening. Type 2B phosphatase inhibitors can maintain the activity of outward-rectifying potassium channels in guard cells of *Vicia* despite of high [Ca^{2+}]$_{cyt}$ (Luan et al., 1993). Positive regulation by type 1/2A proteinphosphatases was described for the activity of plasma membrane K$^+_{out}$ and K$^+_{in}$ channels of guard cell plasma membrane, as type 1/2A phosphatases agonists lead to their inhibition (Thiel and Blatt, 1994; Li et al., 1998). Inhibitors of 1/2A proteinphosphatases caliculin A and ocadaic acid evoke inhibition of blue-light induced proton transport through guard cell plasma membrane and stomatal opening (Kinoshita and Shimazaki, 1997), supposing a role of 1/2A phosphatases as positive regulators of blue light-

induced stomatal opening. Okadaic acid stimulated also the activity of S-type anion channels and ABA-induced stomatal closure in *Vicia* (Schmidt et al., 1995; Schwarz and Schroeder, 1998), *Nicotiana* (Grabov et al., 1997), *Commelina* (Esser et al., 1997), *Pisum* (Hey et al., 1997) and *Arabidopsis* (Pei et al., 1997) guard cells, supposing the role of 1/2A phosphatases as negative regulators of ABA signaling (Schroeder et al., 2001). Upon cytoplasmic ATP depletion both ABA and ocadaic acid were able to maintain the activity of plasma membrane anion channels in guard cell protoplasts of *Vicia*, indicating possible inhibition of 1/2A type proteinphosphatases by ABA (Schwarz and Schroeder, 1998).

Analysis of *Arabidopsis* mutants, insensitive to ABA (a group of so-called *abi*, abscisic acid insensitive mutations, Korneeff et al., 1984) revealed two genes ABI1 and ABI2, encoding homologous 2C proteinphosphatases (Meyer et al., 1994; Leung et al., 1994, 1997). Both mutant alleles *abi1-1* and *abi2-1* are dominant and have set of overlapping phenotypical characteristics, including insensitivity of the seed germination and seedling growth to ABA, disruption of stomatal aperture regulation and many other responses, related to drought resistance (Merlot et al., 2001). Analysis of intragenic revertants *abi1* and *abi2* pointed, that 2C phosphatases ABI1 and ABI2 represent negative regulators of ABA signaling (Gosti et al., 1999, Merlot et al., 2001).

Guard cell protoplasts, derived from *Arabidopsis* plants, carrying dominant mutant alleles *abi1* and *abi2* showed disrupted anion channel activation in response to ABA treatment (Pei et al., 1997). Induced by type 1/2A phosphatase antagonist ocadaic acid inhibition of ABA-induced anion channel activation in *Arabidopsis* guard cells did not change the kinetic parameters of the channels activation, whereas during the investigation of anion channels regulation in isolated epidermal strips of transgenic *Nicotiana benthamiana* plants, expressing mutant allele *abi1*, application of ABA and type 1/2A phosphatase antagonist caliculin A evoked changing of S-type anion channels gating (Grabov et al., 1997). Tobacco plants, expressing *abi1* showed also significant (2- to 6-fold) reduction of plasma membrane outward-rectifying K^+ channels activity and insensitivity of outward- and inward-rectifying K^+ channels to ABA. Parallel registration of cytoplasmic pH changes upon ABA action although did not reveal any difference in pH_{cyt} response between transgenic and wild-type plants, supposing that other than pH_{cyt} mechanism is involved in of K^+_{out} channels regulation (Armstrong et al., 1995).

In *Arabidopsis* guard cells, carrying *abi1* and *abi2* mutations a reduction of the amplitude of ABA-induced $[Ca^{2+}]_{cyt}$ elevations comparing to wild-type plants was also reported (Allen et al., 1999a). The precise points of type 2C proteinphosphatases ABI1 and ABI2 ac-

tivity application is not known yet, but apparently the enzymes activity regulates very early steps in ABA signal transduction chain, as the rises of $[Ca^{2+}]_{cyt}$ supposes to be one of the earliest events (Grabov and Blatt, 1998; Schroeder et al., 2001).

1.4.3. Ca^{2+} and H^+-coupled signaling mechanisms. As a large number of proteins have developed the ability to regulate their activity upon Ca^{2+} binding during evolution, Ca^{2+} cations became important for the regulation and coordination of many cellular processes. The profile of stimulus induced cytoplasmic Ca^{2+} concentration changes, is supposed to encode the information about nature and strength of stimulus (Sanders et al., 2002).

The Ca^{2+} signaling system consist of transport proteins, responsible for Ca^{2+} influx into the cytoplasm and it's removal into the intracellular stores and apoplastic space. Both the in- and efflux mechanisms are Ca^{2+}-dependent themselves and thus are presumed to form the base for the autotuning of Ca^{2+} level (Ca^{2+} homeostasis). Besides Ca^{2+} transport pathways responsible for the generation of $[Ca^{2+}]_{cyt}$ signals or patterns, the Ca^{2+} signaling system also consists of large number of sensory proteins, performing different functions, including the control of Ca^{2+} homeostasis.

Generation of Ca^{2+} signals. The generation of defined patterns of $[Ca^{2+}]_{cyt}$ changes, which encode the specific information about the character and the strength of the external stimulus is the result of coordinated activity of Ca^{2+}-translocating proteins in the plasma membrane and endomembranes of guard cell. Activation of guard cell plasma membrane and endomembrane Ca^{2+} channels is an initial step in generation of $[Ca^{2+}]_{cyt}$ signal. Plasma membrane Ca^{2+} channels are activated by membrane hyperpolarization (Grabov and Blatt, 1998), a rise in the external concentration of divalent cations (Hamilton et al., 2001), ABA treatment (Grabov and Blatt, 1998; Hamilton et al., 2000) and H_2O_2 application (Pei et al., 2000). The activity of plasma membrane voltage-gated Ca^{2+}-channels is also subjected to regulation with proteinphosphatases I and II (Köhler and Blatt, 2002).

The vacuolar membrane and membranes of other intracellular compartments in guard cells (endoplasmic reticulum, Golgi apparatus, mitochondria's and chloroplasts) possess a number of ligand-activated Ca^{2+}-permeable channels which are also likely to participate in generation of $[Ca^{2+}]_{cyt}$ signals. In *Commelina communis* guard cells $[Ca^{2+}]_{cyt}$ rises could be induced by photorelease of conjugated IP_3, previously microinjected into the cytoplasm (Gilroy et al., 1990). Release of Ca^{2+} from isolated plant vacuoles upon IP_3 and cADPR application have also been reported (Allen et al., 1995; Leckie et al., 1998). In addition, sphingosine-1-phosphate (S1P) was shown to be able to induce Ca^{2+} release from guard cell vacu-

oles. Application of S1P induced oscillations of $[Ca^{2+}]_{cyt}$ in *Commelina communis* guard cells (Ng et al., 2001), with an amplitude and shape that were dependent on the S1P concentration (section 1.4.4). A metabolite of NADP, nicotinic acid adenine dinucleotide phosphate (NAADP) induced mobilization of Ca^{2+} from endoplasmic reticulum fractions, derived from red beet and cauliflower tissues (Navazio et al., 2000). Release of Ca^{2+} from endomembrane fractions of *Vicia faba* guard cells were registered also upon IP_6 application (Lemtiri-Clieh et al., 2003).

Characterization of Ca^{2+} signals. A considerable number of experimental studies have been devoted on the relation between $[Ca^{2+}]_{cyt}$ behavior and the stomatal aperture changes. Many stimuli reported to be capable of inducing $[Ca^{2+}]_{cyt}$ rises in guard cells of higher plants, including ABA treatment (Allen et al., 1999a; Staxen et al., 1999), application of high external Ca^{2+} (McAinsh et al., 1995), rise of CO_2 concentration (Webb et al., 1996), introduction of organic elicitors (Klusener et al., 2002) and the temperature changes (Allen et al., 2000, Wood et al., 2000). The shape of of $[Ca^{2+}]_{cyt}$ curves triggered –by different stimuli was marked by symmetrical or asymmetrical oscillations, or could represent a single $[Ca^{2+}]_{cyt}$ transient.

Elevation of the external Ca^{2+} concentration is a well studied stimulus, that can induce $[Ca^{2+}]_{cyt}$ responses in guard cells. In guard cells of *Commelina communis* microinjected with fluorescent probe Fura-2, application of 0.1 mM Ca^{2+} induced symmetrical $[Ca^{2+}]_{cyt}$ oscillations with an average amplitude 430 nM and period of 8.3 minutes. A further increase of the external Ca^{2+} concentration to 1 mM changed the shape of the $[Ca^{2+}]_{cyt}$ signal, the oscillations became asymmetric, the the amplitude rose to 625 – 850 nM and the average period increased to 13.6 minutes (McAinsh et al., 1995). External Ca^{2+} also induces $[Ca^{2+}]_{cyt}$ oscillations in *Arabidopsis* guard cells. In guard cells acid-loaded with Fura-2, increasing the external Ca^{2+} concentration from 50 μM to 1 mM induced $[Ca^{2+}]_{cyt}$ oscillations with amplitude ~ 60 nM and period of 5.8 min. Further increasing the Ca^{2+} concentration from 50 μM to 10 mM lead to generation of $[Ca^{2+}]_{cyt}$ oscillations with the amplitude 120 nM and period of 6.7 minutes (Allen et al., 1995). Registrations of Ca^{2+} responses in *Arabidopsis* guard cells, expressing Ca^{2+}-reporting protein cameleon (Allen et al., 1999b) also showed the induction of oscillate $[Ca^{2+}]_{cyt}$ behavior in response to the increasing external Ca^{2+} concentration. Increasing Ca^{2+} in the perfusion buffer from 0 to 1 mM induced $[Ca^{2+}]_{cyt}$ oscillation with the amplitude of 160 nM and the period of 2.6 min, upon increasing Ca^{2+} concentration to 10 mM the amplitude of oscillations increased to ~1020 nM and had a period of 6.6 minutes.

Later in *Arabidopsis* guard cells were characterized Ca^{2+}-sensory protein CAS and has been proposed the model, supposing involvement of IP_3-dependent signal transduction and intracellular Ca^{2+} stores participation in generation of $[Ca^{2+}]_{cyt}$ oscillations in guard cells (Han et al., 2003). The gene for CAS has several homologues in other plant species, but showed no similarity with any animal genes. showed strong plasma membrane localization and presented in shoot tissues including guard cells. The CAS receptor proposed to carry function of low affinity high capacity Ca^{2+} binding with Kd of ~ 1.5 mM. Interestingly, the signal from CAS probably transduces in the cytoplasm via IP_3-dependent mechanism as inhibitor of phospholipase C neomycin abolished external Ca^{2+}-induced elevations of $[Ca^{2+}]_{cyt}$ in *Arabidopsis* guard cells. Analysis of the antisense-expressing plants showed also reduced Ca^{2+}- but not ABA-induced stomatal closure and impaired bolting upon Ca^{2+} deficiency, indicating important role of the Ca^{2+}-receptor protein in plant vital activity and development (Han et al., 2003).

A large number of experimental studies describe the generation of $[Ca^{2+}]_{cyt}$ signals induced by ABA. The role of $[Ca^{2+}]_{cyt}$ in the transduction of the ABA signal was based on early experimental observations (DeSilva et al., 1985a). These studies revealed that ABA and external Ca^{2+} inhibit stomatal opening in epidermal strips of *Commelina communis*, in a synergistically manner, whereas Ca^{2+} channel blockers have the opposite effect (DeSilva et al., 1985b).

Later studies could show that ABA triggers asymmetrical oscillations of $[Ca^{2+}]_{cyt}$, in guard cells of *C. communis* injected with Fura-2. The ABA induced oscillations started with a delay of 1 – 15 minutes and were characterized by signal parameters that remain stable over the whole period of stimulus presence, up to 3 hours. The period of $[Ca^{2+}]_{cyt}$ oscillations, induced by abscisic acid in a concentration of 10 nM and 1 μM were 11 and 18 minutes. The amplitude of the responses was 200 – 600 nM and did not show an obvious dependence on the hormone concentration (Staxen et al., 1999).

Changes in $[Ca^{2+}]_{cyt}$, triggered by ABA treatment in *Arabidopsis* guard cells of different ecotypes (Col, Ler, WS) were characterized in a number of experimental studies, published by a research group of J. Schroeder (Allen et al., 2001, 2002; Hugouvieux et al., 2001; Jung et al., 2002; Klusener et al., 2002; Kwak et al., 2002, 2003). In these studies the $[Ca^{2+}]_{cyt}$ level was determined as a ratio between the emission signals obtained at two wavelengths of the Ca^{2+}-reporting protein cameleon (Allen et al., 1999b). In the presence of ABA, *Arabidopsis* guard cells showed regular oscillations of$[Ca^{2+}]_{cyt}$ of 500 nM amplitude with a period of ~ 7.8 minutes, or spontaneous Ca^{2+} spikes with no periodicity. These spontaneous

oscillations were altered in the presence of ABA. Interestingly, the repetitive $[Ca^{2+}]_{cyt}$ changes observed in the presence of ABA differ between *Arabidopsis* epidermal fragments loaded with the fluorescent probe Fura-2 and those recorded with the Ca^{2+}-reporter cameleon. Loaded with Fura-2 guard cells only displayed a single transient increase of $[Ca^{2+}]_{cyt}$, or permanent increase in $[Ca^{2+}]_{cyt}$ up to 0.8 – 1 µM (Allen et al., 1999a).

Decoding Ca²⁺ signals. One of the most intriguing questions regarding Ca^{2+} signaling is, how signal specificity can be achieved. How can changes in the concentration of a single non-protein molecule forward a variety of intracellular signals, which lead to completely different cell reactions. The main point of view, accepted in plant biology was in adopted from the animal cell physiology and assumes spatiotemporal principle for coding of $[Ca^{2+}]_{cyt}$ (Sanders et al., 1999; Harper, 2001; Evans et al., 2001). Experimental studies on animal cells have shown, that specific spatio-temporal patterns of $[Ca^{2+}]_{cyt}$ changes encodes the information about the character and the strength of the cell response. Induction of artificial $[Ca^{2+}]_{cyt}$ spikes of varying frequency and amplitude in human lymphocytes lead to change in the gene expression level and activation of different transcription factors (Dolmetsch et al., 1997, Dolmetsch and Lewis, 1998).

Experimental evidence, supporting the idea of information encoding by the $[Ca^{2+}]_{cyt}$ patterns were presented in experiments on stomatal guard cells of epidermal strips of *Arabidopsis*, carrying *det3* mutation (Allen et al., 2000). Oscillations of $[Ca^{2+}]_{cyt}$ and the stomatal closure, induced by ABA in wild type *Arabidospsis* guard cells by Ca^{2+} and H_2O_2 application were disrupted in *det3* mutant cells. However, the induction of artificial $[Ca^{2+}]_{cyt}$ elevations, similar to those registered in wild-type cells, by repetitive transitions to low-potassium perfusion buffer (the change of K^+ concentration from 100 to 0.1 mM), leading to plasma membrane hyperpolarization, was shown to restore the stomatal closure in epidermal strips of *det3* mutant. Using the same method, it was shown that successive $[Ca^{2+}]_{cyt}$ transients at a defined period were necessary to promote prolonged stomatal closure. The duration of the peiod at which stomata remained closed was dependent on the duration, number and the amplitude of experimentally imposed $[Ca^{2+}]_{cyt}$ spikes (Allen et al., 2001).

The general cell biologic role of $[Ca^{2+}]_{cyt}$ signals is not known yet and still is discussed controversially. For example, responses to ABA seem to be the result of different $[Ca^{2+}]_{cyt}$ patterns, whereas similar patterns of $[Ca^{2+}]_{cyt}$ changes in some cases (e.g. osmotic shock and salt shock induce calcium signatures that are very similar in terms of magnitude, timing and spatial localisation within both the cells and the whole plant) can induce different physiological responses. Finally, cell responses may remain virtually unchanged despite of a sig-

nificant variation in $[Ca^{2+}]_{cyt}$ behavior, as found for the induction of *Fucus* rhizoid or pollen recognition of incompatibility factors. These experimental data could suppose that Ca^{2+} most likely serves as a simple chemical switch, which can initiate a large range of programmed cell responses (Scrase-Field and Knight, 2003).

H⁺-coupled signaling mechanisms. The function of the pH_{cyt} in guard cell physiology has received much less attentions as that of $[Ca^{2+}]_{cyt}$ (Blatt, 2000). Early experiments, conducted with guard cells in epidermal strips of the orchid *Paphiopedilum tonsum*, demonstrated that hormones could induce changes of pH_{cyt}. An increase of pH_{cyt} by 0.05 – 0.3 units was measured upon treatment with 80 μM ABA, whereas kinetin and 50 μM auxin evoked an acidification of the cytoplasm of 0.1 – 0.4 pH units (Irving et al., 1992). A similar ABA evoked cytoplasm alkalization of ~ 0.3 pH units also has been registered with pH-selective microelectrodes in guard cells of *Vicia faba* (Blatt and Armstrong, 1993). Using the same method, auxin was found to acidify the cytoplasm in *Vicia* guard cells, causing downregulation of plasma membrane outward-rectifying potassium channels (Blatt and Thiel, 1994).

Several ion channels were found to be sensitive to cytoplasmic pH changes. The activity of plasma membrane inward-rectifying channels is enhanced at a defined membrane potential by cytoplasmic acidification (Hoshi, 1995; Hoth et al., 1997; Hoth and Hedrich, 1999), whereas that of outward-rectifying K^+ channels is inhibited (Miedema and Assmann, 1996). In addition, the cytoplasmic pH also affects the activity of plasma membrane anion channels (Schulzlessdorf et al., 1996). The effect of altered pH_{cyt} on guard cell ion transport most likely is not restricted to direct manipulation of ion channel proteins, but it also may interfere with signaling components the proteinphosphatase ABI1, which has a pronounced pH-dependency (Leube et al., 1998; Armstrong et al., 1995). Transgenic *Nicotiana benthamiana* plants, expressing a dominant allele of *abi1* showed reduced degree of regulation by ABA of outward- and inward-rectifying K^+ channels (Armstrong et al., 1995).

1.4.4. Second messengers function in guard cells. The generation of Ca^{2+} signals in guard cells in many cases has been related to the activation of ligand-dependent Ca^{2+}-permeable channels. These ligands normally represent small non-protein molecules, with tightly controlled cytoplasmic concentration. Ligands appear and disappear quickly in the cytoplasm as a result of the enzymatic activity, responsible for their synthesis and degradation. Such non-protein factors have been named second messengers. A number of signaling pathways in stomatal guard cells have been suggested to utilize messengers as IP_3, IP_6, PtdOH, NAADP, cADPR, cAMP, cGMP and S1P.

Inositol-3-phosphate (IP_3) is a well-described second messenger in animal cells and it is involved in release of Ca^{2+} from intracellular stores. The synthesis of IP_3 has been related to the activity of phospholipase C, an enzyme that splits phosphatidylinositol-2-phospahte (PIP_2). Early experiments showed that the photorelease of caged IP_3 induced a rise in $[Ca^{2+}]_{cyt}$ that was followed by stomatal closure (Gilroy et al., 1990). Photolysis of caged IP_3 was also shown to inhibit plasma membrane inward-rectifying K^+-channels and activate an instantaneous component of membrane current, most likely mediated by IP_3-induced elevation of $[Ca^{2+}]_{cyt}$ level (Blatt et al., 1990). Analogous to animal signaling pathways it is supposed that IP_3 can participate in an amplification of Ca^{2+} signals by release of Ca^{2+} from the intracellular stores. Indeed, the release of Ca^{2+} from isolated plant vacuoles upon IP_3 treatment could be demonstrated experimentally (Allen et al., 1995).

Several lines of experimental evidence indicate the involvement of IP_3 and phospholipase C in ABA signal transduction. Treatment of guard cell protoplasts with ABA lead to a small increase of the cytoplasmic IP_3 content (Parmar and Brearley, 1995; Lee et al., 1996). The ABA-induced pattern of $[Ca^{2+}]_{cyt}$ oscillation and stomatal close could be inhibited with U73122, a pharmacological inhibitor of phospholipase C (Staxen et al., 1999). However, the degree of inhibition of stomatal closure, induced by U73122 only was 20%, while the complete inhibition of ABA-induced stomatal closure could only be achieved by a combination of U73122 and nicotineamide (Staxén et al., 1999). An inhibitor of cADPR synthesis and the latter results thus suggests a joint action of IP_3 and cADPR in the signaling chain controlling the stomatal aperture (McRobbie, 2000). These experimental data led to a model, in which an first ABA-induced Ca^{2+}-rise activates phospholipase C, which generates IP_3 and in turn causes further release of Ca^{2+} from intracellular stores. Thus phospholipase C, may participate in the magnification of initial Ca^{2+}-signal (Hunt et al., 2003).

In addition to IP_3, a second inositol-phosphate, inositol hexakisphosphate (IP_6), could serve as a second messenger in ABA signal transduction chain. Intracellular IP_6 release after flash photolysis of a caged precursor led to a generation of short period (few seconds duration) Ca^{2+} transients. Furthermore, the release of cytoplasmic IP_6 led to the inhibition of the inward-rectifying K^+ channels, through a Ca^{2+}-dependent mechanism, although IP_6 was 100 times more effective in inhibition of K^+_{in} channels comparing to IP_3. Patch-clamp registrations on whole vacuoles showed that IP_6 could induced a reversible activation of tonoplast Ca^{2+}-permeable channels. (Lemtiri-Clieh et al., 2003).

Phosphatidic acid can be generated by phospholipase D and also may serve as a second messenger in guard cells. Treatment of *Vicia faba* guard cells with abscisic acid led up to

2.5-fold increase of phosphatidic acid level. Application of PtdOH evoked stomatal closure and inactivation of plasma membrane inward-rectifying K^+ channels in *Vicia faba* guard cell protoplasts. PtdOH did not evoke an increase in $[Ca^{2+}]_{cyt}$ application was not observed, suggesting that PtdOH acts via a Ca^{2+} independent pathway of signal transduction (Jacob et al., 1999).

A second messenger that has attracted a special interest of researchers, working on the signal transduction in stomatal guard cells, is cyclic adenosine diphosphoribose (cADPR). Cyclic ADPR is produced from NAD by the activity of ADP-rybosylcyclase, and participates in mobilization of Ca^{2+} from intracellular stores in animal cells, through the activation of Ca^{2+}-permeable channels of endomembranes, known as rhyanodine receptors (Lee, 1997). In vacuoles derived from red beet, the induction of Ca^{2+} currents was found upon application of submicromolar cADPR concentrations (Allen et al., 1995). However, the genome of *Arabidopsis* has not revealed any sequences with similarity to the animal rhyanodine receptors.

Cytoplasmic cADPR microinjection initiated increases of the $[Ca^{2+}]_{cyt}$ in guard cells of *Commelina communis*, which could occur as oscillations with the amplitude ~200 nM and a period of 3.75 minutes. Cyclic ADPR involvement in ABA signaling was demonstrated by the inhibition of ABA-induced stomatal closure with cADPR antagonist 8-NH$_2$-cADPR (Leckie et al., 1998). Path-clamp registrations on whole *Commelina* vacuoles showed cADPR-dependent reversible activation of instantaneously-activating cation currents with high permeability for Ca^{2+} (~20 : 1 as compared with the permeability to K^+). These currents were inhibited by high ($\geq$600 nM) cytoplasmic Ca^{2+} concentrations, which suggests that cADPR are not involved in of Ca^{2+}-induced Ca^{2+} release from guard cell vacuoles (Leckie et al., 1998).

Sphingosin-1-phosphate (S1P) potentially also is a molecule, with second messenger function in stomatal guard cells. Application of 6 μM S1P to guard cells of *C. communis* in epidermal strips evoked oscillations of $[Ca^{2+}]_{cyt}$ level with the amplitude up to 50 nM and a period of 3.8 minutes. A lower S1P concentration of 50 nM lead to an increase in amplitude of the $[Ca^{2+}]_{cyt}$ oscillations to 100 nM and shortening of the period to 2.8 minutes (Ng et al., 2001). This study suggested a role of S1P in ABA signal transduction chain. Abscisic acid activation of guard cell sphingosin kinase was supposed to induce the production of S1P. The interaction of S1P with the yet unknown receptor, then leads to the generation of $[Ca^{2+}]_{cyt}$ signals, which depends on the interaction with the G-α sunbunit encoded by *GPA1* (Coursol et al., 2003).

In addition to the potential signaling molecules mentioned above, other second messengers in plant cells NADP metabolite nicotinic acid adenine dinucleotide phosphate (NAADP), a signaling agent, detected in some marine invertebrates. Nicotinic acid adenine dinucleotide phosphate was shown to trigger efflux of $^{45}Ca^{2+}$ from microsomal fractions of the endoplasmic reticulum, derived from beet roots and cauliflower tissues (Navazio et al., 2000). Calcium release induced by NAADP was insensitive to Ca^{2+}, which implies that NAADP in the magnification of Ca^{2+} signals. The NAADP-dependent $^{45}Ca^{2+}$ release showed a binding constant of was as low as 96 nM. The release of $^{45}Ca^{2+}$ was insensitive to inhibitors of L-type Ca^{2+}-channel blockers, like diltiazem and verapamil as well as and the specific inhibitors of IP_3 and cADPR-dependent Ca^{2+}-mobilizing pathways heparin and 8-NH_2-cADPR.

II. MATERIALS AND METHODS.

2.1 PLANT MATERIAL AND PREPARATIONS

Broad been plants *(Vicia faba* L. cv. Französische Weisskeimige, Gebag, Hannover, Germany) were grown in conditioned box of the cultivation house or in the climatic chamber upon 12h : 12h day : night light cycle and the temperature conditions 22 : 16ºC (day : nigh). For making electrophysiological registrations 4-6 weeks-old plants were selected with undistorted intensive green leafs, without indications of physical damage or presence of insects. For the registrations of the guard cell reactions the first fully expanded leaf of intact plants was used. Measurements were started at the end of dark growing phase (i.e. in the morning), or before start of the measurements plants were specially kept in the darkness for 4-5 hours for assure the stomata to be in a closed state. Electrophysiological registrations on the closed stomata among more high probability of cell ABA response appearance were characterized also with greatly high stability of the registrations and reproducibility of physiological reactions.

The strips of isolated epidermis were preparing 3-4 hours before the start of the measurements and were kept dip into the layer of working buffer in closed Petri dish.

For making the epidermal strips the first or second fully expanded leaf was excised from the adult *Vicia faba* plant. With the use of blunt razor blade a superficial rectangular incision of the epidermis from the lower (abaxial) side of the leaf was made and the strip of epidermal tissue was carefully peeled out under the acute angle from the leaf. Epidermal strips were immediately put on the microscope cover sleep, covered with the thin layer of medical adhesive (Medical adhesive B liquid, Aromando Medizintechnik, Düsseldorf, Germany), slightly pressed with the finger and put dip into working buffer.

Commelina plants Commelina communis (L.) were grown from the seeds in conditioned box of the cultivation house under 16h : 8h day: night lighting cycle. For carring out the measurements second or third fully expanded leaf of adult, not reached the flowering phase plants was selected.

Tobacco plants (*Nicotiana plumbagnifolia*) were grown in conditioned box of the cultivation house upon 12h : 12h day : night lighting cycle. Since immobilization of whole tobacco plants was not possible on the measuring setup, an isolated leaf of 3-4 week old plants were used. Leaves were dip with the petiole into the vessel with working buffer.

2.2 CHEMICALS AND WORKING SOLUTIONS.

Electrophysiological registrations on stomatal guard cells were conducted under continuous perfusion of working buffer (section 2.3). Intact guard cells, located in the leafs of living plants were perfused with a standard measuring buffer, including 5 mM KCl, 0.1 mM $CaCl_2$, 0.1 mM $MgCl_2$ and 5 mM potassium citrate, titrated with TRIS to pH 5.0. Guard cells of isolated epidermal strips were perfused with working buffer, containing 10 mM KCl, 1 mM $CaCl_2$ and 5mM MES/BTP, pH 6.0. The concentrations of K^+ or Ca^{2+} were changing upon the necessity of different ionic conditions creation, where it specially denoted.

All inorganic salts and bases, used in the presented work (KCl, KOH, $CaCl_2$, $MgCl_2$, $BaCl_2$, CsCl, $LaCl_3$) where bought in Sigma.

Signaling agents IP_3, IP_6, cADPR, NAADP were obtained from Sigma.

The calcium chelator BAPTA and proton buffers MES, TRIS and BTP - in Sigma.

Abscisic acid was obtained in Lancaster (Newgate, UK). Methanol was used for the preparation of 100 mM stock solution.

Fluorescent probe FURA-2 (pentapotassium salt, crystal) was obtained from Molecular Probes (Eugene, OR, USA) (1mg package).

2.3 EXPERIMENTAL SETUP.

The experimental setup used for performing the electrophysiological measurements (fig 2-1) consist of the vibration-free table (*1*) with the upright binocular microscope (Axioscop 2FS, Carl Zeiss, Göttingen, Germany) mounted on it (*2*) and the preparation table, located under the microscope (*3*). The preparation table had the possibility of two-dimensional movement of the working plane and was hard mounted on the vibration-free table. The preparation table carry micromanipulator (type 5171, Eppendorf, Hamburg, Germany) with electrical drive (*4,5*). Remote high input resistance buffer preamplifiers (*6*) were fixed in aluminum frames and by use of flexible brackets mounted on the movable bar of micromanipulator. The movable bar of the micromanipulator had a possibility of the slope regulation. The highest success rate of electrophysiological registrations was achieved with the microelectrode position under 58° to the impalement plane.

Microelectrode positioning was performed with the electrically-driven micromanipulator and was controlled by sight under the microscope. Impalement of the microelectrode into guard cells was achieved with piezo translator (P-280.30, Physik Instrumente, Waldbronn, Germany).

For the protection of high resistance input chain of the measuring setup against the electromagnetic pick-up from the surrounding and accidental voltage jumps, all metal parts of the setup were connected together electrically with the cupper wire and enclosed by the star principle on the isolating Faraday cell (*7*), provided with the doors from the front side.
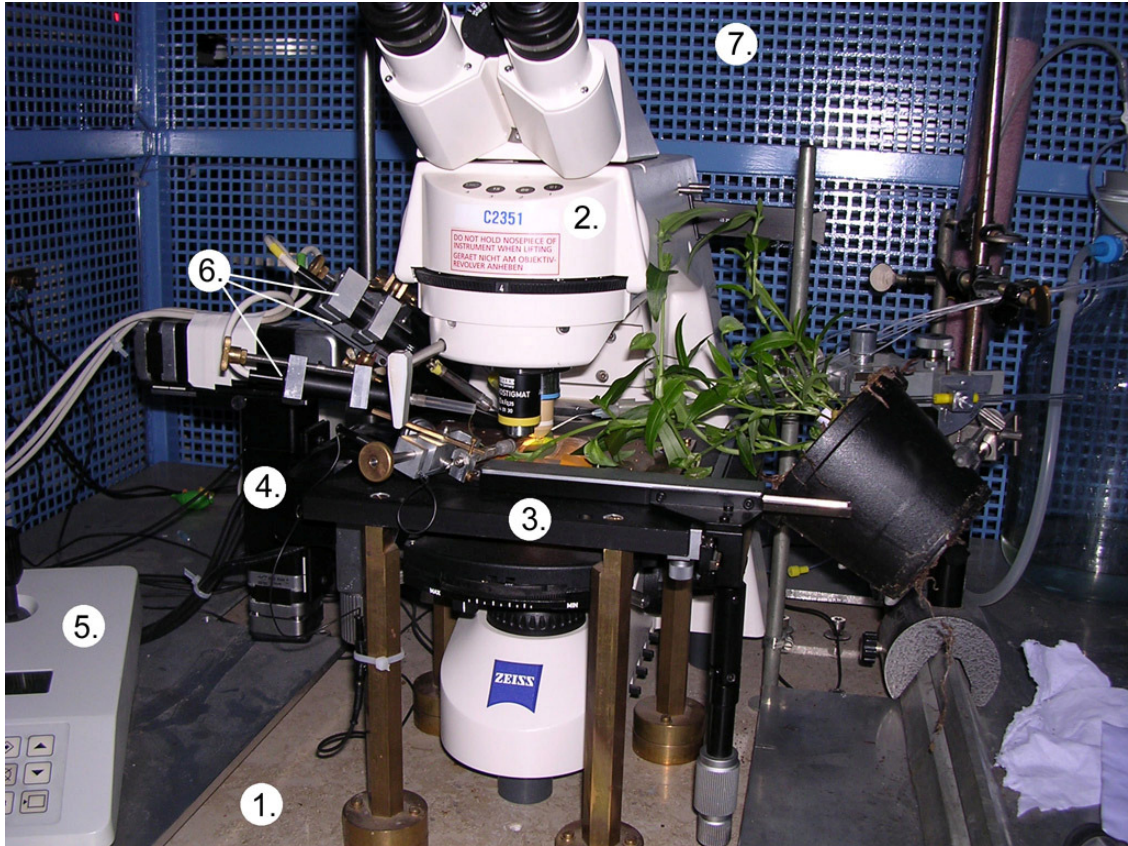

Fig. 2-1 The outer sight of the experimental setup, used for conducting electrophysiological measurements. 1 – vibration-free table; 2 – microscope; 3 – preparation table; 4,5 – micromanipulator and the control unit; 6 – remote buffer preamplifiers; 7 – isolating Faraday's case.

The close view of the working area of the preparation table during the measurement is presented on fig. 2-2. The leaf of an intact plant was fixed with double-sided adhesive tape on top of square plexiglass mount (4 x 4 sm) of cylindrical half-face (*1*) with the adaxial (upper) side in such a way, that lower (abaxial) side was accessible for microelectrode impalement of guard cells.

For illumination of the studying object (region of the leaf of intact plant or the strip of isolated epidermal tissue) the microscope lamp HAL 12V/100W (Carl Zeiss, Göttingen, Germany) was used. Photon density flux was ~500 $\mu M/m^2c$. Most measurements were carried out in darkness, unless it specially indicated, the illumination was only switched on during the impalement procedure. During registrations the cells were visualized with long-distance water-immersed microscope objective Achroplan 40x/0.80W, Carl Zeiss, Jena, Germany (*2*). Manipulations under smaller magnification (bringing of the microelectrode to

the leaf surface and it's positioning over the impalement place) were made by using of an alternative socket of the microscope with the installed long-distance objective Achrostigmat 10x/0.25, Carl Zeiss (*3*).
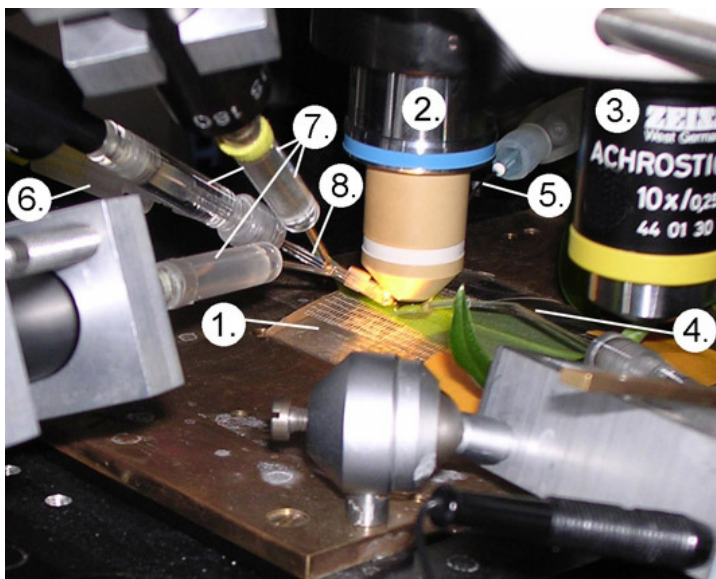

Fig. 2-2. Working area of the preparation table. 1 – plexiglas mount, serving for the intact plant leaf fixation; 2 – water-immersed objective; 3 – long distance 10x objective; 4 – reference electrode; 5 – influx tubing; 6 – suction tubing; 7 – microelectrode holders; 8 – microelectrode.
More details in the text.

The reference electrode (*4*) was made from glass capillary, filled with 300 mM KCl solution and fixed in a plexiglass holder. End of the capillary was interconnected with the short cut of the polyethylene tubing, serving as agarose bridge (300 mM KCl + 1.5% agarose). During measurements the reference electrode was placed into the drop of working buffer, perfused between the water-immersion objective and the leaf surface. Continuous perfusion of the working buffer was implemented via the perfusion system, including influx tubing system (*5*) and the suction tubing (*6*), connected to permanently running electric vacuum pump. Influx were made up from six single-use plastic syringes of 50 ml volume, supplied with valves and connected by thin flexible tubing's (d = 0.8 мм) into a common estuary, ending by the single-use syringe needle. Plastic syringes had a possibility of the regulation of the height of the elevation, used for the control of the flux velocity.

2.4 MICROELECTRODES MANUFACTURE AND USE.

Three types of microelectrodes were used in the presented experimental work: double- and triplebarreled microelectrodes, with the electrical resistance of single barrel filled with 300mM KCl of 70-100 and 100-150 MΩ correspondingly, and also singlebarreled blunt microelectrodes, with electrical resistance of 4-10 MΩ, which were used for measuring of the surface potential, appearing on the cuticle of intact plant leaves (section 3.4.5).

Double- and triplebarreled microelectrodes, used for currying out the experiments in a voltage clamp mode and for the iontophoretical microinjection of organic substrates (section

2.5.3) were produced from standard borosilicate glass capillaries Hilgenberg (Malsfeld, Germany), outer diameter 1.0 mm, inner diameter 0.58 mm. Pulling out of microelectrodes was performed in two stages. On the first stage glass capillaries were put together and fixed in the modified vertical puller (LM3P/A, List Medical Electronic, Darmstadt, Germany), equipped with the calibrated spacer disk. In the case of triplebarreled microelectrodes fabrication the ends of joint together capillaries were fixed together by Parafilm type to avoid of breakage during the pulling manipulations.

Vertical puller was modified in such a way, that lower bar, serving for the fixation of lower capillaries end could freely rotate around it's axis. On the first stage of pulling the capillaries were heated till glass softening, rotated to 360° and cooled. After changing the spacer disk capillaries were heated again and pooled aside for the reduction of the diameter of the section between two future microelectrodes, preparing for rupture. Further the capillaries, prepared for the rupture were transferred into horizontal laser pooler (S2000, Sutter Instrument Co., Novato, CA, USA) for the second, final stage of pulling guaranteeing the required geometry of the microelectrode tip, defined by the specificity of the studied object.

After pooling out, the capillaries with the use of riser blade were liberated from fixing Parafilm tape, side barrels of the microelectrode were heated on the open flame and bend apart for the shaping of the microelectrode to the appropriate spatial configuration (fig. 2-3), necessary for the ready microelectrode installation into the wholes of salt bridges, fixed on the ends of remote buffer preamplifiers.
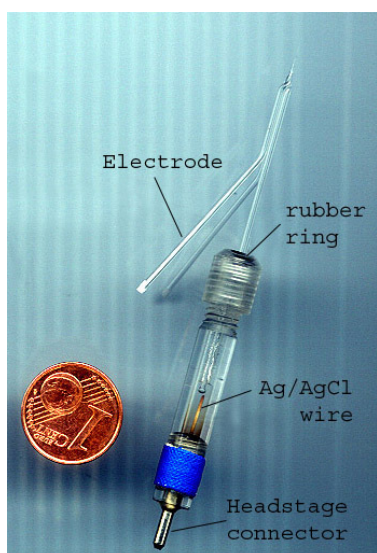

Fig. 2-3. Ready to use triplebarreled microelectrode. Central barrel of the microelectrode tightly fixed in a plexiglass holder by the rubber ring, two remaining barrels are bent apart for giving the appropriate spatial configuration. Back end of the plexiglass holder made represents a metal contact, inserting into the socket of remote buffer preamplifier.

The inner cavity of the holder was filled up with 300 mM KCl solution. Metal contact, serving for the fixation in the socket of the preamplifier connected with non-polarizing half-cell, made from the segment of silver wire, coated with AgCl.

2.5.1. Registrations of electrophysiological parameters of guard cells.

Electrical resistance of the microelectrode barrels before start of the measurements was checked by injection of a current pulse of 1 nA amplitude to each of the barrels and estimation of caused voltage drop.

Insertion of the microelectrode into the guard cell was performed from the inner side of the stoma (fig. 2-4) with use of piezo translator (P-280.30, Physik Instrumente).
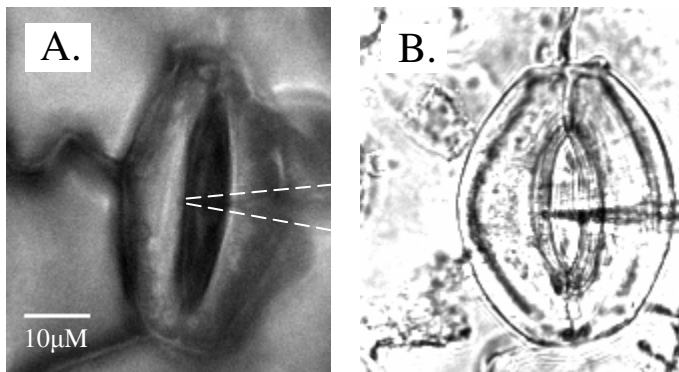

Fig. 2-4. Intact guard cell, localized in the leaf of *Vicia faba* plant (A) and the guard cell, located in isolated epidermal strip (B) impaled with microelectrodes. (In the first case the microelectrode location is emphasized by dashed lines).

Electrophysiological registrations were carried out using of the microelectrode amplifier VF-102 (Bio-Logic, Claix, France). The voltage clamp conditions were provided by using double-electrode differential amplifier CA-100 (Bio-Logic). For the electrical stimulation of the cells and the registration of cell responses served remote buffer preamplifiers HS-180 (Bio-Logic) with the input resistance $\sim 10^{11}\Omega$.

All the electrophysiological data, obtained during the experimental work was sampled in the digital form and stored on hard drive of PC-compatible computer. Before digitization all electrical signals were filtered with 8-pole Bessel filter (type 902, Frequency Devices, Haverhill, MA, USA)

In case of the membrane potential changes or slow membrane current responses registration the signal was filtered at a corner frequency of 12 Hz and digitized with the sampling time of 20 ms (50Hz). In case of quick membrane current responses registration, – upon scanning of membrane conductance characteristics with bipolar staircase voltage protocol (fig. 2-5), or with short voltage ramps, the signals were filtered at 250 Hz corner frequency and digitized with 1 ms sampling time (1kHz). Digitization of electric signals were made with the use of DAC/ADC interface LIH1600 (HEKA Electronics, Lambrecht, Germany) under the control of stationary PC-compatible computer with use of Pulse+Pulse Fit v.8-62 software package (HEKA Electronics). Electrophysiological registrations were stored on

hard drive of the personal computer and analyzed off-line using Pulse software (HEKA Electronics).

The source of potential artifacts during the registrations of membrane potential and conducting the measurements of membrane current in voltage clamp conditions could represent a surface potential, appearing at the leaf cuticle as a result of unequal permeability of inorganic anions, namely Cl^- and K^+ through waxy cuticle layer (Tyree et al., 1990). The causes of the surface potential jumps appearance could be the extreme experimental treatments, for example the cold shock, which evoked quick and massive efflux of K^+ and anions from the mesophyll tissue. As a result during the membrane potential registrations on guard cell plasma membrane an additional error peak could appear up to -70 mV (section 3.4.5).

For the direct registration of the surface electrical potential a blunt singlebarreled microelectrodes filled with 300 mM KCl were used. The microelectrode was inserted into the stomatal cavity and brined into the tight seal with the guard cells wall, thus providing possibility of the electric potential difference registration, appearing between the apoplast and the perfusion buffer. Measured values of surface potential of young illuminated *Vicia faba* leaves were around –4 mV and did not change upon ABA application.

2.5.2. Processing the electrophysiological data.

For determining of the plasma membrane ion channels activity, guard cell plasma membrane was studied under voltage clamp conditions by imposing the bipolar staircase voltage protocol. Starting from the holding potential of – 100 mV, the potential on the guard plasma membrane was stepwise shifting to the range of testing potentials starting from -180 mV and further up to 0 mV with an increase of 20 mV. The duration of testing voltage steps was 2s, interval between voltage steps application was also 2 s. Every such step-like change of the membrane potential value led to a current activation with the kinetics corresponding to the present state of the membrane conductances. The families of such current responses for the whole range of testing potential levels (fig. 2-5) can give the information about the time-course of the different ion channels activity change during the cell responses to different stimuli application (sections 3.2.1, 3.2.2).

Electrophysiological data, stored on the hard drive of PC-compatible computer were analyzed off-line using the Pulse + Pulse Fit v.8-62 software package (HEKA Electronics). For the quantitative analysis of the families of membrane current responses, obtained during bipolar staircase voltage protocol application, the values of instantaneously activating and steady-state currents were exported to get corresponding current-voltage relations (fig. 2-5

A, B). The values of instantaneously activating currents were exported at time range 10-30 ms, ride after fading out the capacitance component of the current, evoked by the change in clamping voltage level. The values of steady-state current were exported from the time interval 1970-1990 s after the start of voltage step, when the time-activated current component have reached the steady level of activation.

Analysis of the families of current traces, obtained during application of voltage step protocols can give the knowledge's about the activity of different ionic conductance's since the difference of time- and voltage dependency of their activation kinetics (sections 1.3.1 – 1.3.3).
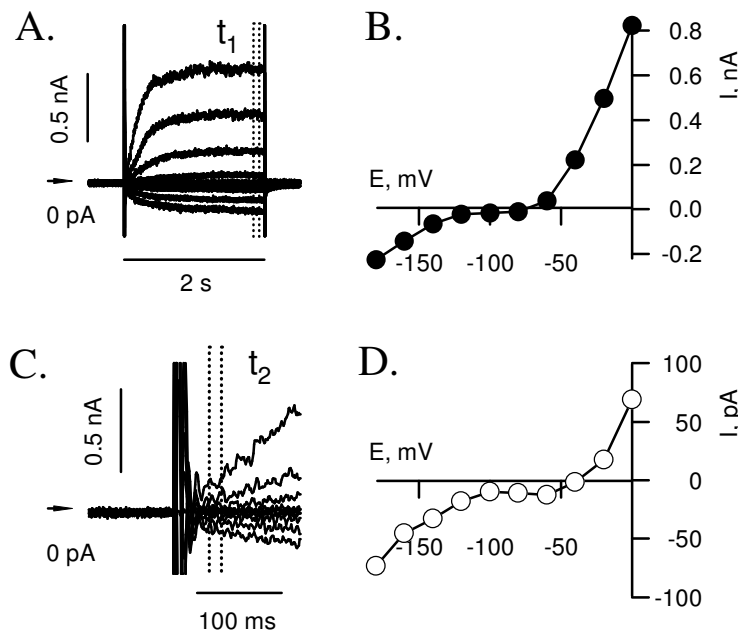

Fig. 2-5. Family of the current traces, obtained during the application of bipolar staircase voltage protocol. (A) Full family of current responses, obtained in -180 – 0 mV voltage range. (B) Values of the time-activated current component plotted against corresponding membrane potential values (an IV-curve). (C) Instantaneous, time-independent values of the membrane current. (D) Values of instantaneously activating current, plotted against corresponding membrane potential values.

Dotted lines on A and C mark the time regions, used for the export of corresponding current components. Arrows indicate 0 current position.

Determination of the time-dependent component of membrane current, which correspond to the activity of inward- and outward-rectifying K^+-selective channels was made by a subtraction of the values of instantaneously activated current from corresponding values of steady-state currents.

For the determination of the relative contribution of R- and S-type anon channels activity in the generation of total anion conductance of the guard cell plasma membrane during the generation of cell responses to ABA application (section 3.2.1) the following equation was used (Kolb et al., 1995) :

$$I_m = (V_m - V_{rev}) \frac{G_{slow} + G_{rapid}}{1 + e^{(\sigma F (V_{half} - V_m)/RT)}} , \qquad (4\text{-}1)$$

where I_m – the membrane current, V_m – potential on the plasma membrane, V_{rev} – reversal potential of the current; G_{slow} – voltage-independent conductance (corresponds to the

activity of S-type anion channels), G_{rapid} – voltage-dependent conductance (corresponds to the activity of R-type anion channels), σ – the charge of gating particle, F –Faraday's constant, V_{half} – the half-maximal activation potential of the current, R – the gas constant, T - temperature. Following assumptions were used for the simulation of the curves: G_{slow} >0; G_{rapid} > 0; -150мВ < V_{half} < -50мВ; 1 < σ < 5. Simulation was done using the program SIGMAPLOT 2000 (SPSS Science, Chicago, IL, USA). For the analysis were selected the curves, which gave the fit regression coefficient not less than 0.9.

2.5.3 Iontophoretical microinjection of organic compounds.

Application of triple-barreled microelectrodes gave the exclusive possibility of iontophoretical microinjection of different organic compounds – ABA, putative cell signaling components (second messengers) or fluorescent probes directly into the cytoplasm of guard cells. Iontophoretical microinjection was achieved via the current application to the loading barrel of the triple-barreled microelectrode, tip-filled with the solution, containing the injecting substrate. The rest of the loading barrel was filled with 300 mM KCl. For ABA loading 0.1 mM water solution was used, for putative second messengers microinjection (IP$_3$, IP$_6$, cADPR, NAADP) – 10 mM water solution were used. Fluorescent probe Fura-2 was used for microinjection as 2 mM water solution.

As all organic compounds, used for microinjection had a state of anion in dissociated form, the loading current had an inward direction (corresponding to anion movement from the barrel of the microelectrode into the cytoplasm). Iontophoretic microinjection were performed in voltage clamp conditions on the plasma membrane, applied to prevent the membrane hyperpolarization upon loading current imposition. Actually the loading current flowed from the loading barrel of the microelectrode to the current barrel, used for the current application, performing the voltage clamp. The amplitude of loading current did not exceed 500 pA, loading time was not more than 60 s, and were determined by the specific case of the treatment.

Distribution of loading substrates over the cell volume occurred probably with the participation of the cytoplasmic streaming (cyclosis). The velocity of the distribution of fluorescent probes BCECF (M_r = 460.4) and Fura-2 (M_r = 936.5) in the cytoplasm of *Vicia faba* guard cells was high and it needed seconds for fluorescence to appear at distant ends of the cell. (see Levchenko et al., 2005 supplementing data[1]).

---

[1]Available at PNAS home page http://www.pnas.org/content/102/11/4203/suppl/DC1

2.6 FLUORESCENT MICROSPECTROSCOPY.

The activity of free Ca^{2+} ions in the cytoplasm of stomatal guard cells was measured by fluorescent microspectroscopy with use of UV-light stimulated double excitation wavelength fluorescent probe Fura-2 (Molecular Probes, Eugene, OR, USA).

For obtaining the fluorescent pictures of guard cells and measuring the fluorescent signals were used intensified charge-coupled device (CCD) camera Cool SNAP-HQ (Ropper Scientific, Tucson, AZ, USA). The schematic representation of the optical setup, used for the excitation of microinjected single guard cells is shown on fig. 2-6. The optical signal, coming from the polychromator failed to the dichroic mirror, reflecting the UV light and directing it to the microscope objective. Fluorescent probe was excited with serial flashes of ultraviolet light of 345 and 390 nm wavelengths, transduced from the polychromator (Visi-Chrome, Visitron Systems GmbH, Puchheim, Germany). Emission signal in the visible region of the light (510 nm), coming from the excitation of Fura-2, microinjected into the cytoplasm of single guard cell further passed the microscope objective, dichroic mirror, was filtered by band-pass filter D510/40 M (Analyzing Technic, Tübingen, Germany) and captured by a CCD camera.
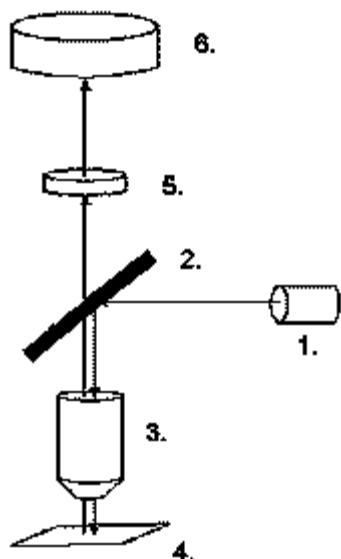

Fig. 2-6. Schematic representation of the optical setup, used for making fluorescent microspectroscopy measurements. (1) optical output of polychromator (2) dichroic mirror (3) water-immersed objective (4) preparation (5) band-pass optical filter (6) optical input of the camera.

The fluorescent camera and the polychromator were controlled by a PC- computer from the Metafluor v 6.2 program (Universal Imaging, Dawnington, PA, USA). Serial flashes of UV light of 345 and 390 nm wavelengths and 200 ms duration were imposed with 1 or 0.5 second interval. Imprinted by the camera images (taking one after another for both

wavelengths with 50 ms interval) were stored as an indexed sequence on PC-compatible computer and further analyzed off-line in Metafluor program (Universal Imaging).

Intracellular loading of the fluorescent probe Fura-2 were performed using the method of iontophoretical microinjection via third (loading) barrel of microelectrode by applying inward-directed electrical current up to –500 pA. After completing the loading procedure, fluorescent signal in both intact guard cells and in guard cells of epidermal strips started to decay exponentially, what strongly reduced the time of registrations (10-20 minutes on the average, fig. 2-7). The process of fluorescent dye loading was controlled visually on the screen of PC-compatible computer and was stopped upon fluorescent signal reached certain level, sufficient for carrying out the measurement.

Dye concentration was estimated by the comparison of fluorescence intensity signal from Fura-2 microinjected guard cells and guard cell protoplasts, loaded by Fura-2 via the diffusion from the patch pipette with known dye concentration. Fura-2 concentration during the registrations both on intact guard cells and guard cells of isolated epidermis din not exceed 100 μM. and measurements were stopped when dye concentration dropped to <10 μM.
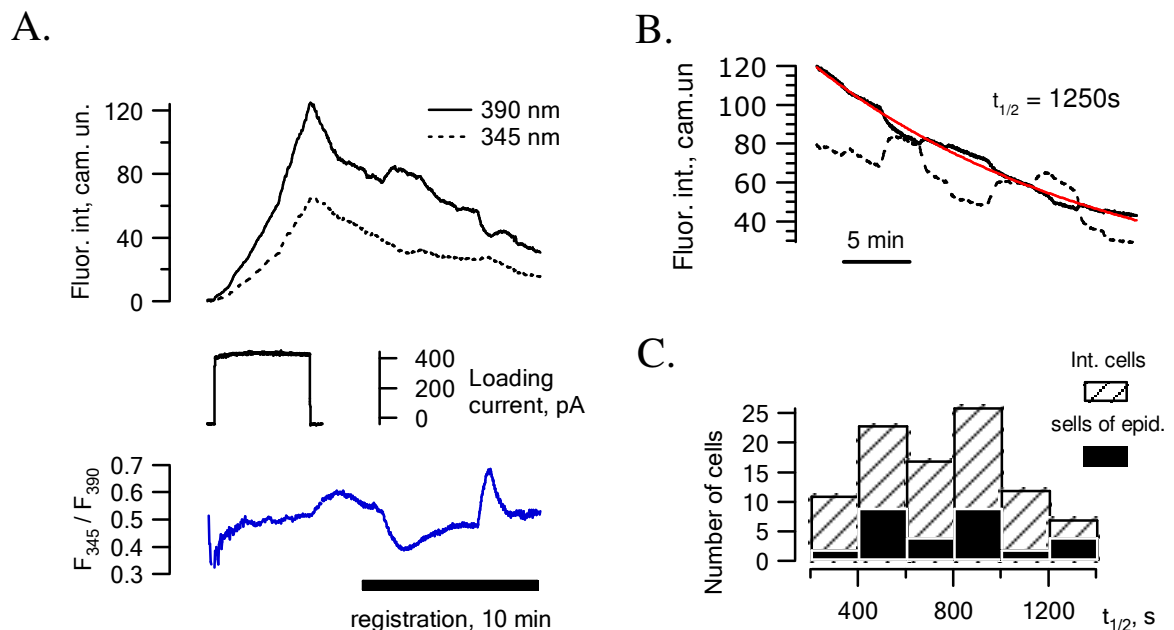

Fig. 2-7. (A) Registration of ratiometric signal from microinjected with fluorescent dye Fura-2 single intact guard cell of *Vicia faba*. Application of loading current (middle trace) led to the increase of the fluorescence intensity (upper pair of traces) and quick stabilization of the ratiometric signal (lower trace). After finishing of the loading current application, the fluorescent signal starts to decay. The time period, in which the registration was performed (reaction of $[Ca^{2+}]_{cyt}$, induced by the membrane depolarization) is marked by black bar under the ratio trace. (B) Characterization of the fluorescence decay in Fura-2 microinjected guard cells. Signal, obtained by stimulation with 345 nm wavelength, recorded during the measurement, carried out on single *Vicia faba* guard cell of isolated epidermis was fitted by the single exponential function for determination of the half-time of the fluorescence decay process (C) The distribution of half-times of the fluorescence decay during measurements, carried out on intact *Vicia* guard cells (n = 113) and of isolated epidermis (n = 34).

In many cases upon reaching the minimum of the fluorescence signal the cell could be loaded by fluorescent dye one or two times more (fig. 2-8), reasoning from the consideration of an expediency of continuing the experiment. From 145 cells examined, 51 cells were loaded with fluorescent probe twice during the experiment, 8 cells – three times, and one cell was uploaded with Fura-2 four times during one measurement.

Fluorescent signal (the stream of 10-bit numbers with the discretization of 1 or 0.5 s for each of two wavelengths) was exported as a value of average fluorescence intensity from three regions – the region of the whole cell, the cytoplasmic region (in most cases corresponding to the center of the cell), where the intensity of the fluorescent signal was maximal, and the background region, representing the part of campaigning non-injected guard cell or neighboring to the microinjected guard cell part of the leaf surface (fig. 2-8).
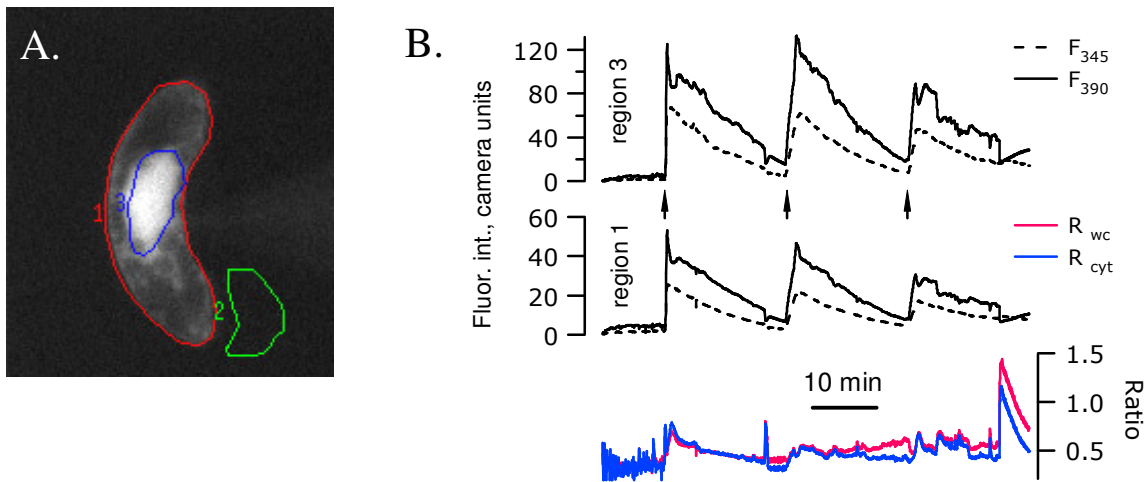

Fig.2-8. (A) Fluorescent photomicrography of a single *Vicia faba* guard cell, located in epidermal strip, loaded with fluorescent dye Fura-2. Color lines outline three regions, used for exporting the values of fluorescent intensity: 1 – the whole cell region, 2 – cytoplasmic region, 3 – background region. (B) Graphical representation of the registration, carried out on the cell, depicted on (A). Upper and middle pairs of traces represent the timecourse of the fluorescence intensity change in the cytoplasmic region and the fluorescent intensity, coming from the whole cell, lower pair of traces represent bahavior of the ratiometric signal in the cytoplasmic region and the signal, coming from whole cell. During the timecourse of the measurement cell was loaded with the dye three times (marked by arrows).

Pure values of intensity of Fura-2 dependent fluorescence were calculated by pairs for each of wavelengths (345nm and 390 nm) by subtracting of the intensity of the fluorescence in the background region (including autofluorescence of guard cell walls and the noise of perceiving crystal of the camera) from the intensities, exported from the whole cell and cytoplasmic regions for each separate image. For the analysis and publication of the data only the intensity values were used, which were exported from the cytoplasmic region of the cell, where the fluorescent probe were equally distributed over the whole depth of the cell (see also below). The distant regions of the cell were characterized with less fluorescence inten-

sity because of the localization of vacuoles, in most cases could be easily distinguished on fluorescent pictures (fig.2-8 A).

The ratiometric signal, expressing Ca^{2+}-dependent behavior of the fluorescent probe excitation, was calculated as a ratio between the pure values of the intensity of probe fluorescence upon excitation with shorter wavelength to the intensity of the probe fluorescence upon excitation with longer wavelength:

$$R_{cyt} = \frac{F_{345(cyt)} - F_{345(bgr)}}{F_{390(cyt)} - F_{390(bgr)}} \quad , \tag{4-2}$$

Excepting the qualitative similarity in the behavior of the ratiometric signal, calculated for two regions, the signal calculated for the cytoplasmic region of the cell were characterized with greater stability during the timecourse of the experiment comparing to the ratiometric signals calculated for the whole cell, which always were tending to rise slowly (fig. 2-8 B) and were selected for the analysis and data publication.

2.7 CALIBRATION OF RATIOMETRIC MEASUREMENTS.

For the calculation of the activity of $[Ca^{2+}]_{cyt}$ from the ratiometric data, obtained during experimental registration with use of Fura-2 were used the standard formula for the calibration of double-wavelength fluorescent dyes (Tsyen et al., 1985; "Fura and Indo Ratiometric Calcium Indicators" information sheet[2]):

$$[Ca^{2+}] = K_d Q \frac{(R - R_{min})}{(R_{max} - R)} \quad , \tag{4-3}$$

where K_d – is a dissociation constant of fluorescent dye, R_{min} and R_{max}, - maximal and minimal values of ratiometric signal, corresponding to ion-saturated and ion-free forms of the probe, Q – coefficient, which expresses the degree of emission signal change upon excitation with longer wavelength between ion-free and ion-saturated forms of the dye (F_{max} / F_{min} for $\lambda = 390$ nm).

For determination of K_d value were performed the procedure of *in vitro* Fura-2 calibration. For this purpose were used standard buffer for Fura-2 calibration #1, containing 1 mM free $[Mg^{2+}]$ (Molecular Probes, Eugene, OR, USA). The fluorescent probe in concentration 2

---

[2] "Fura and Indo Ratiometric Calcium Indicators" information sheet at the Molecular Probes home site, http://probes.invitrogen.com/media/pis/mp01200.pdf

51

μM (corresponding to the "Ca^{2+} calibration buffer kit" information sheet[3]) was added to standard buffer dilutions, containing free [Ca^{2+}] in concentrations from 17 nM to 39 μM. Buffer aliquots of 5 μl volume were placed to the microscope object-plate between two cover sleeps and covered by the third for getting the standard thickness of the fluorescent layer. Further the preparations in turn were placed under the microscope for scanning the spectral characteristics. The scanning was performed in 300 – 430 nm excitation wavelength range with 1nm step (fig. 2-9).

The K_d value, corresponding to the using optical configuration were calculated from the obtained data on probe fluorescence with help of the on-line script, available on-line at the web-site of Molecular Probes[4] company and was 210 nM.
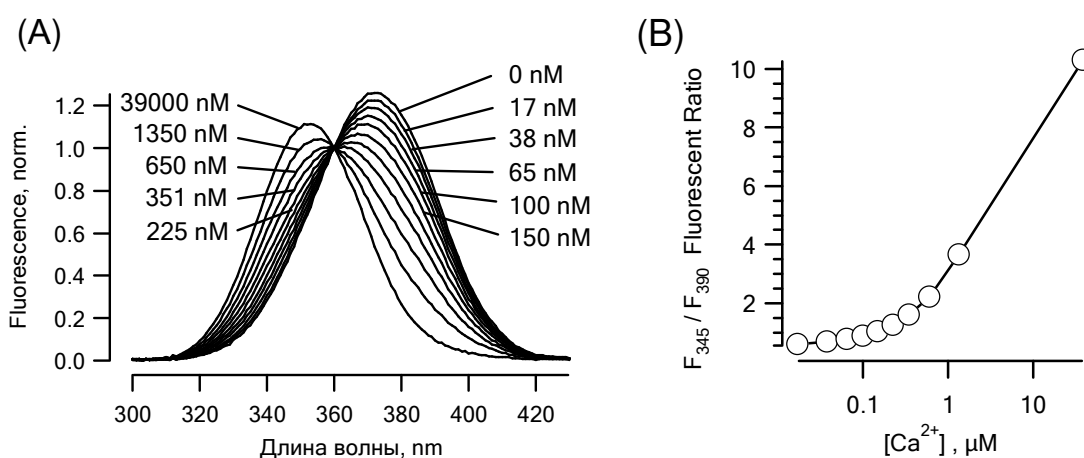

Fig. 2-9. (A) Set of spectral curves, characterizing the emission of Fura-2 upon excitation with UV light in the wavelength range 300 – 430 nm in the presence of [Ca^{2+}] in concentration from 0 nM to 39 μM. Spectral curves were normalized by the isosbestic point of Fura-2 excitation ($\lambda = 360$ nm). (B) The values of fluorescent 345 nm/390nm excitation ratio, plotted against corresponding Ca^{2+} concentrations.

For obtaining of the maximal and minimal ratiometric signal values (R_{max} and R_{min}) and also of the values of maximal and minimal Fura-2 emission upon excitation by longer wavelength (F_{min} and F_{max}), corresponding to real measuring conditions was performed the procedure of *in vivo* Fura-2 calibration. For this purpose to the standard 2 mM Fura-2 solution, used for tip-filling of the microelectrode loading barrel, 50 mM of Ca^{2+}-chelating agent BAPTA was added which lead to the buffering of [Ca^{2+}]$_{cyt}$ level upon it's coming into the cytoplasm. Upon finishing the loading of the cell with the mixture of the fluorescent dye and Ca^{2+} chelator, the holding potential was quickly changed from the standard value of –100 mV to the strongly hyperpolarized values (up to – 0.5 V) for the time period 10 – 20 seconds

---

[3] "Ca^{2+} Calibration Buffer Kit" information sheet at Molecular Probes homesite, available on-line at: http://probes.invitrogen.com/0media/pis/mp03008.pdf

[4] Molecular probes home site, available on-line at: http://probes.invitrogen.com/resources/calc/kd.html

with intension to evoke the events, close to the electrical breakdown of the membrane. As a consequence of such short membrane hyperpolarization a big rise of $[Ca^{2+}]_{cyt}$ level appears, reaching the saturating levels and in most cases coming back to the background level after short time (fig. 2-10).

Experimentally obtained values of R_{min} and R_{max} for intact guard cells were 0.47 ± 0.05 and 3.05 ± 0.29, for guard cells of isolated epidermis – 0.62 ± 0.04 and 6.58 ± 0.78. The F_{min}/F_{max} ratio for 390 nm excitation wavelength (coefficient Q, eq. 4-3) for intact guard cells were determined in range 6.38 ± 1.14; for guard cells located in isolated epidermal strips – 9.61 ± 1.12.
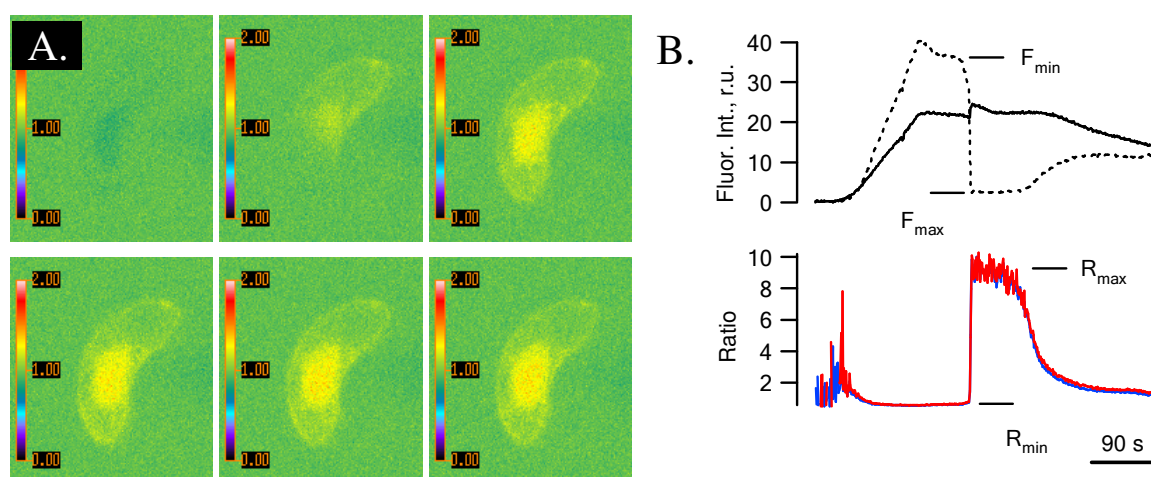

Fig. 2-10. Procedure of *in vivo* Fura-2 calibration. Fluorescent pictures of a single guard cell of isolated epidermis of *Vicia faba*, microinjected with the mixture of fluorescent dye Fura-2 and Ca^{2+}-chelating agent BAPTA. Pictures were made with 0.5 s interval before (1-st picture) and after (all remaining pictures) starting of the hyperpolarizing front, see text. (B) Step like change of the spectral properties of microinjected into the guard cell cytoplasm Fura-2, induced by the application of strong hyperpolarizing voltage front. Upper pair of traces depicts changes of the fluorescence intensity in both wavelengths, lower pair – change of the whole cell ratiometric signal and signal from the cytoplasmic region.

During the combined analysis of all conducted experiments, in particular upon calculating the $[Ca^{2+}]_{cyt}$ values in the experiments with the plasma membrane depolarization in intact guard cells (section 3.4.3) some cells were found with the level of ratiometric signal, coming out of R_{min} values, determined during the *in vivo* calibration. The $[Ca^{2+}]_{cyt}$ represents strongly nonlinear function with the extent of error appearance strongly decreasing by moving from the end points of function definition (which correspond to R_{min} and R_{max} values). Into this region of well-defined values matches background $[Ca^{2+}]_{cyt}$ level and all values of ratiometric signal which correspond to induced calcium signals, normally meaning increase in $[Ca^{2+}]_{cyt}$. This way the difficulties has appeared with the calibration of $[Ca^{2+}]_{cyt}$ values, meaning fall in $[Ca^{2+}]_{cyt}$ level and the corresponding determination of R_{min} value. For this reason as R_{min} parameter during the calibration of spectroscopic measurements, done in in-

tact guard cells was used the minimal value of ratiometric signal, have ever been observed during registrations in guard cells of intact plants, which was equal to 0.2 (see also section 3.4.1).

III. RESULTS.

3.1 ABA-INDUCED STOMATAL CLOSURE AND MEMBRANE POTENTIAL CHANGES.

3.1.1 Response of the stomatal apparatus to ABA application. Stomatal conductance changes in response to the application of abscisic acid were recorded with the use of infrared gas analysis. A leaf of *Vicia faba* was put with it's the petiole into an Eppendorf tube with water. After obtaining a stable conductance, ABA was added at a concentration of 100 μM, as indicated by the arrow (fig. 3-1). Application of ABA led to stomatal closure, which started after delay of approximately 10 minutes. Stomatal closure continued for 20 min and came to a steady state in which only a small residual conductance remained.
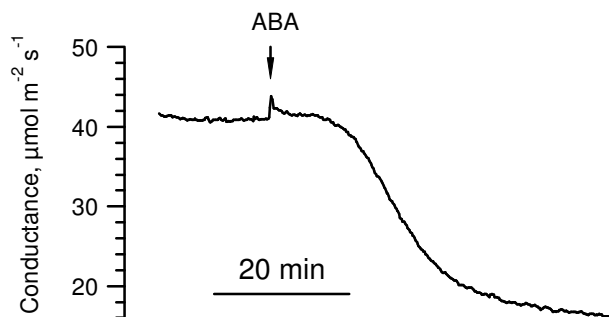

Fig. 3-1. Changes of stomatal conductance of a *Vicia faba* leaf upon 100 μM ABA application.

For registration of electrophysiological responses of guard cells and stomatal movements another method of ABA application was used, as abscisic acid feeding via the petiole requires long lag-time for the stimulus to reach its destination sites and a stimulus wash out is unfeasible. Furthermore, ABA also leads to responses of other cell types within the leaf, causing movement within the fixed tissues and thus loss of impalement (Roelfsema MRG, personal communication).

For the registration of stomatal movements in response to ABA application, the leaf of an intact *Vicia faba* plant was placed under the microscope and fixed with the adaxial side to the plexiglass holder. The abaxial side was continuously perfused with standard working buffer, containing 5 mM KCl, 0.1 mM $CaCl_2$, 0.1 mM $MgCl_2$ and 5 mM potassium citrate pH 5.0. Abscisic acid at a concentration of 10 μM was applied via the diffusion through leaf cuticle from externally perfusing buffer. The solutions with- and without ABA could easily be changed during the experiment by quick switching between two influx pathways. Registrations of stomatal aperture changes were made with use of a Spot Insight Color Camera (Visitron Systems GmbH, Puchheim, Germany). Images of the leaf surface were made automatically with intervals of 2 minutes. The pictures obtained with the camera were stored on hard drive of a PC-compatible computer and analyzed off-line. In each series of meas-

urements the changes in aperture of two or three stomata, localized in the area of the focal plane of microscope were analyzed (fig. 3-2).

From 37 stomata analyzed, 14 were closed after ABA application, while 23 remained stayed open. Based on this heterogeneity in stomatal behavior it can be expected that approximately 30% of guard cells could show a change of the electrical properties at the plasma membrane, upon ABA application.
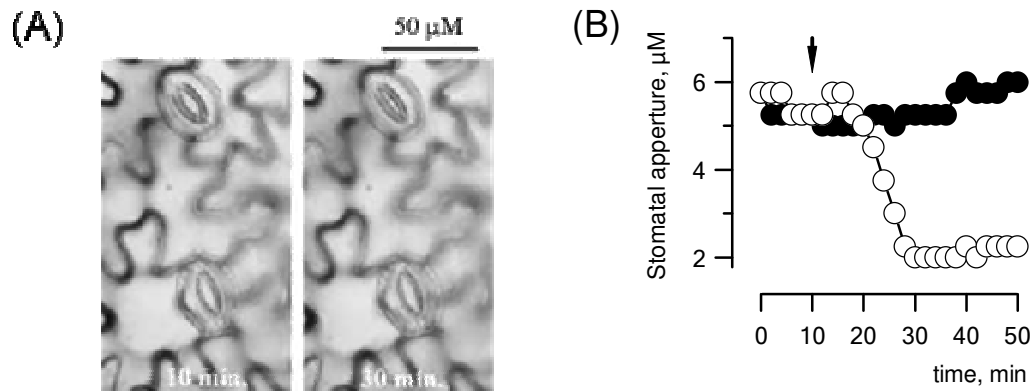

Fig. 3-2. Stomatal closure, induced by 10 μM ABA applied at the leaf surface of an intact *Vicia faba* leaf. (A) Two neighboring guard cells before (left panel) and 20 minutes after (right panel) ABA application. While the upper stoma closed upon ABA treatment, the lower stoma slightly opens within this time period. (B) Graphical representation of the aperture changes of upper (○) and lower (●) stomata shown in (A). The arrow indicates the time point of ABA application (t = 10 min).

3.1.2 ABA-induced membrane potential changes. Changes in the electrical properties of the guard cell plasma membrane, related to ABA-induced stomatal closure, were studied with the use of double-barreled microelectrodes. Experiments were carried out under continuous illumination with white light provided by the microscope lamp.

Following the impalement with double barreled microelectrodes, the membrane potential of guard cells depolarized, thereafter it slowly recovered and in 2-5 min reached a stable value. Basing on the value of the established free running potential guard cells could be divided into two groups. In 71 out of 85 cells, the membrane potential stabilized at a value slightly positive of the K^+-Nernst potential (E_m = -74 ± 1.2 mV) and such cells were classified as "depolarized" according to Roelfsema et al. (2001). The second group of cells (n = 14) displayed a membrane potential negative of the K^+-equilibrium potential (E_m = -112 ± 4.3 mV) and thus were classified as "hyperpolarized" cells.

ABA-induced membrane potential changes were elicited through application of a buffer containing ABA at 10 μM concentration to the leaf surface. Responses of the membrane potential initiated by ABA application could be divided into four groups (fig. 3-3). Approximately half of cells (40 from 75 analyzed) did not show any changes in membrane

potential after ABA application and thus were classified as non-responding cells (fig. 3-3, A). In all other cells typical membrane potential changes were observed in response to hormone application. Cells that were already depolarized before ABA application displayed a further depolarization of the membrane potential after a lag phase of ~2 minutes (fig. 3-3, B). The ABA-induced depolarization showed a peak value 4 - 5 minutes after start of ABA application (fig. 3-3 B). On average, depolarized cells displayed a membrane potential change of 22 ± 10 mV (n = 33). After reaching a peak value, the membrane potential repolarized again and reached a steady state value slightly more positive than the membrane potential before the stimulus application. After washout of the hormone, the membrane potential recovered to the pre-stimulus level in 5-6 minutes. During this period, approximately half of cells switched temporary to hyperpolarized state (fig. 3-3 C).
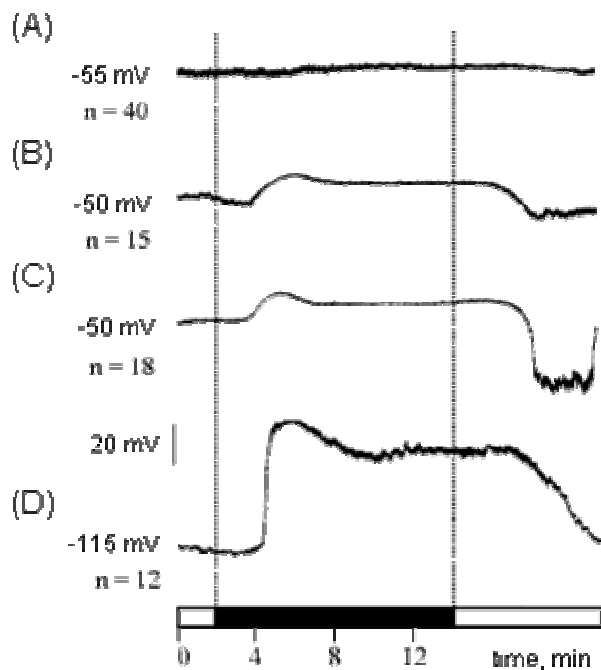

Fig. 3-3. Changes of the membrane potential of intact guard cells of *Vicia faba* plants, induced by 10 μM ABA application (indicated with the black bar below the traces).
(A) Depolarized cells that do not show any membrane potential change. (B) Depolarized cells, displaying a typical response, starting after ~2 min delay with a transient depolarization, followed by a new plateau level of membrane potential that preserves over whole period of ABA presence and followed by a complete recovery of the membrane potential after ABA washout. (C) Depolarized cells with a typical ABA response, but showing hyperpolarization of the plasma membrane after ABA washout. (D) Hyperpolarized cell, returning back to the hyperpolarized state after ABA removal.

Hyperpolarized cells were more likely to respond to ABA, comparing to initially depolarized cells. Out of 14 cells tested 12 displayed a depolarization after hormone application. Furthermore, these cells showed a larger membrane potential changes that had an average peak value of 57 ± 19 mV (n = 12). All initially hyperpolarized cells returned hyperpolarized membrane potentials after washout of ABA (fig. 3-3 D). Despite the difference in the magnitude of depolarization, depolarized and hyperpolarized cells reached comparable peak values of -52 ± 12 mV (n = 33) and -55 ± 12 mV (n = 12), respectively.

3.2 ABA-INDUCED CHANGES OF ION CONDUCTANCE ON GUARD CELL PLASMA MEBRANE.

3.2.1 Anion channels activation. The guard cell plasma membrane was studied under voltage clamp conditions, to explore the changes in the activity of ion transporters that underlie the ABA-induced depolarization. For this purpose cells that depolarized during exposure to ABA were challenged with bipolar staircase voltage clamp protocols (section 2.5.2).
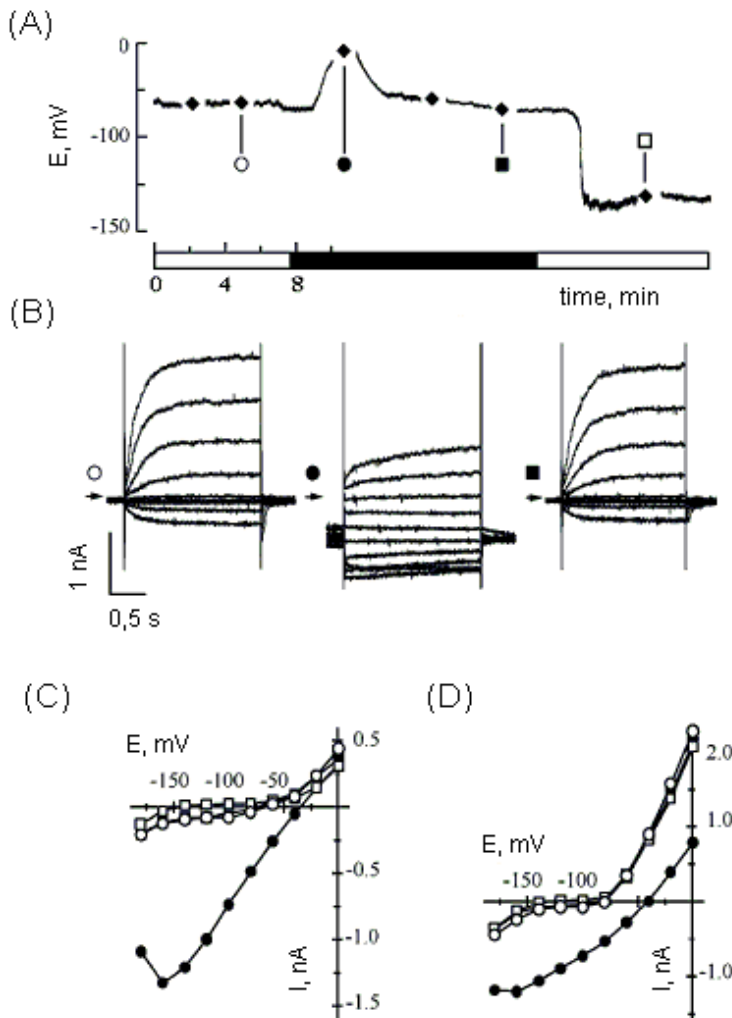

Fig. 3-4. (A) Membrane potential trace of a guard cell depolarizing in the presence of 10 μM ABA (indicated with the black bar below the trace). At time points, depicted in the trace with markers (♦), the amplifier was switched to the voltage-clamp mode and conductance changes were explored through the application of a bipolar staircase voltage protocol. (B) Current traces, obtained before ABA application (○), during the peak of the membrane depolarization (●), by reaching a steady state level of membrane depolarization (■) and after ABA washout (□).

Current voltage relations of instantaneous (C) and time-dependent (D) membrane current components before, during and after ABA application as in (A), markers correspond. Note the activation of an instantaneous current component at the maximum of membrane current activation (●).

The membrane current traces obtained from a single intact *Vicia faba* guard cell before ABA application, during the maximum of depolarization and after reaching the plateau level of depolarization showed significant changes of membrane conductance state during ABA action (fig. 3-4). A typical feature observed during ABA responses manifestation is the stimulation of instantaneously activating conductance during the maximum of membrane depolarization (fig. 3-4 B, middle traces). The instantaneously activating component of the membrane currents was reduced after the membrane potential reached a new stable value, despite of the continuous hormone presence (fig. 3-4 B, left traces). After removal of ABA, the current at -100 mV frequently got positive values (fig. 3-4 C), corresponding to the observed plasma membrane hyperpolarization. The outward current with the reversal potential

at approximately -140 mV may originate from the activity of the guard cell plasma membrane H$^+$-ATPase that possibly becomes activated as a result of hormone wash out (section 4.1.2).

The ABA-stimulated instantaneously activated ion conductance shown in fig. 3-4 B (middle traces) had a virtually linear current-voltage relation (fig 3-4 C) and displayed a time-dependent inactivation at membrane potentials more negative than -100 mV. These features resemble those of S-type anion channels characterized by slow activation and deactivation kinetics (Schroeder and Keller, 1992; section 1.3.2).

In addition to ABA-activation of S–type anion channels, the hormone could also activate channels with characteristics that were similar to those of R-type anion channels, displaying typical rapid activation and deactivation kinetics (Keller et al., 1989; Marten et al., 1995, section 1.3.2). In the recording presented in fig. 3-5, the microelectrode was filled with 300 mM CsCl solution. Using of CsCl in the microelectrode enables blockage of outward-rectifying potassium channels in the plasma membrane. The elimination of K$^+$-selective outward-rectifying channels gave the possibility to determine the activity of R-type anion channels with application of quick ramps of clamping voltage. In the cell displayed in fig. 3-5 ABA induced an inward current that displayed a peak current at -70 mV, typical for R-type anion channels. The reversal potential of membrane current shifted from -30 mV to 20 mV in line with the activation of a conductance for anions. Apparently, ABA can induce the activity of S- as well as R-type anion channels in the plasma membrane of guard cells.
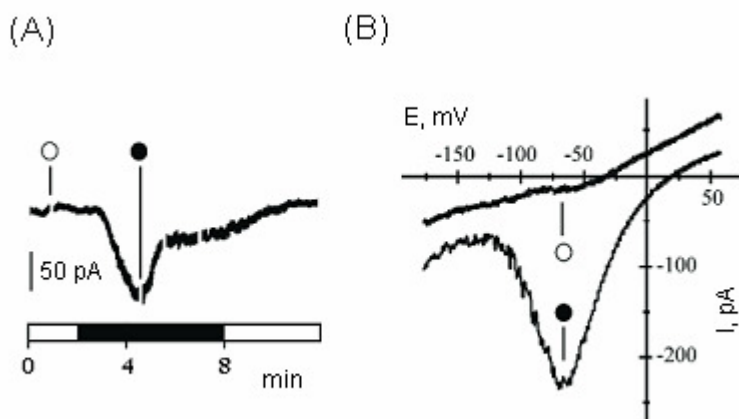

Fig. 3-5. (A) Membrane current response of a single intact *Vicia* guard cell upon application of 10 μM ABA (black bar on the time scale). (B) Current-voltage dependences of plasma membrane conductance obtained before (○) and during the maximum (●) of membrane response, obtained with 1.8 s voltage clamp ramps from -180 to 60 mV.

More negative value of the reversal potential before ABA application may be determined by incompletely blocked plasma membrane outward-rectifying K$^+$ channels and background activity of the plasma membrane H$^+$-ATPase.

In few cells ABA activated predominantly S- or R-type anion channels, according to the current-voltage plots of the instantaneous-activated conductance (fig. 3-6 B, D). In most

cells, however, both channels were activated simultaneously. In search for conditions that would lead to preferential activation of S-or R-type anion channels by ABA, the relative contribution of each channel type in membrane responses generation was determined. For this purpose, current-voltage plots of the instantaneously activated conductance, taken at the maximum of ABA-induced current were fitted as described in section 2.5.2.

The analysis of current-voltage plots revealed a preferential activation of R-type anion channels during responses with large amplitudes, whereas S-type anion channels were the dominating conductance during responses with smaller amplitudes. The amplitude of the cell response was determined as the total increase of anion conductance stimulated by ABA at the peak current. In 24 cells with the amplitude of the response less than 5 nS, slow anion channels were dominating in 18 cells, among cells with the amplitude of anion conductance activation exceeding 5 nS the number of cells with dominating R- (n = 5) and S-type (n = 5) anion conductance was equal (fig. 3-6 E). Interestingly, the relative contribution of R- and S-type anion channels can change also upon consequent transients induction with serial ABA applications in the same cell (Roelfsema et al., 2004).
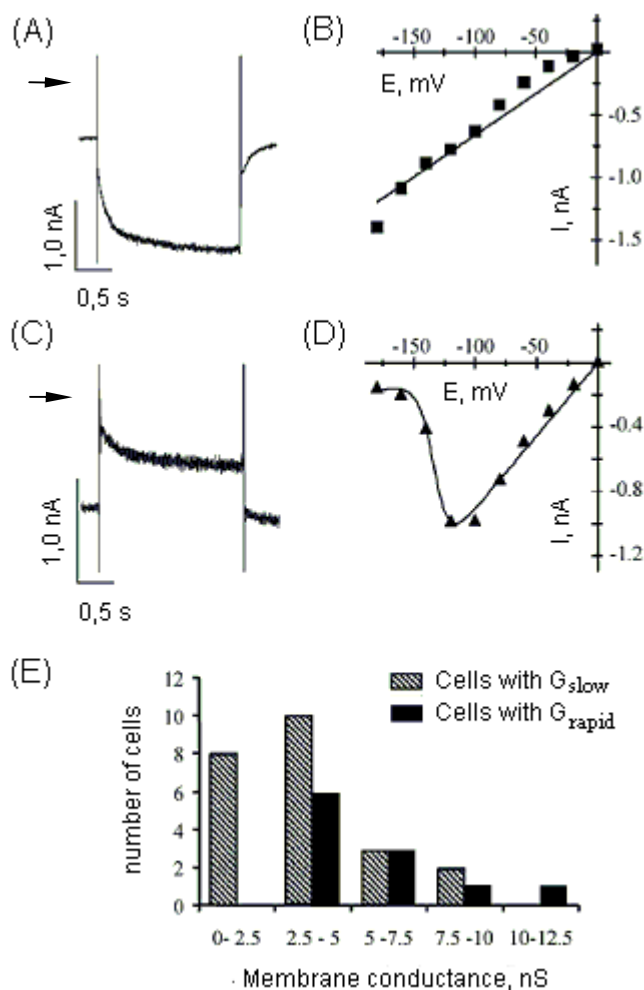

Fig. 3-6. Relative contribution of R- and S-type anion channels in the generation of ABA-induced inward plasma membrane current responses.

(A, C) Inward membrane currents, activated in intact *Vicia faba* guard cells by ABA. The plasma membrane was clamped from a holding potential of -100 to -180 mV for 2s. The activation kinetics resembles S-type (A), and R-type (C) anion channels. *Note*, that the inward current through instantaneously activating channels at -180 mV is smaller than at -100 mV. Arrow indicates 0 nA current value.

(B, D) Current-voltage relation of instantaneously activated conductance, obtained from the same cells as presented on (A and C).

(E) Distribution of guard cell responses with either R- or S-type anion channels as the dominating conductance, in relation to the amplitude of the ABA-activated conductance.

Apart from the relation between the amplitude of the ABA-induced current and the occurrence of one of both types of anion channels, no other obvious correlations with the electrical properties of the guard cells could be observed.

3.2.2. Responses of plasma membrane K⁺-selective channels to ABA. Effects of ABA on K^+-selective channels of guard cell plasma membrane were described in a number of previous experimental publications (Blatt, 1990; Blatt and Armstrong, 1993; Lemtiri-Clieh and MacRobbie, 1994; Shwartz et al., 1994) where the effects were studied in guard cell preparations, including isolated epidermal strips and guard cell protoplasts.

The responses of K^+-channels of intact guard cells to ABA were recorded parallel to the registration of anion channels activity. The membrane conductance was probed with bipolar staircase voltage clamp protocol that was applied at regular time intervals during the guard cell responses to ABA. The activity of K^+-selective channels was determined from the time-dependent components of the membrane current, recorded during bipolar staircase voltage protocol application (section 2.5.2).
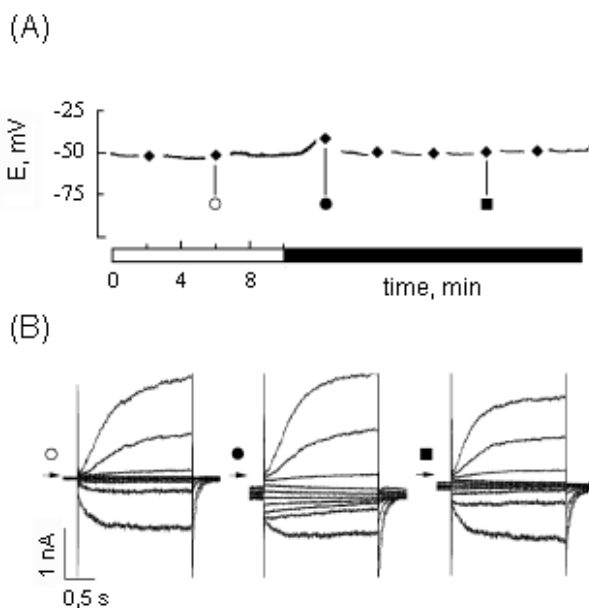

Fig. 3-7. *V. faba* guard cell in which the activity of K^+_{out} channels was not affected by ABA. (A) Membrane potential trace of a guard cell stimulated with ABA (marked by the black bar below the trace on the time scale). Bipolar staircase voltage protocol was applied at time intervals, marked with (♦). (B) Membrane current traces, obtained with a bipolar staircase voltage clamp protocol executed before ABA application (○), at the maximum of membrane depolarization (●) and 9 min after the peak of membrane depolarization (■). In spite of the significant increase of instantaneously activated currents during the maximum of membrane depolarization, the activity of outward rectifying channels remains virtually unchanged.

The effect of ABA on outward-rectifying K^+-channels differed between cells, judged on the activation of anion channels to hormone application. In 14 out of 24 cells ABA evoked an inhibition of currents through K^+_{out} channels, which coincided with the maximum of anion channels activation and membrane depolarization (fig. 3-4 B, D). After the peak of the depolarization, the activity of outward rectifying channels returned to the control level, in spite of the presence of ABA (fig. 3-4 A, B). In the remaining 10 cells (fig. 3-7) the activity

of K$^+$-channels remained virtually unchanged (the amplitude of registered current changes did not exceed 10 %).

The analysis of inward-rectifying potassium channels activity changes could not be performed because of the overlapping of the process of voltage-dependent K$^+_{in}$ channels activation with slow deactivation of S-type anion channels at hyperpolarized membrane potentials (see for example, fig. 3-7 B or 3-4 B, middle traces).

3.3. TIMING OF ABA-INDUCED PLASMA MEMBRANE CURRENTS.

3.3.1 Membrane current transients, induced by extracellular ABA. The kinetic parameters of inward current responses of guard cells plasma membrane triggered by ABA were explored in the continuous voltage clamp mode.

The plasma membrane potential was clamped at –100 mV, since this value corresponds to a state in which outward- and inward-rectifying potassium channels are deactivated (section 1.3.1). Under such conditions, all registered changes of membrane current are likely caused by changes in the activity of plasma membrane anion channels.
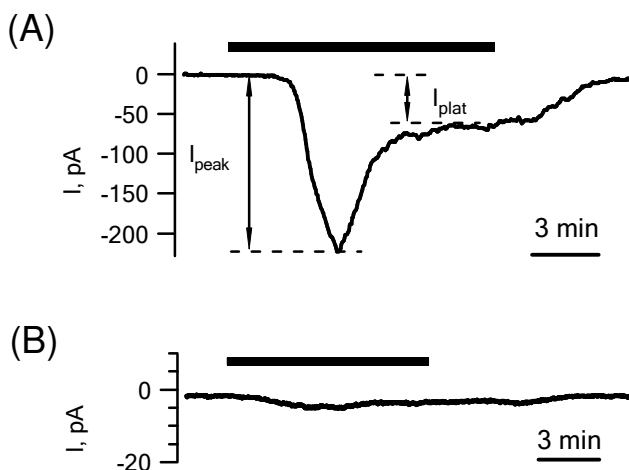

Fig. 3-8. ABA effects on inward membrane current in *V. faba* guard cells. (A) Typically observed activation of anion current across the plasma membrane of intact *Vicia faba* guard cells induced by ABA. (B) Reaction of membrane current, registered in single guard cell of isolated epidermal strip.

In both registrations the membrane potential was clamped at –100 mV, the period of 10 µM ABA application is marked with black bars over current traces.

Abscisic acid at a concentration of 10 µM was added together with the perfusion buffer at the leaf surface to cells that displayed stable membrane currents at control conditions. The guard cell responses started after a delay of ~ 2 minutes with a transient activation of inward current that reached a maximum in next 2 – 3 minutes. After reaching a peak value (I$_{peak}$, fig. 3-8 A), the membrane current declined again to a new stationary level of activation (I$_{plat}$, fig. 3-8 A), located although more negative than the background current level preceding ABA stimulation. Hormone washout led to a complete deactivation of inward current to the prestimulation levels, which occurred in 5 – 6 minutes. The kinetics of membrane current changes thus resembled that of the membrane potential changes evoked by abscisic acid. In line with the membrane potential changes triggered by ABA (section 3.2.2), the membrane

current frequently crossed the 0 pA value after stimulus removal. Such reversion of the membrane current indicates underlying membrane hyperpolarization, and likely comes from plasma membrane proton pump activation.

Membrane current responses in guard cells of intact plants of typical shape could also be elicited with ABA at concentrations less than 1μM (Roelfsema et al., 2004).

Abscisic acid application to guard cells of isolated epidermal strips showed no significant effect on inward current at –100 mV. Two out of six cells tested displayed a little increase of anion current upon ABA application. The profile of the current response was very similar to those observed in guard cells of intact plants, but the amplitude did not exceed 5 pA (fig. 3-8 B).

The described typical ABA response of intact guard cells, with a single transient inward current peak followed by a reduced plateau current, completely deactivating upon stimulus removal, showed high reproducibility excepting the variations in terms of I_{peak} / I_{plat} relation (fig. 3-8 A). Apparent interest could also represent cases of non-typical responses. In few cells ABA evoked an oscillating behavior of membrane current (fig. 3-9). Through out the whole period of experimental work 3 cells were registered, in which ABA triggered such oscillations of membrane current. The period of oscillations varied and was equal to ~ 4 minutes in one cell and ~ 10 minutes in the two other cells. All non-typical responses with oscillating current behavior were also characterized with a bigger delay of ~ 10 minutes.

Fig. 3-9. Non-typical ABA response of intact *Vicia* guard cell appeared as oscillations of the plasma membrane current. Membrane potential was clamped at –100 mV, the period of 10 μM ABA application is marked with black bar.

An interesting feature of intact guard cell responses to ABA application was the possibility of their recurrent induction in the same cell with sequential hormone applications. Full membrane current responses could be reproduced in single guard cell up to 3 – 4 times. Guard cells were able to sense a new portion of ABA already 2 – 3 minutes after recovery from the plateau phase of previous response to ABA.

 The ABA-stimulated current transients in intact guard cells also can be evoked with short-time ABA applications (fig. 3-10). The kinetics of the current responses, stimulated by short ABA pulse showed no difference to those initiated by front of ABA, excepting the absence of the plateau phase of current activation. Instead of coming to a plateau phase, after

passing the peak, the membrane current directly returned to background level, in most cases preceded by a transient overshoot of positive current (fig. 3-10 A). These current values indicate activation of the proton pump and correspond to plasma membrane hyperpolarization, as in case with full ABA response deactivation. Repetitive current transients can be also elicited with sub sequential short-time ABA applications.
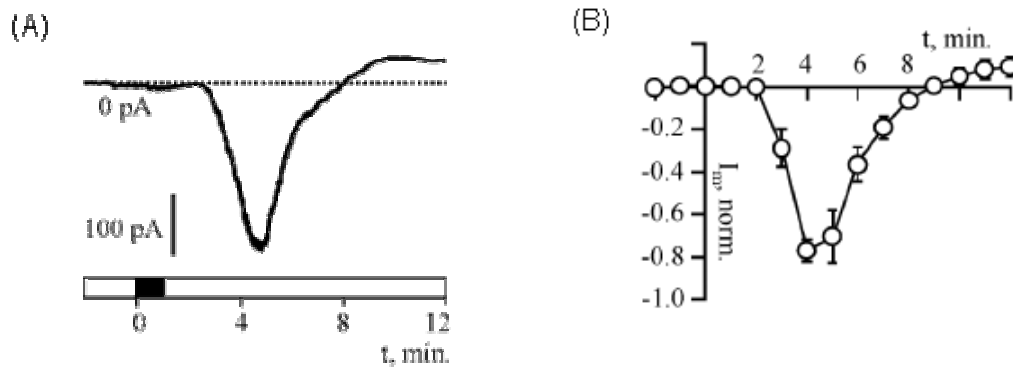

Fig. 3-10. Inward membrane current transients induced in *Vicia* guard cells by short-time ABA applications. (A) Inward current response of single intact a *Vicia faba* guard cell induced by short ABA pulse. A 60s period of ABA application is marked with black bar on the time scale. (B) Averaged kinetics of the membrane responses, induced by short ABA applications, n = 8. Current values were normalized to the maximal amplitude of inward current.

Anion current responses stimulated by ABA, similar to those observed in intact *Vicia faba* guard cells were also recorded in stomatal guard cells of intact *Commelina communis* and tobacco (*Nicotiana plumbagnifolia*) plants (fig. 3-11).

All phases of the anion current responses, induced by ABA in intact guard cells of *Commelina* plants were approximately two times slower compared to the responses of *Vicia faba* guard cells. The delay of the ion current activation took approximately 4 – 5 minutes; the maximal activation of the membrane current was reached 8 – 10 minutes after the beginning of ABA application. Hormone washout also led to the complete deactivation of the membrane current, which was also characterized by slower kinetics compared to the current deactivation in *Vicia* guard cells.

The registration of ABA responses in tobacco guard cells represented big experimental difficulties. In attempts to record any ABA-induced membrane current reaction only one cell was recorded which displayed response with features very similar to those observed in *Vicia faba* (fig. 3-11 B). The membrane current response was recorded upon 100 µM ABA application. The low probability of responses generation most likely was due to a higher extent of gentle tobacco guard cell damaging caused by the impalement procedure, comparing to *Vicia* or *Commelina* guard cells. Later experimental attempts, however, enabled regular

registration of anion current responses to ABA application in *Nicotiana tabacum* cv. SR1 guard cells, similar to those observed in *Vicia faba* guard cells (Marten et al., 2007).
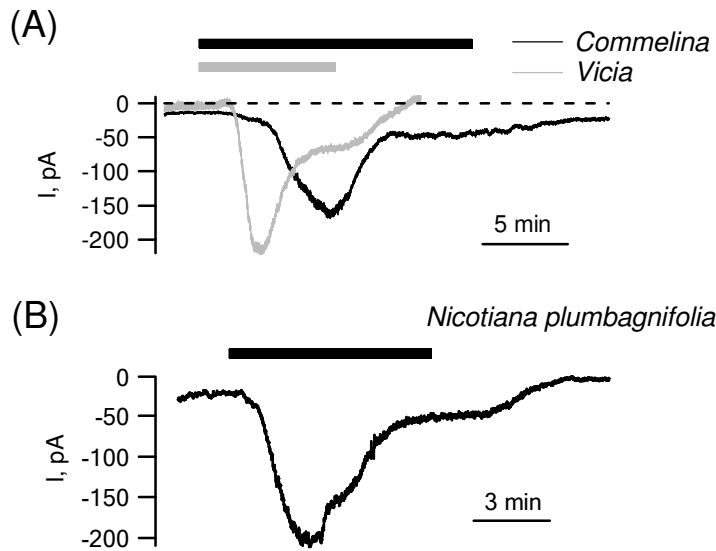

Fig. 3-11. Responses of plasma membrane ion current induced by ABA application in intact guard cells of *Commelina communis* (A) and *Nicotiana plumbagnifolia* (B) plants. A gray trace on (A) depicts typical anion current response, obtained upon 10 μM ABA application in intact *Vicia faba* guard cell.

External ABA concentration, applied to *Commelina* guard cells was 20 μM, membrane response of *Nicotiana* guard cell was obtained with 100 μM ABA application.

3.3.2 Membrane current responses induced by cytosolic microinjection of ABA. For further investigation of open questions about the site of perception of ABA and ABA-induced membrane current initiation, a series of experiments was carried out, in which the hormone was iontophoretically microinjected directly to the cytoplasm of intact guard cells. For this purpose triple-barreled microelectrodes were used (section 2.5.3).

The membrane potential of guard cells was clamped at -100 mV. Microinjection of ABA was achieved by application of negative current pulse to the loading barrel of the microelectrode. The amplitude of loading currents was 0.2 – 0.4 nA, the duration did not exceeded 20 s. The concentration of ABA, filled to the tip of loading barrel of the microelectrode was 0.1 mM.
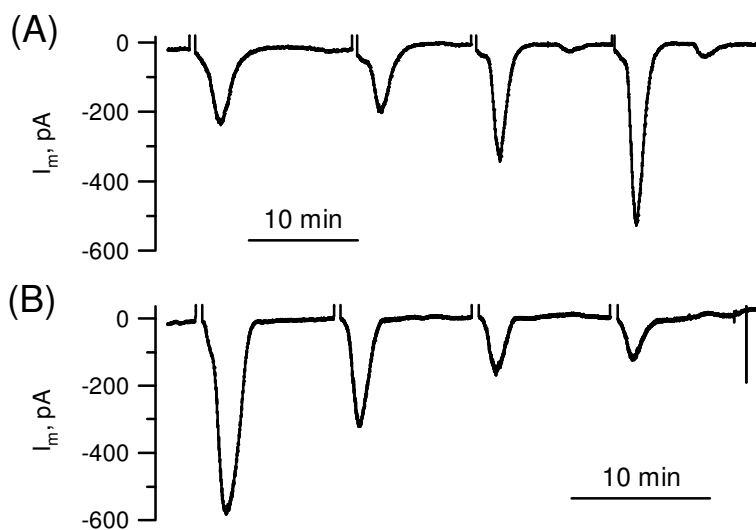

Fig. 3-12. Serial anion current transients initiated in intact *Vicia faba* guard cells by cytoplasmic microinjection of ABA. (A) Example of the registration, where every subsequent microinjection induced cell sentization to ABA. (B) Example of the registration, where every subsequent microinjection evoked desentization of the cell to ABA.

A characteristic feature of guard cell responses induced by cytoplasmic ABA microinjection was absence of the delay in membrane current activation (fig. 3-12), which is typical for the kinetics of guard cell responses triggered by extracellular ABA.

Successive cytoplasmic injections of ABA, like in case of consequent external applications also cause multiple current transients with a reproducible shape. In most registrations consequent cytoplasmic applications of the hormone initiated current transients of nearly the same amplitude, although polar cases of gradual decreasing or increasing of the amplitude were also observed (fig. 3-12). The increase and decrease of ABA responses amplitude by serial ABA applications could point to an existence of possible mechanism of cells sentization and desentization to hormone (section 4.1.4).

3.3.4 Voltage dependence of ABA-induced current responses. ABA-induced current responses, evoked in intact guard cells by ABA were independent of the voltage value, clamped at the plasma membrane. Intact *Vicia* guard cells were able to generate anion current transients upon ABA application even at strongly depolarized membrane potentials.

The anion conductance of *Vicia faba* guard cell plasma membrane was studied in voltage clamp conditions with the double-barreled micro electrodes, filled with 300 mM CsCl for elimination of outward-rectifying potassium currents. The inhibition of voltage-dependent K^+_{out} channels allowed registrations of inward anion currents even at strongly depolarized holding potentials. In the measurement, presented in fig. 3-13 A, three successive current responses, induced by short external ABA pulses were obtained at three different holding potentials at the plasma membrane.
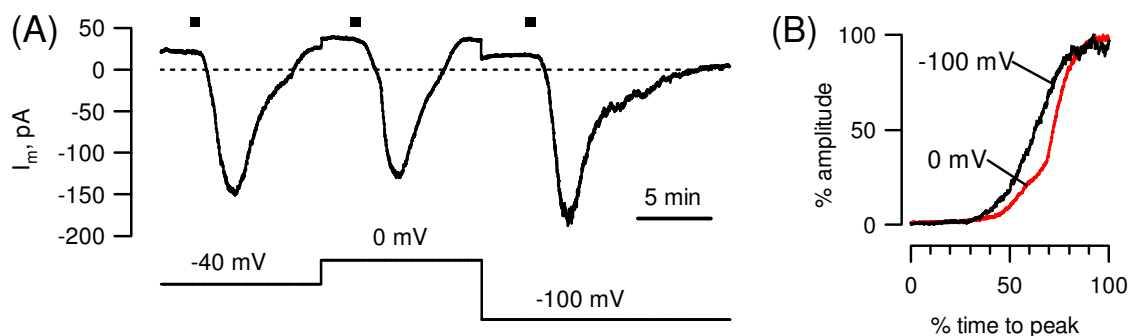
Fig. 3-13. Voltage independence of ABA-induced inward current responses. (A) Successive current transients induced by pulses of external ABA at different holding potentials (lower trace) at the plasma membrane in a single intact guard cell of *Vicia faba*. Periods of short (40s) ABA applications are marked by the black bars above the current trace. (B) Current transients, recorded at 0 and -100 mV (transients 2 and 3 on A). Traces are normalized by the amplitude of the response and the time to maximum. A slowdown of the initial phase of the current activation at 0 mV could be seen.

The ability of guard cells to generate ABA induced anion current transients even at strongly depolarized membrane potentials, likely says that involvement of voltage-dependent Ca^{2+}-selective channels is not necessary point in the signal transduction chain leading to anion channels activation by ABA (sections 1.3.4, 4.2.2).

Even though ABA-induced anion current transients obtained at all membrane potentials tested, small differences could be observed in the shape of the current responses. At depolarized membrane potentials a specific slowdown of the initial phase of membrane current activation was observed (fig. 3-13 B). In some cells the initial phase of anion current activation at depolarized membrane potentials could even get a shape of an additional current peak (fig 3-14).
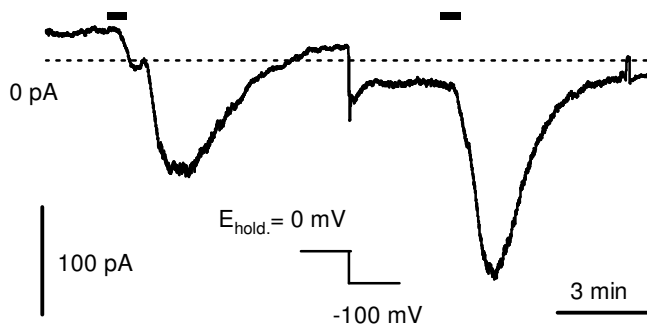

Fig. 3-14 Current transients, induced by 10 µM ABA in a single intact *Vicia* guard cell, recorded at holding potentials of 0 mV and -100 mV. An additional peak of membrane current, appearing at the initial phase of the membrane response could be seen at 0 mV holding potential. Registration was carried out with microelectrode filled with 300 mM CsCl. Pulses of external ABA (40s) are marked with black bars over the current trace.

The initial phase of ABA-induced current transients was further investigated in a series of experiments with fast voltage ramps. During the time course of anion current activation the membrane conductance was scanned with regular voltage ramps ranging from -100 to +60 mV or -180 to +60 mV (fig. 3-15). The duration of ramps was 2 seconds and the interval between ramps applications (18 – 28 s) was chosen to ensure that the time-dependent relaxation of the anion channels was completed before application of the next voltage ramp.

The analysis of these experiments (fig. 3-15) provided information on the dynamics of two parameters; the magnitude of membrane conductance and the reversal potential of the ionic current during the manifestation of plasma membrane responses. For this, the membrane conductance was determined from the slope conductance of current traces ranging ± 10 pA from the zero current value.

After stimulation with ABA, a transient shift of the reversal potential to more depolarized values occurred earlier than the increase in membrane conductance (fig. 3-15 C). The reversal potential shifted from initial value of 19.7 ± 2.6 mV to a peak value of 49 ± 3.2 mV (n=3) and precede maximal activation of membrane conductance for the time 145 ± 15 s. Such anomalous timing of changes in the reversal potential could be explained either by the

activation of additional channels, like potential-independent Ca^{2+}- selective channels, or by an increase in the cytoplasmic anion concentration.
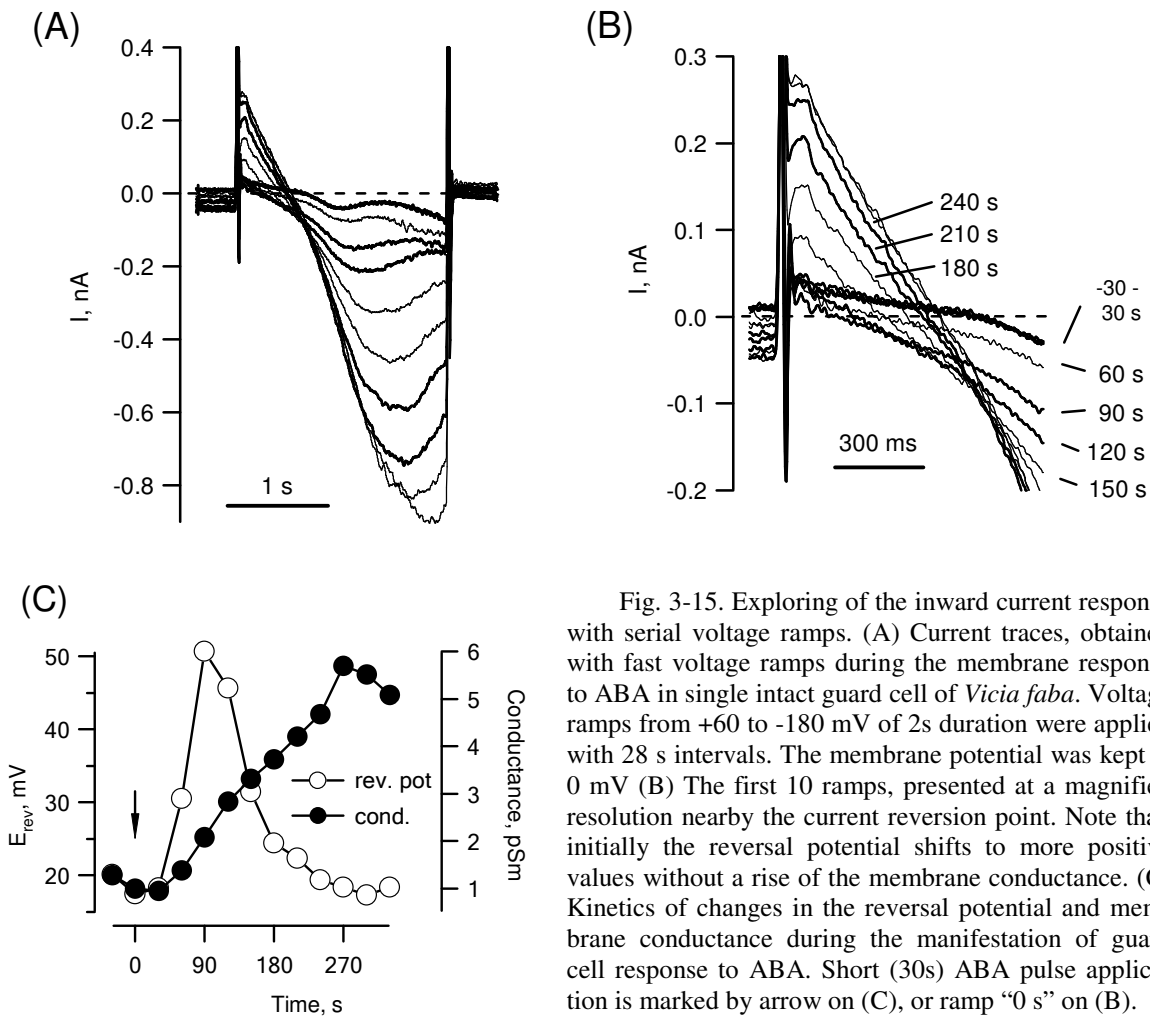

Fig. 3-15. Exploring of the inward current response with serial voltage ramps. (A) Current traces, obtained with fast voltage ramps during the membrane response to ABA in single intact guard cell of *Vicia faba*. Voltage ramps from +60 to -180 mV of 2s duration were applied with 28 s intervals. The membrane potential was kept at 0 mV (B) The first 10 ramps, presented at a magnified resolution nearby the current reversion point. Note that, initially the reversal potential shifts to more positive values without a rise of the membrane conductance. (C) Kinetics of changes in the reversal potential and membrane conductance during the manifestation of guard cell response to ABA. Short (30s) ABA pulse application is marked by arrow on (C), or ramp "0 s" on (B).

The increase in the cytoplasmic anion level presumably could be caused by the initial release of anions from the vacuole and following delayed activation of plasma membrane anion channels, registering as increase of membrane conductance (section 4.2.1).

3.4 STIMULUS INDUCED CHANGES IN GUARD CELL $[CA^{2+}]_{CYT}$.

3.4.1. Fura-2 measurements and calcium homeostasis in V. faba guard cells. After insertion of the microelectrode into guard cell and recovering of the membrane potential, the recording mode was switched to a voltage clamp and cells were microinjected with the fluorescent probe Fura-2 (section 2.5.3).

With the aim of a comparison of $[Ca^{2+}]_{cyt}$ behavior and more detailed investigation of question of cytoplasmic Ca^{2+} level regulation, experiments were carried out on guard cells of intact *Vicia faba* plants, cells of isolated epidermal strips and in guard cell protoplasts. Both intact guard cells and guard cells of in isolated epidermal strips, microinjected with Fura-2

showed cytoplasmic streaming, observed as a continuous cycling of small cytoplasmic parti-cles. The fluorescent dye was equally distributed throughout the cytoplasm except for the distant ends of the cell, with dense inclusion of small vacuoles where the dye was excluded (fig. 2-8 A).

The level of background ratiometric signal, recorded in guard cells of isolated epider-mis was 1.02 ± 0.06. Intact guard cells were characterized with lower level of resting rati-ometric signal of 0.66 ± 0.04 (fig. 3-16 A). The calibrated values of $[Ca^{2+}]_{cyt}$, however, showed a very similar distribution in guard cells of isolated epidermal strips and those in in-tact plants (fig. 3-16 B), except for a higher number of guard cells with increased $[Ca^{2+}]_{cyt}$ in epidermal strips. The average $[Ca^{2+}]_{cyt}$ levels for guard cells of isolated epidermis and intact guard cells were 144 ± 16 (n = 41) and 93 ± 8 nM (n = 100), respectively. The higher degree of variation in resting $[Ca^{2+}]_{cyt}$ of guard cells in epidermal cells likely can be due to the preparation procedure. The sensitivity of guard cells to preparation procedure may differ sig-nificantly in leaves, taken at different physiological states, defined by weather conditions or seasonal changes (own unpublished observation). The Bigger difference in the distribution of the ratiometric signals comparing to the distribution of $[Ca^{2+}]_{cyt}$ levels can be explained by the changes of the excitation ratio as well as emission signals that are likely to occur during cuticle transition in intact guard cells (section 2.7).
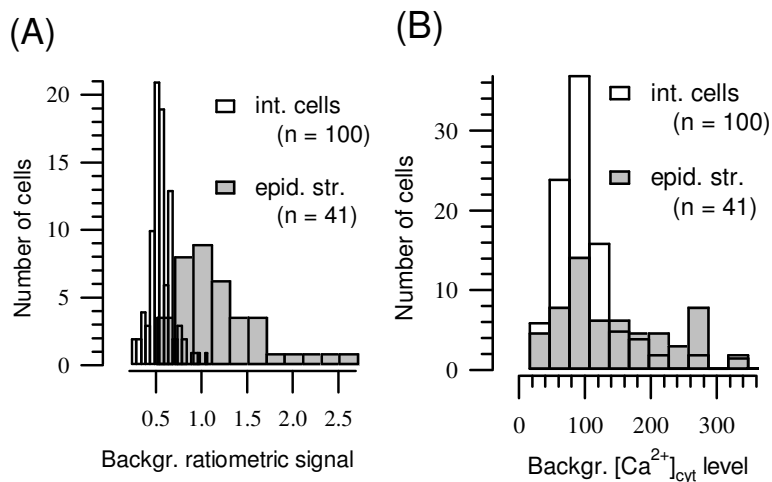
Fig. 3-16. Background $[Ca^{2+}]_{cyt}$ in guard cells of *Vicia faba*. (A) Distribution of the background rati-ometric signals registered at a hold-ing potential of -100 mV in guard cell of intact *Vicia faba* plants and in isolated epidermis (B). Distribu-tion of the calibrated background $[Ca^{2+}]_{cyt}$ levels.

The values were taken as aver-age of 2 min. control level during registrations.

After microinjection of Fura-2, the fluorescent signal slowly decayed in guard cells of intact plants as well as in guard cells of isolated epidermal strips. The half times of the fluo-rescence decay process were similar in both preparations (fig. 2-7 C, section 2.6). This can point that the functioning of the mechanism, performing Fura-2 detoxication or removal from the guard cell cytoplasm is not affected by preparation (Levchenko et al., 2008).

3.4.2. Effect of ABA on [Ca^{2+}]$_{cyt}$. The involvement of Ca^{2+} in the signal transduction of ABA was studied in guard cells of intact plants, which were microinjected with fluorescent dye Fura-2.

Guard cells that were loaded with the fluorescent probe were clamped at a holding potential of -100 mV. The application of abscisic acid at a concentration of 10 µM lead to generation of membrane current responses, which were identical to those of non-injected *Vicia* guard cells (section 3.3.1). In spite of the clear activation of anion current no reproducible changes in the [Ca^{2+}]$_{cyt}$ could be observed in response to stimulation with ABA (fig. 3-17).

The role of the [Ca^{2+}]$_{cyt}$ was further studied with the Ca^{2+} chelator BAPTA. Guard cells first were tested for their ability to respond to ABA, based on anion current activation (fig. 3-17 B). Thereafter, a mixture of 2 mM Fura-2 and 50 mM BAPTA, was microinjected into the cytoplasm. After microinjection procedure, absence of anion current response was observed in any of the six cells measured. In contrast, in six control cells that were only microinjected with Fura-2, five displayed normal ABA-dependent anion current activation (fig. 3-18 A). This result may indicate that a certain physiological resting [Ca^{2+}]$_{cyt}$ level is essential for anion current activation in response to ABA treatment (section 4.2.2).
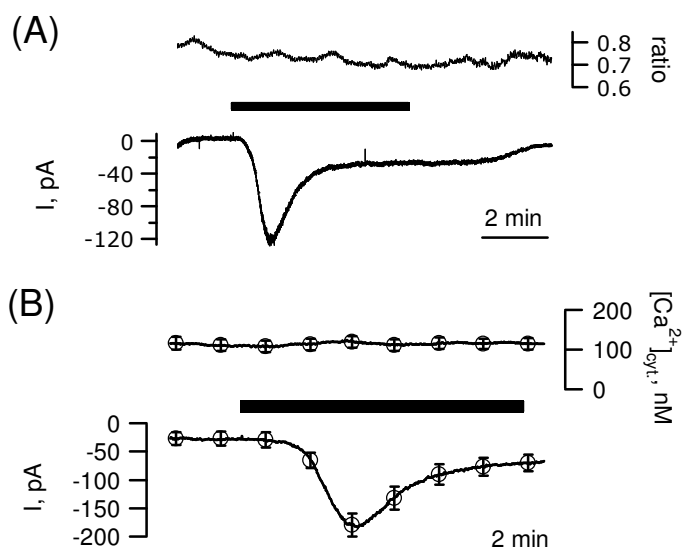
Fig. 3-17 Parallel registrations of membrane current and [Ca^{2+}]$_{cyt}$ reaction, induced with ABA in guard cell. (A) Individual registration conducted on single intact *Vicia faba* guard cell. (B) Averaged data from six measurements identical to presented on (A). Note, that in spite of the significant activation of plasma membrane anion current, no changes in [Ca^{2+}]$_{cyt}$ could be seen. Time of 10µM ABA application is marked with black bar between the traces.

Interesting observation was made in an additional series of experiments, where ABA was applied to guard cells perfused with a standard buffer containing additionally 5 mM Ba^{2+} (fig. 3-18). This resulted in a higher level of registering ratiometric signal of 0.95 (± 0.08, n = 4), as compared to the ratiometric signal, recorded in standard perfusion buffer (0.65 ± 0.048 nM, section 3.4.1).

This can be explained by entering of Ba^{2+} into guard cell and binding to Fura-2, as Ba^{2+} is known to easily permeate plasma membrane Ca^{2+}-channels (section 4.2.2). In guard

cells recorded in the presence of Ba^{2+}, ABA induced a fall of the ratiometric Fura-2 signal (Δ = 0.115, n = 4), along with the membrane current response.

Fig. 3-18. Abolishing of ABA-induced response of *Vicia faba* guard cells, achieved with cytoplasmic microinjection of BAPTA. The first control response to ABA was evoked before- and the second after injection of Fura-2 along (A) or Fura-2 in combination with BAPTA. Co-injection of B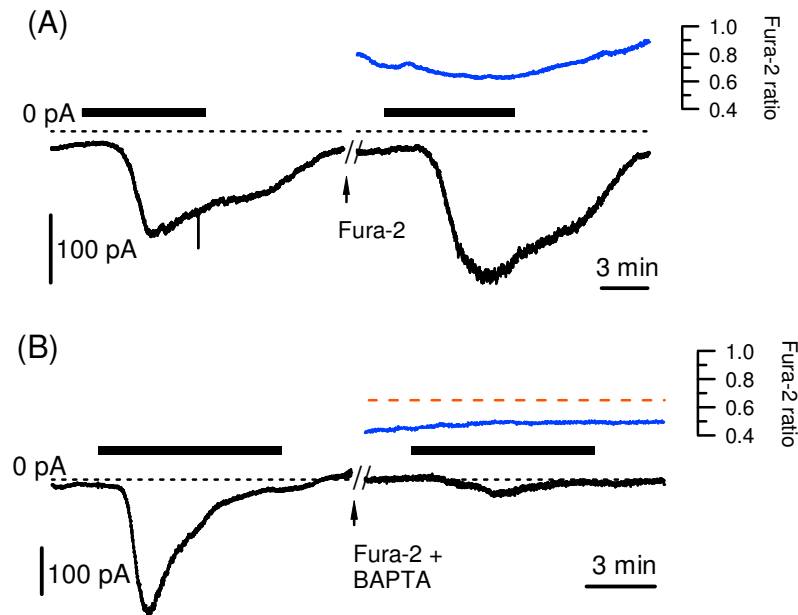APTA reduced the activation of anion current transients generation by guard cells. Red dotted line on (B) indicates average resting level of ratio signal of Fura-2 alone microinjected guard cells. Periods of ABA application are shown with black bars over current traces.

The decrease in ratiometric signal cannot be due to a Ba^{2+} influx into the cytoplasm, since that would cause a rise in the ratiometric signal. More likely, the change in the Fura-2 signal is due to competition with other cations, causing a change of the Fura-2 for binding Ba^{2+} ions. The latter could, for instance, be caused by change in the cytoplasmic pH value, taking into account higher and more labile binding constant of Fura-2 for Ba^{2+} ions (section 4.2.2).
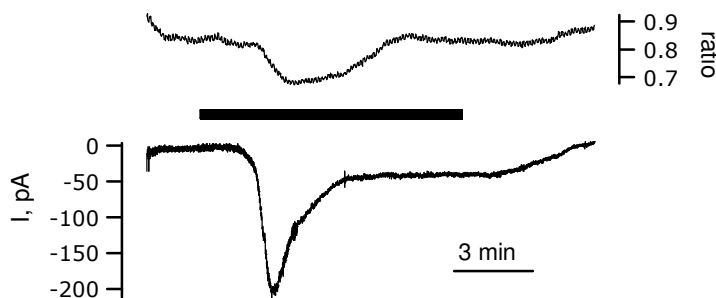
Fig. 3-19. Changes in membrane current and ratiometric Fura-2 signal, evoked with ABA in single intact *Vicia* guard cell. Response was recorded in standard buffer with 5 mM $BaCl_2$.

Application of 10 μM ABA is marked by the black bar over the current trace.

3.4.3 Responses of $[Ca^{2+}]_{cyt}$ induced by membrane potential changes. Several publications suggest that ABA induces transient cytoplasmic Ca^{2+} elevations, through stimulation of hyperpolarization activated non-selective cation channels (Grabov and Blatt, 1998; Hamilton et al., 2000). Since the ability of intact guard cells to generate anion current transients at depolarized potentials likely did not confirm the necessity of hyperpolarization-activated Ca^{2+}-permeable channels for transduction of the ABA signal, further interest represented the

functioning of voltage dependent Ca^{2+}-permebale channels in guard cells. For this reason, $[Ca^{2+}]_{cyt}$ behavior of guard cells in intact *Vicia faba* plants was studied in relation to membrane voltage.

A series of experiments was carried out, in which the membrane potential was stepwise shifted for a period of 5 minutes from resting -100 mV level to depolarized (0 mV) or hyperpolarized (-160 mV) membrane potential values. Hyperpolarization of the plasma membrane from -100 mV to -160 mV evoked a rise in $[Ca^{2+}]_{cyt}$, both in guard cells of intact plants as well as in guard cells of isolated epidermal strips (fig. 3-20). In cells of isolated epidermal strips, the change in $[Ca^{2+}]_{cyt}$ can be described as a single exponential rise, which saturates at a new stationary level (fig. 3-20 C). The amplitude of $[Ca^{2+}]_{cyt}$ increase was ~280 nM, reaching maximal level of 389 ± 46 nM. Unlike to the simple shape of $[Ca^{2+}]_{cyt}$ response of prepared guard cells, the reaction of $[Ca^{2+}]_{cyt}$ in intact guard cells was more complicated and displayed transient increase of $[Ca^{2+}]_{cyt}$ with a peak value of 250 ± 98 nM followed by a decay to a plateau level of 135 ± 52 nM.

Repolarization of the plasma membrane brought $[Ca^{2+}]_{cyt}$ to pre-stimulus levels, both in guard cells of intact plants and guard cells of isolated epidermal strips.

Fig. 3-20. Changes of $[Ca^{2+}]_{cyt}$ level, induced by hyperpolarization of the membrane potential in guard cells. Reactions evoked in single *Vicia faba* guard cells in an epidermal strip (A) and an intact plant (C). (B, D) Corresponding average kinetics of $[Ca^{2+}]_{cyt}$ changes for guard cells (n = 6) in isolated epidermal strips and intact plants (n = 5).

The changes in $[Ca^{2+}]_{cyt}$ eveoked in guard cells by plasma membrane depolarization revealed similar differences between intact guard cells and cells of isolated epidermal strips.

In intact plants, depolarization of the plasma membrane from -100 to 0 mV evoked a transient drop of $[Ca^{2+}]_{cyt}$ that reached a minimum of 13 ± 8 nM. Thereafter, $[Ca^{2+}]_{cyt}$ started to increase again and got to a stationary plateau level at 54 ± 9 nM, located although lower of the resting $[Ca^{2+}]_{cyt}$ level. Repolarization of the membrane potential lead to fast recovery of $[Ca^{2+}]_{cyt}$ to the pre-stimulus value, which was preceded by an overshoot reaching the value 171 ± 22 nM (fig. 3-21 A, B).

In guard cells of isolated epidermal strips a depolarizing voltage step from -100 mV to 0 mV induced a single exponential decrease of $[Ca^{2+}]_{cyt}$ of ~95 nM to a new stationary level of 39 ± 6.8 nM. Like in case of the reaction to hyperpolarizing voltage steps, the newly established level of $[Ca^{2+}]_{cyt}$ remained stable over the whole period of the stimulus presence (fig. 3-20C). Repolarization of the membrane lead to the recovery of $[Ca^{2+}]_{cyt}$, with the same velocity as the initial decrease (fig. 3-21 D).

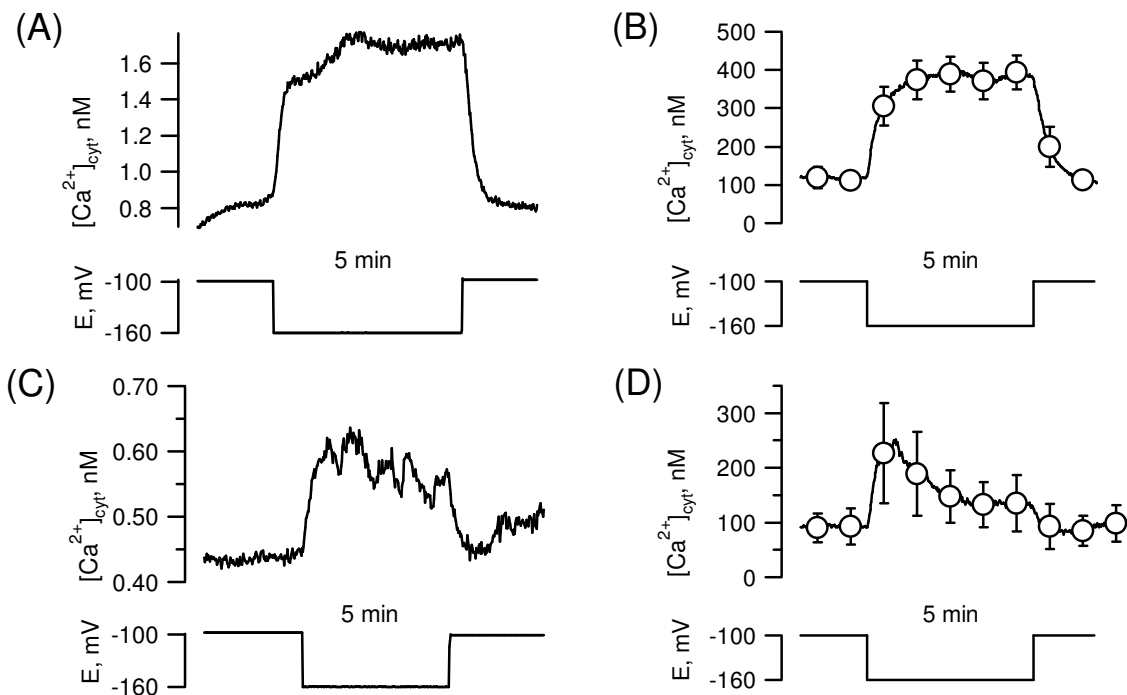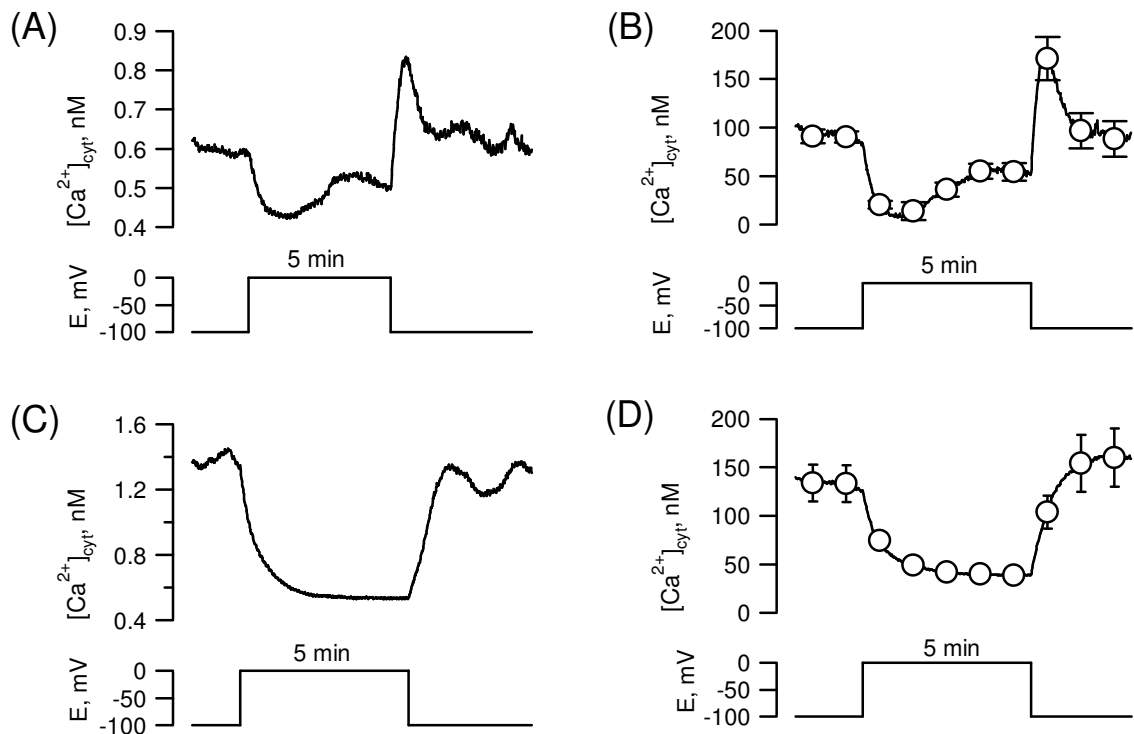Fig. 3-21. Changes of $[Ca^{2+}]_{cyt}$ level, induced by depolarization of the membrane potential in guard cells. Reactions evoked in single *Vicia faba* guard cells in an epidermal strip (A) and an intact plant (C). (B, D) Averaged kinetics of $[Ca^{2+}]_{cyt}$ changes of guard cells in intact plants (n = 8) and guard cells of isolated epidermis (n = 7). Registrations were carried out with microelectrodes, filled with 300 mM CsCl.

3.4.4. Induction of $[Ca^{2+}]_{cyt}$ elevations with short hyperpolarizing pulses. Patch clamp experiments have revealed that plasma membrane anion channels in guard cell protoplasts are activated at elevated $[Ca^{2+}]_{cyt}$ (Schroeder and Hagiwara, 1989). The effect of $[Ca^{2+}]_{cyt}$ was experimentally tested with application of hyperpolarizing pulses with a duration of 1s.
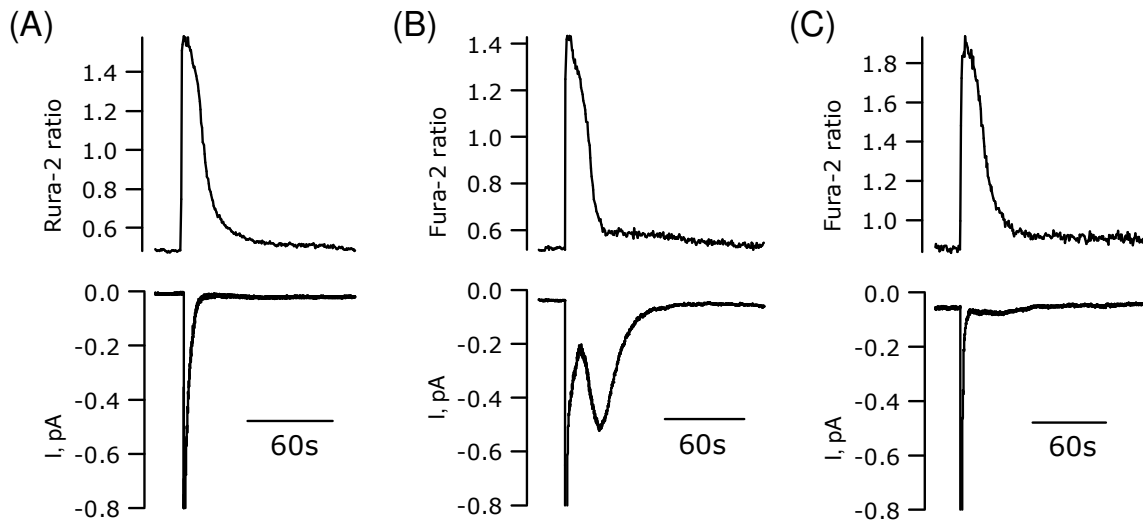
Fig. 3-22. Induction of $[Ca^{2+}]_{cyt}$ elevation with short hyperpolarizing pulses. (A). Changes in $[Ca^{2+}]_{cyt}$ and the membrane current in a single guard cell of *Vicia faba* in an intact plant with single exponential decay of membrane current. (B) As in A, but in the presented cell the decay in current was followed by an additional current peak. (C) Changes in $[Ca^{2+}]_{cyt}$ and the membrane current evoked by a hyperpolarizing pulse in a single *Vicia* guard cell, located in an isolated epidermal strip.

A short-term shift of the clamp potential from -100 to -270 mV led to a massive rise of $[Ca^{2+}]_{cyt}$ and a simultaneous increase of inward current at -100 mV. After returning the clamping voltage to -100 mV, both parameters started to decay again and returned to their initial values (fig. 3-23).
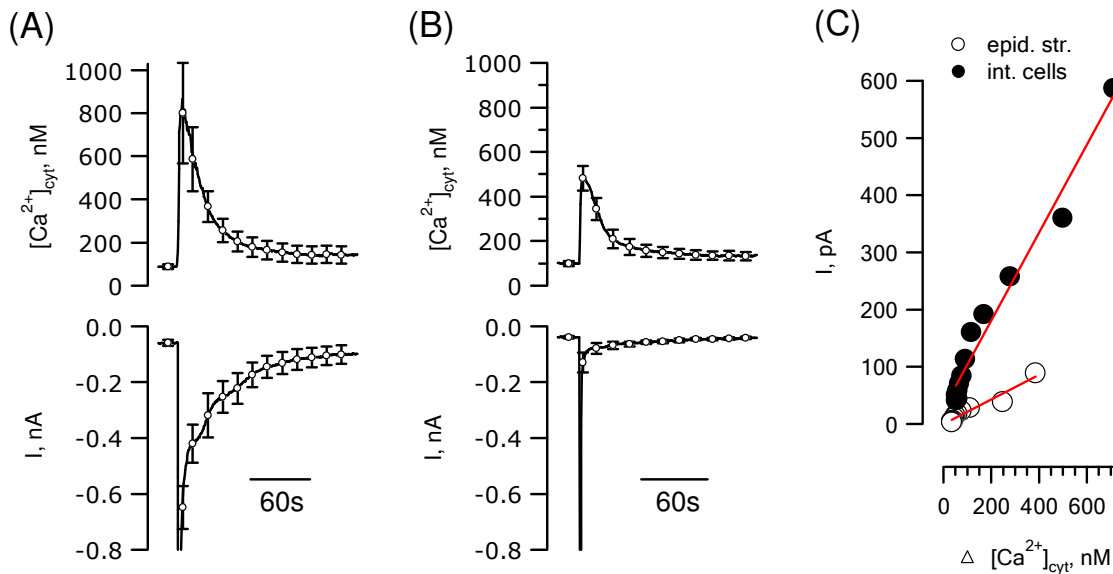
Fig. 3-23. Elevation of $[Ca^{2+}]_{cyt}$ and the concurrent membrane current at -100 mV, induced with short hyperpolarizing pulses in guard cells. (A) Average data for guard cells in intact plants, n = 19 and for guard cells of isolated epidermal strips, n = 14 (B). (C) Ca^{2+}-dependency of the anion current activation in intact guard cells (●) and guard cells of isolated epidermis (○). The lines were obtained by linear regression of both data sets.

In most guard cell in intact plants, the decay in inward current displayed single exponential kinetics (11 out of 19). However, in other 8 guard cells, the exponential decay in inward current was followed by a transient increase (fig. 3-22 B). Such an additional activation

of inward current was not observed in any of the guard cells in epidermal strips tested (fig. 3-22 C). On average, the amplitude of the ionic current, as well as $[Ca^{2+}]_{cyt}$ changes, were higher in intact guard cells than in guard cells of isolated epidermis (fig. 3-23).

An attempt of simple linear approximation of Ca^{2+}-dependent activity of plasma membrane anion channels, supposing the direct correlation between $[Ca^{2+}]_{cyt}$ and the activity of plasma membrane anion channels showed almost four-fold higher Ca^{2+}-sensitivity of anion channels in intact guard cells ($\Delta = 4.67$ pA/nM) compared to the cells in isolated epidermis ($\Delta = 1.29$ pA/nM), (fig. 3-23 C).

3.4.5 $[Ca^{2+}]_{cyt}$ responses evoked by external Ca^{2+} and cold shock. The $[Ca^{2+}]_{cyt}$ in guard cells was also reported to respond to external Ca^{2+} and cold shock in several publications (McAinsch et al., 1995; Wood et al., 2000). To verify reactions of prepared guard cells to those located in intact plants, effects of elevated Ca^{2+} concentrations and cold shock on $[Ca^{2+}]_{cyt}$ was checked experimentally.
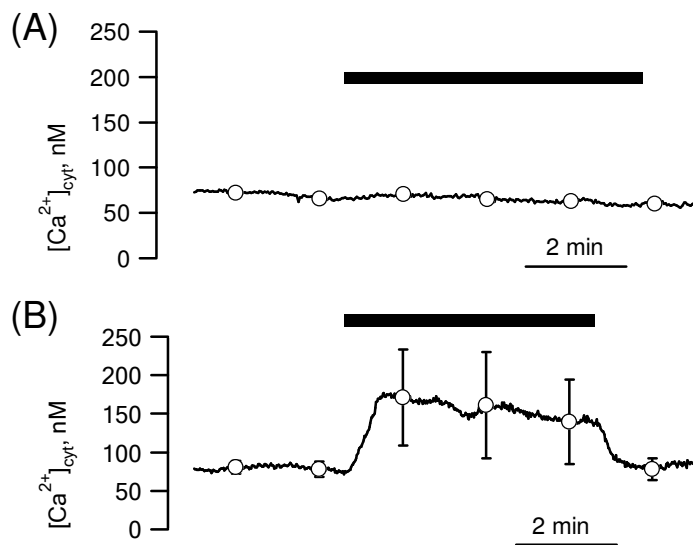
Fig. 3-24. Changes of $[Ca^{2+}]_{cyt}$ level, induced by increasing the external Ca^{2+} concentration from 1 to 10 mM. (A) Averaged data obtained in registrations on intact *Vicia faba* guard cells (n = 6). (B) Averaged data, obtained with the guard cells in isolated epidermal strips (n = 4). The period of application of 10 mM external Ca^{2+} is shown by the black bars over the traces.

The membrane potential of guard cells was clamped at -100 mV. External Ca^{2+} was added at a concentration of 10 mM to the standard perfusion buffer. In intact plants, elevation of Ca^{2+} in the external solution did not affect $[Ca^{2+}]_{cyt}$ of guard cells (fig. 3-24 A). Guard cells, located in isolated epidermal strips, responded to 10 mM external Ca^{2+} with an increase of the cytoplasmic calcium level from 77 ± 10 nM to 170 ± 63 nM, although $[Ca^{2+}]_{cyt}$ started to decay slowly and after 5 minutes reached a value of ~140 nM (fig. 3-24 B). Wash-out of the stimulus brined $[Ca^{2+}]_{cyt}$ to initial background level.

Cold shocks were applied by perfusion of standard buffer solution cooled to 5° C. Most of the registrations in guard cells of intact plant leaves failed, because of the disruption of

electrical contact between the guard cell and the microelectrode. The loss of impalement was the result of low temperature-induced movements of the leaf surface, evoked by the shrinkage of the leaf tissues. In such experiments, the cells displayed a transient increase of $[Ca^{2+}]_{cyt}$ to high levels, which coincided with the appearance of an electrical leak current. In mechanically stable registrations, cold shock evoked strong transient hyperpolarization for 10 – 20s. This change of registering potential of ~20 s duration and 40 – 70 mV amplitude (data not shown), turned to be an artifact, related to the jump of surface electric potential, appearing on the leaf cuticle (section 2.5.1).

Lowering of the temperature, although did not alter the $[Ca^{2+}]_{cyt}$ in guard cells of intact *Vicia faba* in stable impalements (fig. 3-25).
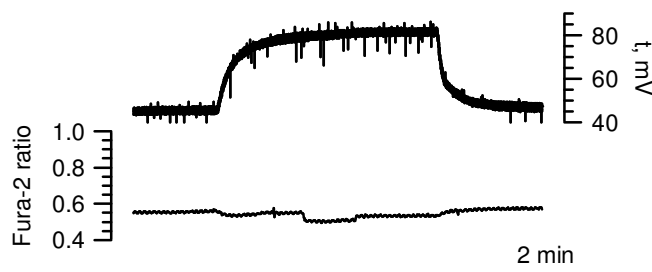
Fig. 3-25. Reaction of $[Ca^{2+}]_{cyt}$, recorded upon cold shock application in single guard cell, located in intact *Vicia faba* leaf. The whole range of the temperature change on the upper trace is equal to 20° C (25° → 5°C)

In guard cells of isolated epidermal strips, a small hyperpolarization of 8.6 ± 2.17 mV (n=5) and corresponding small decrease in inward current of 10-20 pA were recorded upon lowering the temperature of the bath solution to 5° C. The depolarization had sustained nature and preserved over the whole period of stimulus present. The reduction in inward current could be linked to a low temperature-induced inhibition of S-type anion channels activity. Despite of the membrane potential response and typical deactivation of K^{+}_{out} channels (data not shown), no changes of $[Ca^{2+}]_{cyt}$ in response to cold shock could be registered in guard cells of intact plants (fig. 3-25).

3.5 EXPLORING THE PUTATIVE SECOND MESSENGER ACTION.

Because of the lack of Ca^{2+} signals induced by ABA in *Vicia faba* guard cells, putative second messengers of the ABA signal transduction cascade tested were tested for the ability to mimic ABA action in guard cells.

The putative second messengers IP_3, IP_6, cADPR and NAADP were delivered directly to the guard cell cytoplasm by iontophoretical microinjection (section 2.5.3). Before microinjection of signaling molecules, the guard cells were tested for their ability to generate ABA-induced anion current transients. Following the microinjection of the second messenger, guard cells were tested for their ABA-sensitivity again (fig. 3-26).
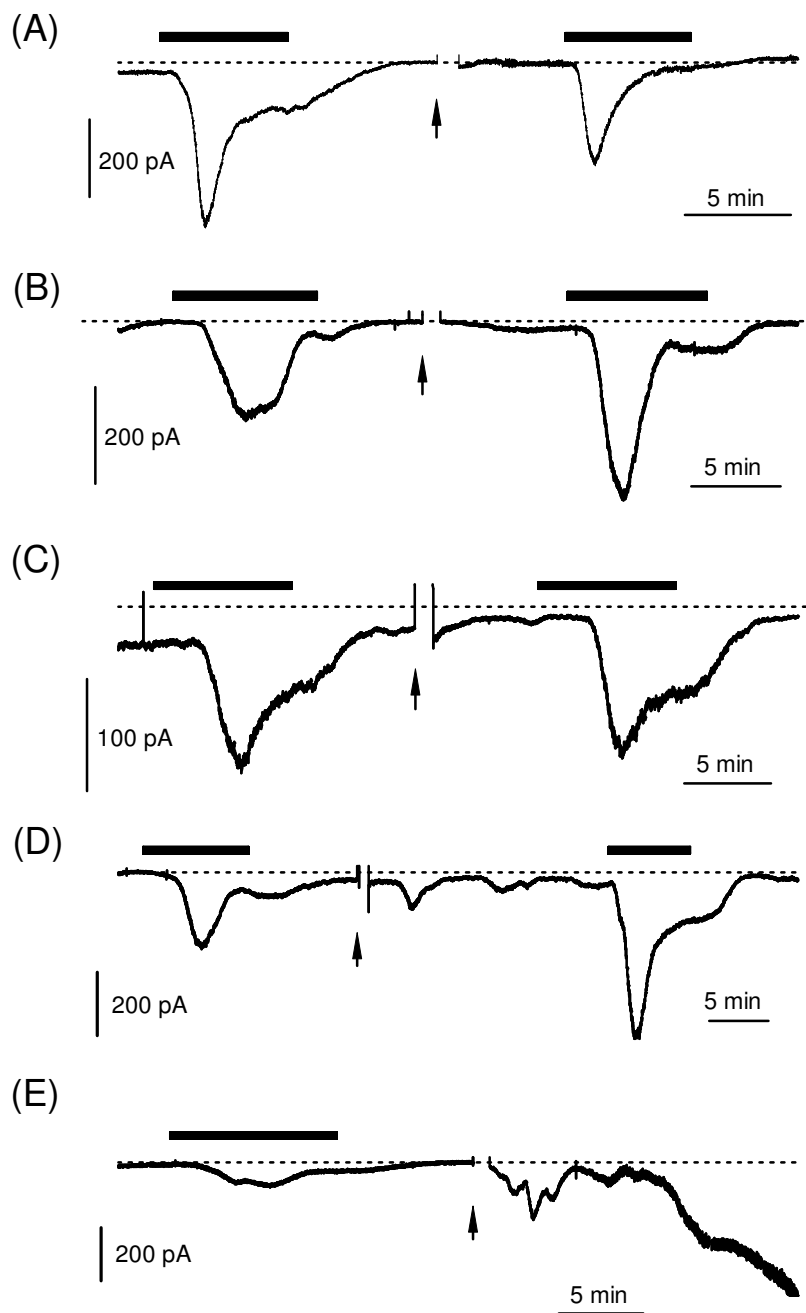
Fig. 3-26. Microinjection of putative second messengers into the cytoplasm of guard cells of *Vicia faba* in intact plants. Microinjection of IP_3 (A), IP_6 (B) and NAADP (C) was started at the arrow and continued for 60s, n = 6 for each signaling agent. The magnitude of the loading current in all experiments was 0.4 nA. In case of the first three signaling compounds no change membrane current was apparent following the cytoplasmic microinjection.

(D, E) Microinjection of cADPR (D) An example of the registration, where the microinjection induced oscillating behavior of the membrane current (n = 8). (E) An example of the registration, were cADPR microinjection lead to non-controlled rise of membrane current, leading to cell collapse (n = 4). The ability of the cells to respond to 20 µM ABA application was tested before and after microinjection of the second messenger. Applications of 20 µM ABA is shown with the black bars over the current traces.

Cytoplasmic microinjection of three out of the four selected signaling compounds – IP_3, IP_6 and NAADP did not evoke any reactions of membrane current during six minutes since intracellular application (fig. 3-26 A-C). Identical results were obtained in six similar measurements for each compound tested.

Microinjection of cADPR into the cytoplasm of intact guard cells induced variable membrane current responses. Out of 18 cells tested, 8 cells responded to cADPR with irregular oscillations in membrane current. (fig. 3-26, D). In four other cells, cADPR microinjection led to a non-controlled and irreversible rise of membrane current, which finally caused

the cell to collapse (fig. 3-26 E). Six remaining cells displayed no membrane current responses.

Among all second messengers tested, cytoplasmic microinjection did not showed no reproducible effect on the amplitude of following to microinjections membrane current responses to ABA (e.g. fig. 3-26 A and B).

IV. DISCUSSION.

4.1 ABA-INDUCED STOMATAL MOVEMENTS AND REARRANGEMENT OF
ION TRANSPORT.

This study is one of the first attempts of experimental investigation of Ca^{2+}- and Cl^- related signaling events, taking place in intact guard cells located in their natural surrounding – leaves of alive plants (Roelfsema et al., 2004; Levchenko et al., 2005, 2008). Keeping the integrity of the studying object will improve the physiological relevancy of the obtained data by two reasons. First is that using intact measuring systems excludes artifacts arising from preparation procedures. The second is naturally occurring interactions within plant organs and tissues, which disappear in case of preparations and may cause registration of non-physiological or significantly deviating reactions. All previous studies were carried out on different guard cells preparations – either guard cells of isolated epidermal peels, or isolated protoplasts lacking cell wall.

The newly applied strategy of *in situ* registrations enabled observation of real-time kinetics and the magnitude of physiological processes, taking place in intact plants. Analysis of responses of intact guard cells and guard cells of isolated epidermis, presented in chapter III and also known from other reports (McAinsh et al., 1990, 1992; Schroeder and Hagiwara 1990; Gilroy et al. 1991; Irving et al. 1992 Grabov and Blatt, 1998; Allen et al., 1999a; Staxen et al., 1999), can point to a significant rate of possible artifacts in description of guard cell signaling machinery function. A comparison of different cell responses, such as stomatal closure, regulation of ion channels and behavior of cytoplasmic Ca^{2+} showed pronounced difference between reactions of guard cells of intact plants and their counterparts in other preparations.

4.1.1. Stomatal closure upon external ABA application. Stomatal movements in intact plant leaves differ from that in isolated epidermis. The differences of stomatal dynamics occur due to interaction of guard cells with surrounding leaf tissues – epidermis and mesophyll. Viable turgescent epidermal cells back-press guard cells, affecting final aperture of opened stomata and causing incomplete closure of stomata with disrupted neighboring epidermal cells (reviewed in Roelfsema and Hedrich, 2005).

In intact *Vicia faba* leaves, stomata started to close 8 min after addition of external ABA with an initial aperture size of 5.25 µM and reached maximal closure within 20 min of ABA perfusion and the final aperture of 2 µM (Fig. 3-2 B). Stomatal closure in isolated epi-

dermal peels upon external ABA application develops much slower. In similar experimental conditions, final closure of stomata in isolated epidermal peels of *Vicia faba* from initial aperture of 8 to final 3.25 µm was reached after 1 hour perfusion with 20 µM ABA (Blatt and Armstrong, 1993).

4.1.2 ABA-induced membrane potential changes. Movements of stomata are the result of redistribution of ions and organic solutes between guard cells and apoplast (Raschke, 1975; Roelfsema and Hedrich 2005). The distribution of ions is under the cell control and strongly depends on the electric potential difference at the plasma membrane which regulates and coordinates ion channel activities (Thiel et al., 1992).

Almost half of intact guard cells challenged with extracellular ABA displayed a typical depolarization of membrane. In a population of resting "depolarized" (section 3.1.2) cells, which had a free running membrane potential value that approximates the K^+ equilibrium potential, almost half of cells showed a typical depolarization response. This depolarization occurred with ~ 2 minutes delay and reached a maximal amplitude at ~5 minutes after ABA introduction. The depolarization is followed by a plateau phase and recovering to initial level of membrane potential after stimulus removal (fig. 3-3 B). The other initially depolarized cells showed additionally transient or sustained hyperpolarization of plasma membrane to values more negative than -100 mV, upon removal of ABA. This hyperpolarization most likely is the result of plasma membrane H^+-ATPase activity, which is essential for energizing K^+ and anions uptake into the cell (Dietrich et al., 2001). Switching of initially depolarized cells to the hyperpolarized state after ABA removal, most likely corresponds to reuptake of ions after a sudden stop of the response to ABA. After such an abrupt termination, the physiological status of the cell differs from the hormone input it receives from the surrounding tissue.

Co-occurrence of non-responding and responding in different ways guard cells on one plant leaf may point to a possible existence of guard cells in different physiological states characterized with different sensitivity to ABA (section 4.2.2). It is very suitable for plants, because such multiplicity of physiological states would give a possibility to produce graduated responses, when less intensive drought will cause closure of only small portion of stomata.

4.1.3 Regulation of K^+-channels activity by ABA. Potassium acts as an osmotically active compound and moves at significant amounts in and out of guard cells during the

stomatal movements. Cytosolic K^+ activity is about 0.1 M in resting closed *Vicia* guard cells; but in fully opened stomata it increases up to 0.5 M (MacRobbie, 1987). Potassium translocation across guard cell plasma membrane is passive process mediated by voltage-dependent K^+ channels.

External ABA did not change the activity of outward rectifying K^+ channels in intact *Vicia* guard cells. In 14 of 27 cells tested, a down-regulation of time-dependent outward current has been found (fig. 3-4). In other cells ABA produced no effect on K^+ outward currents (fig. 3-7), showing that the conductance of outward rectifying K^+ channels is not on average modified by ABA *in vivo*.

These results do not confirm previous experimental data on ABA regulation of guard cell K^+_{out} channels, which reported their activation by ABA. K^+_{out} channel activation has been described in guard cells of isolated epidermal strips (Blatt, 1990) and protoplasts thereof (Lemtiri-Chlieh and MacRobbie, 1994). However, the effect of ABA on this channel could not be reproduced by others (Schwartz et al., 1994). The activation of K^+_{out} channels by ABA has been proposed to be mediated through alkalization of the guard cell cytoplasm (Blatt and Armstrong, 1993). The observed transient reduction of K^+_{out} currents in about 50 % of cells tested, occurring at the peak of the anion channel activation, could be due to a second messenger that acts on both channels. It is unlikely that this response was due to a $[Ca^{2+}]_{cyt}$ elevation, since ABA does not induced such an event in intact guard cells of *V. faba*. A transient cytoplasmic acidification may explain the inhibition of K^+_{out} (Roelfsema et al., 1998), which could be tested in future experiments.

The lack of an effect of ABA on K^+_{out} channels has also been observed with intact *Nicotiana tabacum* guard cells. External ABA application showed no significant effect on K^+_{out} channel activity, even though it activated anion channels (Marten et al., 2007b). The lack of K^+_{out} channel activation by ABA in intact guard cells, measured in two different plant species, suggests that ABA does not induce cytosol alkalization, a signaling event known to stimulate K^+_{out} channels (Blatt and Armstrong, 1993).

The effect of ABA on the activity of inwardly rectifying K^+ channels could not be determined because it overlaps with a large conductance increase that is due to activation of anion channels. Previous studies demonstrated the inhibition of inward K^+ currents by ABA, in guard cells of isolated epidermal strips (Blatt and Armstrong, 1993) and guard cell protoplasts (Lemtiri-Chlieh and MacRobbie, 1994).

Regulation of K^+_{in} channel activity by ABA may act through the elevation of $[Ca^{2+}]_{cyt}$, because K^+_{in} channels are inhibited at high $[Ca^{2+}]_{cyt}$ (Grabov and Blatt, 1999). However, a

study with guard cell protoplasts reports inactivation of K^+_{in} channels by ABA at experimental conditions with buffered $[Ca^{2+}]_{cyt}$ (Romano et al., 2000).

__4.1.4. Anion channels activation by ABA.__ Intact *Vicia faba* guard cells impaled with multi-barreled microelectrodes were able to generate a characteristic ABA-activated anion current transients (section 3.2.1). Voltage-dependence, kinetics and reversal potential of the activated channels show that they were mediated by rapidly activating-deactivating (R-type) and slowly activating (S-type) anion channels.

ABA activation of S type anion channels has been reported before in guard cell protoplasts from *Arabidopsis* (Pei et al., 1997) and isolated epidermis of *Nicotiana benthamiana* (Grabov et al., 1997). R type anion channels were activated by ABA in two independent studies with intact guard cells of *Vicia faba* (Raschke et al., 2003; Roelfsema et al., 2004) but this response has not been observed in guard cell protoplasts. The co-existence of these two types of anion channels (Hedrich et al., 1990; Schroeder and Keller, 1992) thus could been confirmed here by experiments carried out on intact *Vicia* guard cells. The ABA-induced anion conductance consisted of both slow and rapid current components (Roelfsema et al., 2004, section 3.2.1). A search for conditions that lead to preferential activation of one of both channel types yielded no results (fig. 3-6), apart from the observation that R type anion channels dominate in responses with bigger amplitude (section 3.2.1). No obvious difference in kinetics of transient responses has also been found between transients with dominating S- or R-type conductance.

Both R- and S- channel types mediate anion efflux from guard cells, leading to the plasma membrane depolarization, loss of solutes and stomatal closure. As R-type anion channels are not active at hyperpolarized membrane voltages (negative of -100 mV), they unlikely participate in triggering membrane depolarization in hyperpolarized guard cells. In contrast, only slow anion channels, which are active at very negative voltages promote depolarization of hyperpolarized cells. The physiological role of R type anion channels was assumed in a feed-back mechanism of high CO_2 sensing by guard cells, as these channels respond to a rise of the external malate concentration with a shift of the activation threshold towards more negative membrane potentials (Hedrich and Marten, 1993). The activation of R-type anion channels during large conductance changes suggests that they are involved in controlling the rate of anion efflux from guard cells in response to ABA.

The activation of inward current correlates closely with the kinetics of membrane potential changes, observed upon external ABA application (section 3.3.1). After a 2-min lag

phase, the current starts to increase and reaches maximal values in 4 - 5 min. Thereafter, it declines to a steady-state level. The steady-state inward currents in the presence of ABA are larger than control currents observed before ABA application. Upon ABA washed-out, the membrane current either recovers to the original level, or even becomes more positive.

Guard cells of intact *Vicia* plants also responded to short-term ABA treatment by generation of typical inward current transients (fig. 3-10). Responses to short-term ABA treatments were characterized by a complete return to pre-stimulus values. In most cases, however, the inward current transient was followed by a time dependent outward current, –indicating the activation of plasma membrane H^+ pump activation. The ability of intact guard cells to generate delayed anion transients in response to short-term ABA treatment suggests an autonomous signal transduction chain, which is triggered even by short-term hormone perception.

Several successive cell responses to extracellular ABA, as well as responses to short-term ABA treatments, can be repeatedly reproduced in single guard cells. The ability of intact guard cells to generate successive anion current transients, even after a few minutes shows that guard cell ABA signaling mechanism can be re-setted within such short time.

Unfortunately, no obvious conclusions about ABA pretreatment history impact on the amplitude of consequent anion transients could be drawn. Guard cells were found to increase as well as decrease ABA-sensitivity during repetitive ABA treatments (fig. 3-12). Apart from these polar changes in the current response amplitude, no indications of systematic tuning of the system, regulating ABA sensitivity of guard cells with respect to anion channel activation was found. The observed time-dependent alterations in ABA-sensitivity of guard cells could be due to intrinsic guard cell rhythms, which to some extent may be provoked by surrounding cells. The well documented phenomenon of "patchy" stomatal aperture (Mott and Buckley, 2000) strongly suggests the regulation of guard cell ABA-sensitivity by surrounding tissues.

Variability in ABA sensitivity could also explain the oscillating behavior of inward current, observed in few cells upon long-term ABA exposure (fig. 3-9). During these "oscillating" responses successive anion current transients develop after completing the first one, suggesting that these guard cells are able to respond to ABA soon after completing the first anion channel transient. The occurrence of repetitive transients may relate to a complete closure of stomata, whereas single transient anion channel responses is likely to cause only a restricted reduction of the stomatal aperture.

A transient increase of anion channels activity in response to ABA reaching a steady-state state after approximately 10 min seems to be ubiquitous among plant species. Guard cells of intact *Nicotiana tabacum*, *N. plumbagnifolia* and *Commelina communis* plants also responded to ABA by activating plasma membrane anion current with the virtually the same kinetics as in *Vicia faba*. The timing of changes in anion conductance was very similar in guard cell of *Nicotiana* and *Vicia*, but *Commelina* guard cell responses were approximately two times more prolonged (section 3.3.1, see also Marten et al., 2007b).

A temporary activation of anion channels is well in agreement with the predicted temporary activation of guard cell plasma membrane anion conductance, based on a transient tracer efflux from epidermal strips upon ABA treatment (MacRobbie, 1981). A transient nature of the anion efflux was also confirmed by measurements of ABA-induced Cl$^-$ activity changes in the apoplast of intact *Vicia faba* leaves recorded with ion-selective microelectrodes (Felle et al., 2000).

The transient anion current induced by ABA, followed by a steady-state state inward current most likely facilitates quick stomatal closure followed by a conditions that prevent a re-opening of the stomata. Such an initial closure of stoma could be incomplete, however, it will reduce the transpiration stream and thus set a new rate of ABA delivery to guard cells. The new rate of ABA delivery will determine if the stoma will further go close or reopen, as guard cells were found to respond to the rate of ABA arrival to plasma membrane, instead of the apoplastic ABA concentration (Trejo et al., 1995).

Future studies could be aimed to elucidate the factors controlling ABA-sensitivity, which may be related with inner rhythmic processes in guard cells.

4.2 INDUCTION OF ANION CONDUCTANCE BY ABA: INSIGHTS INTO EARLY ABA SIGNALING STEPS.

4.2.1. ***Exploring the early phase of anion current transients.*** Since the discovery of hyperpolarization-activated Ca^{2+}-permeable channels in the guard cell plasma membrane (Blatt and Grabov, 1998; Pei et al., 2000), these channels have been a component of most ABA signaling models (Schroeder et al., 2001; Li et al., 2006). ABA has been shown to increase $[Ca^{2+}]_{cyt}$ by shifting the activation threshold of Hyperpolarization Activated Cation Channels (HACC) to more depolarized voltages (Grabov and Blatt, 1998). Elevations of $[Ca^{2+}]_{cyt}$ are thought to activate downstream signaling events leading to plasma membrane anion channel activation, membrane depolarization and stomatal closure.

HACCs are inactive at depolarized voltages more positive than -50 mV (Hamilton et al., 2001). Therefore, the involvement of these channels in the ABA signal transduction chain was studied by testing the ability of guard cells to generate anion current transients at depolarized membrane potentials. These studies showed that anion current transients can be triggered in intact *Vicia* guard cells even at very depolarized voltages (0 mV, section 3.3.3). This questions the involvement of voltage-gated Ca^{2+}-channels in the signaling chain causing activation of anion channels by ABA.

The ABA-induced conductance changes attained a biphasic nature in a number of guard cells clamped to depolarized membrane potentials (fig. 3-14, section 3.3.3). The nature of both current peaks, was studied with short voltage ramps. During current transient, a shift of the reversal potential occurred to strongly depolarized values (positive of +50 mV, fig. 3-15). The large shift of the reversal potential was associated with only small increase of the membrane conductance. At the second phase, a strong increase in membrane conductance was accompanied by a return of the reversal potential to less negative values. At the conductance of the second phase the reversal potential approximated 20 mV indicating that this current was due to the activation of plasma membrane anion channels.

The nature of the conductance activating during the first phase of the ABA response at depolarized values has remained unclear. One possibility could be that activation of a Ca^{2+}-selective channel precedes that of anion channels. Considering the extremely positive value of the reversal potential during this early phase, some unknown Ca^{2+}-selective channels, active at depolarized potentials must be assumed. However, a Ca^{2+}-selective channel active in this voltage range has so far not been identified in guard cells. Furthermore, measurements with cytoplasmic microinjection of Ca^{2+}-sensitive fluorescent probe Fura-2, did not provide evidence for an influx of Ca^{2+} preceding the anion current transient in the second phase of the ABA response.

Alternatively, the transient shift in reversal potential during the first phase of current transient may be due to a short-term increase of anion concentration in the cytoplasm. Such increase of the cytoplasmic anion concentration could be the result of an initial anions efflux from the vacuole, preceding the activation of plasma membrane anion channels. The delayed activation of plasma membrane anion channels thus may create a temporary barrier for anion efflux from the vacuole that causes the accumulation of anions in the cytoplasm. Theobserved 30 mV reversal potential shift corresponds to a cytosolic Cl- concentration increase from approximately 10 mM to 45 mM, based on the Nernst equation and assuming a Cl⁻ selective channel and an apoplastic Cl- concentration of 5 mM.

Very little is known about the role of the vacuole in guard cell physiology; despite its significant role in ion accumulation. Future studies with ion-selective microelectrodes are needed to answer the question of the vacuole involvement in the regulation of the guard cell turgor ant ion homeostasis.

4.2.2. *Cytosolic Ca^{2+} level and anion current activation by ABA.* The participation of [Ca^{2+}]$_{cyt}$ in the ABA signal transduction chain, which starts from ABA perception by guard cells and ends by the activation of plasma membrane anion channels, is still unclear. It is known, that both R- (Hedrich et al., 1990) and S-type (Schroeder and Hagiwara, 1989) anion channels, that participate in stomatal closure, can be activated by the elevation of [Ca^{2+}]$_{cyt}$. In line with these observations, Ca^{2+} and ABA have a synergistically effect in triggering stomatal closure (DeSilva et al., 1985a, b; section 1.4.1). This suggested that ABA stimulates anion channels through an increase of [Ca^{2+}]$_{cyt}$. However, so far no direct experimental evidence for the requirement of [Ca^{2+}]$_{cyt}$ elevation for anion channel activation by ABA has been obtained. Experimental registrations of [Ca^{2+}]$_{cyt}$ during cell response manifestation would help to understand the exact role of cytosolic Ca^{2+} in ABA signaling in guard cells. To this end, the [Ca^{2+}]$_{cyt}$ changes were monitored in parallel to ABA-induced anion transients in intact *Vicia* guard cells. These experiments revealed no detectable [Ca^{2+}]$_{cyt}$ changes, even though inward anion current transients with typical time kinetics were found in Fura-2 microinjected intact *Vicia* guard cells (fig. 3-17).

Despite of the absence of ABA-dependent [Ca^{2+}]$_{cyt}$ transients, other experimental results point to an important role of the physiological resting [Ca^{2+}]$_{cyt}$ for the ability of guard cells to respond to ABA. Intact guard cells, microinjected with mixture of Fura-2 and Ca^{2+} buffer BAPTA displayed a lower ability of generating anion transients in response to ABA (section 3.4.2). Similar results have been obtained in patch-clamp experiments on *Vicia* guard cell protoplasts, in which ABA was applied via the pipette. Inclusion of 50 mM BAPTA in the pipette solution completely abolished ABA-stimulated anion channel activation in guard cell protoplasts (Levchenko et al., 2005).

Instead of inducing a rise in the Fura-2 ratiometric signal, ABA induced a decrease in the presence of 5 mM Ba^{2+} in the perfusion buffer (fig. 3-19, section 3.4.2). Apart from its sensitivity to Ca^{2+}, Fura-2 also binds to the range of other divalent cations like Ba^{2+}, Sr^{2+}, Mn^{2+} and Ni^{2+} (Hatae et al., 1996). As HACCs are easily permeable to Ba^{2+} (Hamilton et al., 2001), their activation should lead to Ba^{2+} influx into the cytoplasm and a corresponding increase of Fura-2 ratiometric signal. Instead of such an increase, the Fura-2 ratio signal

dropped adding to the evidence that HACC channels are not activating in response to ABA. A possible explanation for the decrease of the Fura-2 ratio signal is a change of ionic conditions in the cytosol during the ABA-induced anion transient. Taking into account a more labile binding of Ba^{2+} to Fura-2, in comparison to Ca^{2+} ions, the Fura-2 signal may become sensitive to cytosolic conditions such as pH_{cyt}. A change of pH_{cyt} may well occur during anion transient, since anions are though to be taken up in symport with H^+. The observed changes of Fura-2 ratiometric signal thus may reflect changes in the cytoplasmic pH.

Absence of Fura-2 ratiometric signal rise in Ba^{2+}-containing media further shows that HACC or other plasma membrane Ca^{2+} channels are not involved in ABA signal transduction.

Recent studies of the ABA effect on ion transport in intact *Nicotiana tabacum* guard cells showed that in this species a $[Ca^{2+}]_{cyt}$ elevation occurred in response to ABA treatment, in 80% of cells responding with an anion current transient (Marten et al., 2007b). The time-dependent change in $[Ca^{2+}]_{cyt}$ in *Nicotiana tabacum* guard cells had a shape of a single transient up to 250 nM. However, in most cases, the Ca^{2+} peak was not synchronic with the anion current transient. In 50% of cells that displayed $[Ca^{2+}]_{cyt}$ increase, the $[Ca^{2+}]_{cyt}$ peak was delayed in comparison to anion channel activation. This suggests that $[Ca^{2+}]_{cyt}$ increase does not serve as a signaling event leading to anion channel activation. In *N. tabacum*, 20 % of the guard cells did not show $[Ca^{2+}]_{cyt}$ elevation; but displayed similar anion current transients as in cells with a $[Ca^{2+}]_{cyt}$ change.

Most obviously, there are two ways of ABA signal transduction existing in guard cells – a Ca^{2+}-independent and a Ca^{2+}-dependent pathway. The latest probably, represent an alternative or additional way of the stress hormone signal transduction. Oscillations of $[Ca^{2+}]_{cyt}$ of changing frequency and amplitude are known to alternate genes expression profile in animal cells (Dolmetsch et al., 1997, 1998). The registered rises of cytoplasmic Ca^{2+} in *Nicotiana* guard cells thus could have an impact, for example, on gene expression related or long-term adjustment of ABA responsiveness status of guard cell.

4.2.3. ***Effects of intracellular ABA and second messengers.*** The nature of the ABA receptor and its subcellular localisation still are not answered yet (section 1.5.1). The delayed activation of the anion current in response to extracellular ABA is probably because of an intracellular localization of the receptor. The lag phase could be explained by the transport of ABA from the cell wall to the cytoplasm. Microinjection of ABA directly into guard cell cytoplasm evoked an immediate response of the anion channels, supporting an intracellular lo-

calization of the ABA receptor. Cytosolic ABA microinjection during 30s induced a transient anion current which completely deactivated passing the maximum. Before the plasma membrane current reached it pre-stimulus value, positive currents were recorded that are indicative of the H^+ pump stimulation. The shortened response to a quant of ABA injected to the cytosol indicates a fast cell desensitization or quick ABA destruction or removal from the cytoplasm (Cutler and Krochko, 1999).

A number of signaling molecules, such as IP_3 (Allen et al., 1995), IP_6 (Lemtiri-Clieh et al., 2003), NAADP (Navazio et al., 2000) and cADPR (Leckie at. al., 1998) have been proposed to participate in guard cell ABA signal transduction. The effect of these putative second messengers on the activation of anion channels has been examined in this work (section 3.5). Microinjection of IP_3, IP_6 and NAADP had no effect on the anion current of intact guard cells responding to ABA (fig. 3-26 A, B, C). This indicates that these compounds are unable to mediate the ABA activation of plasma membrane anion channels. Microinjection of cADPR, however, induced variable responses of the anion channels in intact *Vicia* guard cells. More than half of cells showed irregular oscillations of the plasma membrane anion conductance, in some cases, ending with extreme increase of the membrane current and the cell collapse (fig. 3-26 D, E). This result provides a strong evidence for the ability of cADPR to mediate the ABA-induced activation of anion channels.

4.3 CYTOSOLIC CA^{2+}: SIGNALING AND HOMEOSTASIS.

4.3.1. *$[Ca^{2+}]_{cyt}$, changes induced by different stimuli.* The potential function of Ca^{2+} as a key second messenger inspired a large number of guard cell researches to study the role of changes in the cytosolic free Ca^{2+} concentration in a number of cell functions and transduction pathways of various signals. Many of these studies have been carried on guard cell preparations – such as isolated epidermal peels, epidermal fragments or guard cell protoplasts. With the first two preparations, stimulus induced transient, sustained or oscillating responses of $[Ca^{2+}]_{cyt}$ were found (section 1.4.3).

Even though various stimuli can induce Ca^{2+}-signals, an elevation of the external Ca^{2+} concentration is probably the most reproducible and therefore often used to induce $[Ca^{2+}]_{cyt}$ elevations (Allen et al., 1999b; McAinsh et al., 1995; Hann et al., 2003). A ten-fold increase of the external Ca^{2+} concentration, from 1 to 10 mM, leads to a sustained elevation of $[Ca^{2+}]_{cyt}$ level by ~ 100 nM over background level in guard cells of isolated *Vicia faba* epidermis (fig. 3-24). The same treatment evoked no response of $[Ca^{2+}]_{cyt}$ in guard cells of intact plants, demonstrating an obvious difference in behavior of $[Ca^{2+}]_{cyt}$ in guard cells of in-

tact plants and cells of prepared epidermis. The possibility that Ca^{2+} may not reach guard cells due to limited diffusion through leaf cuticle can be excluded, as increasing Ca^{2+} evoked changes of free-running membrane potential (data not shown). The difference in $[Ca^{2+}]_{cyt}$ responses could be explained by higher activity of Ca^{2+}-gated Ca^{2+}-permeable channels in isolated guard cells or a non selective leak of the plasma membrane of isolated guard cells to Ca^{2+}. These stable (not a transient) $[Ca^{2+}]_{cyt}$ elevation points to an inability of guard cells to maintain a steady cytosolic Ca^{2+} level.

The application of "cold shocks" induced neither $[Ca^{2+}]_{cyt}$ increases in guard cells of intact plants neither in epidermal peels (section 3.4.5, fig. 3-25). This result is in disagreement with that of the effect of cold on guard cell $[Ca^{2+}]_{cyt}$ registered in aequorin-transformed guard cells of *Nicotiana plumbagnifolia* epidermal strips (Wood et al., 2000). In the latter species cold induced an extreme Ca^{2+} elevations up to 6 μM.

The absence of $[Ca^{2+}]_{cyt}$ increases in intact guard cells of *Vicia faba* in response to ABA, high external Ca^{2+} and cold, may be due to differences in organization of Ca^{2+} signaling pathways in different plant species. For example, a similar study of ABA activation of anion channels in *Nicotiana tabacum* revealed the generation of $[Ca^{2+}]_{cyt}$ elevation in 80 % of cells responding to ABA (Marten et al., 2007b). Responses of $[Ca^{2+}]_{cyt}$ to same stimuli are different in different species and even in different preparations with same species (section 1.4.3). Guard cells of isolated epidermal strips of *Commelina communis* demonstrates regular oscillations of specific shape in response to ABA (Staxen et al., 1999), but in *Arabidopsis thaliana* these oscillations in most cases have an irregular shape and amplitude (Allen et al., 1999a). Thus, in case of guard cell preparations one should be careful with interpreting the data, especially in relation of oscillation processes. As every signaling system is likely to represent a self-organizing loop, preparation procedures can disrupt the integrity of such a signaling system. For this reason, it is favorable to study signaling events with the use of minimal invasive experimental approaches.

4.3.2. ***Responses of $[Ca^{2+}]_{cyt}$ induced by membrane potential changes.*** In a classical paper reporting for the first time on an existence of HACC in guard cells (Grabov and Blatt, 1998), the authors used a short hyperpolarizing pulses to increase $[Ca^{2+}]_{cyt}$ in guard cells of *Vicia* epidermal strips. In our studies we found that long-term hyperpolarisation from -100mV to -160 mV induced a step-like increase of $[Ca^{2+}]_{cyt}$ level up to 300 nM in guard cells of epidermal strips. Returning membrane potential to -100 mV caused $[Ca^{2+}]_{cyt}$ recovery to the original level of ~ 100 nM. The changes in $[Ca^{2+}]_{cyt}$ during the long-term hyperpolarisa-

tion in guard cells of intact plant was different. After reaching a 150 nM maximum at 50 s, $[Ca^{2+}]_{cyt}$ slowly decreased to a level that was only ~25 nM higher than the background level. A subsequent depolarization to the pre-stimulus potential of -100 mV caused a complete $[Ca^{2+}]_{cyt}$ recovery. The hyperpolarization induced increase of the $[Ca^{2+}]_{cyt}$ level confirms the activity of voltage-gated Ca^{2+}-channels in both guard cells of isolated epidermis and intact *Vicia* plants. The difference in the responses following the initial rise of $[Ca^{2+}]_{cyt}$ suggests that the mechanisms for $[Ca^{2+}]_{cyt}$ regulation in guard cells is impaired in isolated epidermal peels.

Long-term depolarization of guard cells, in isolated epidermis, from -100 to 0 mV evoked step-like decrease of $[Ca^{2+}]_{cyt}$ up to 100 nM below the resting level. This decrease fully recovered after the repolarization to the initial voltage level. Just as for the hyperpolarization, the response to a 5-min depolarization of the plasma membrane in resulted in more complex $[Ca^{2+}]_{cyt}$ changes in intact plants. Guard cells in their natural environment, displayed a the short-term $[Ca^{2+}]_{cyt}$ decrease from the background level of 98 nM to approximately 13 nM and a recovery to a steady-state level of approximately 55 nM, thereafter. Stepping back to -100 mV caused a transient $[Ca^{2+}]_{cyt}$ elevation up to 170 nM, which rapidly decreased again to a background level of ~100 nM (fig. 3.21 B).

The transient changes of $[Ca^{2+}]_{cyt}$ after membrane potential changes, nicely demonstrate a mechanism in guard cell of intact plant leading to Ca^{2+} homeostasis. A depolarization closes a part of voltage-gated Ca^{2+}-channels that are still active at -100 mV, and therefore leads to a decrease of $[Ca^{2+}]_{cyt}$, probably caused by a continuous active Ca^{2+} pumping from the cytoplasm. After reaching the minimum $[Ca^{2+}]_{cyt}$ level partially recovers and gets to a plateau level, indicating a new balance between the passive Ca^{2+} influx and an active Ca^{2+} efflux from the cytoplasm. A subsequent repolarization opens HACC and induces an influx of Ca^{2+} into the cytoplasm. The faster increase of $[Ca^{2+}]_{cyt}$ during membrane repolarization comparing to a hyperpolarization from -100 mV may demonstrates emptying of cytoplasmic Ca^{2+} buffer capacity after prolonged depletion of cytoplasmic Ca^{2+} during depolarization. Alternatively, the increased velocity of $[Ca^{2+}]_{cyt}$ increase could be due to additional modifications in the activity of Ca^{2+} translocating proteins, which are likely to be regulated by $[Ca^{2+}]_{cyt}$ themselves (section 1.3.4).

The $[Ca^{2+}]_{cyt}$-dependent activation of plasma membrane anion cannels and mechanisms involved in the maintaining resting $[Ca^{2+}]_{cyt}$ levels, was studied with short hyperpolarization pulses of large amplitude (section 3.4.4). Short-term voltage pulses (up to -0.5 V) induced massive elevation of the $[Ca^{2+}]_{cyt}$ level both in guard cells of isolated epidermis and intact

plants. The large increases of $[Ca^{2+}]_{cyt}$ may well be due to electroporation, which is based on a temporary electrical breakdown of the plasma membrane. After reaching a maximum, a rapid rise of the $[Ca^{2+}]_{cyt}$ level that stops and begin to decrease exponentially to the initial level both in guard cells of isolated epidermis and intact plants. In intact plants, guard cells showed a large inward current following the hyperpolarizing pulse, which exponentially decayed to the pre-stimulus level within 1-2 min. In most guard cells an additional delayed transient current activated after the exponentially decaying initial (fig. 3-22 B).

In guard cells of isolated epidermal peels only a small inward current was observed in response to hyperpolarization pulses (fig. 3-23 B). Based on a presumed linear relation between the $[Ca^{2+}]_{cyt}$ elevation and the inward current the activation, the ability of anion channels regulation with $[Ca^{2+}]_{cyt}$ was ~ 3.7 times less in guard cells in isolated peels compared to intact plants. This difference may indicate to a disruption of a Ca^{2+}-dependent mechanism of anion channels regulation in guard cells of isolated epidermal strips as well as to the reduced number of anion channels in prepared cells.

The more complex voltage induced $[Ca^{2+}]_{cyt}$ changes in guard cells of intact plants as compared to those in isolated preparations clearly points to the disruption of endogenous guard cell mechanisms maintaining a Ca^{2+} balance in the cytosol. By one mean or other, guard cells of intact plants seem to monitor the resting $[Ca^{2+}]_{cyt}$ and try to maintain it independently of changes in the Ca^{2+} influx, while isolated guard cells may not possess such monitoring mechanism and capable of displaying only a steady activity of Ca^{2+} pumping proteins. Bceause of a lack of such regulation a change in the Ca^{2+} influx causes only a simple shift of $[Ca^{2+}]_{cyt}$ level.

Guard cell protoplasts displayed even a stronger dependence of $[Ca^{2+}]_{cyt}$ level on the membrane voltage. In combined $[Ca^{2+}]_{cyt}$ measurements and patch-clamp recordings, *Vicia* guard cell protoplasts were able to keep stable background $[Ca^{2+}]_{cyt}$ level only at holding potential of -50 mV, as hyperpolarization of the membrane to -100 mV caused a steady increase of the $[Ca^{2+}]_{cyt}$, to levels exceeding 400 nM (Levchenko et al., 2008). Protoplast isolation procedures have been shown to change gene transcription levels (Birnbaum et al., 2003) and the observed differences in Ca^{2+} homeostasis between cells in different preparations also very likely could reflect changes in the transcription level of various genes.

CONCLUSION

There are many questions that are still not solved in the field of plant physiology. Among them function of stomatal guard cells is one of the most intriguing and important to date. Right understanding of gurd cell function requires highly relevant physiological data. Such data might be only obtained during registrations in measuring systems where maximal intactness is kept, such as whole leave of intact living plant.

Guard cells located in whole plant leaf are in their natural environment and therefore appeared to be turned in to the full set of regulatory circuits existing in plant organism. On one hand measuring in such system may seems to complicate the experiment by mean of excessive input variables. On the other the observed reactions do represent the naturally occurring plant behavior and thus, of unargueble importance.

Experimental work presented here was designed initially as an attempt of a registration of ABA-induced reactions of guard cells located within intact leaves of living plant. Unexpectedly, the newly applied experimental approach yielded highly-reproducible registrations of ABA-induced anion current responces of 10-100 times biger amplitude than that reported for the guard cells of isolated epidermal peels. One to two orders of magnitude bigger plasma membrane electrical responces very likely represent the amplitude of the real physiological reactions, as it well correspond to calculated rates of anion efflux during stomatal closure. High reproducibility of the experimental results also uncompromisingly point to guard cells of intact leaves as an excellent system for performing highly relevant physiological experiments.

Further research was aimed to detalize the data on $[Ca^{2+}]_{cyt}$ participation in ABA signaling in guard cells. Surprisingly, experiments carried out in intact Fura-2 microinjected guard cells did not confirm $[Ca^{2+}]_{cyt}$ elevations during ABA action. This finding rose a consequent set of questions, which could be solved through a comparison of different $[Ca^{2+}]_{cyt}$ reactions and homeostasis in guard cells of prepared epidermis and intact leaves. A series of conducted experiments revealed significant deviations of $[Ca^{2+}]_{cyt}$ reactions in guard cells of epidermal peels from those of intact plant leaves, indicating impairment $[Ca^{2+}]_{cyt}$ homeostasis in prepared guard cells.

Insignificance of $[Ca^{2+}]_{cyt}$ elevations during ABA signal transduction and unimportance of some potential second messengers operating in animal cells, reported in the presented study may suggest that some of currently accepted opinions concerning ABA signaling in guard cells must be reassessed.

Altogether, the main results of the experimental work outline next:

1) Guard cells of intact plants respond to ABA with activation of anion efflux current via plasma membrane. The response has strongly reproducible kinetics and likely, is conserved between different plant species.

2) Anion efflux current in guard cells of intact *Vicia faba* leaves is curried via both R- and S-type plasma membrane anion channels and has an amplitude and kinetics which correspond to naturally observing ABA-induced stomatal closure.

3) ABA-signaling machinery of guard cell represents an autonomously functioning circuit with the amplification mechanism, requiring only short-time signal perception for the initiation of delayed response. Signaling mechanism completely resets within short times (comparable to the duration of the response) and could be started repeatedly within the same cell upon serial stimulus applications.

4) Tuning of the signaling mechanism sensitivity is rather complex and do not obviously depend on serial stimulus applications.

5) The ABA receptor, responsible for the initiation of stomatal closure most likely localized from the cytoplasmic side of the plasma membrane.

6) Elevation of $[Ca^{2+}]_{cyt}$ level is not necessary event in the signal transduction chain leading from ABA perception to the activation of guard cell plasma membrane anion channels. Physiological resting $[Ca^{2+}]_{cyt}$ level is important for the ability of guard cells to respond to ABA.

7) Most of potential second messengers of animal cells could not mimic ABA in its ability to initiate anion efflux currents via guard cell plasma membrane.

8) Mechanism of $[Ca^{2+}]_{cyt}$ homeostasis is impaired in guard cells of detached epidermis. Impairment of $[Ca^{2+}]_{cyt}$ homeostasis together with crucially reduced plasma membrane responses may characterize guard cells of isolated epidermis as measuring system which may provide registration of responses far from normal physiological reactions taking place *in vivo*.

This new experimental data, obtained in registrations on guard cells of intact plant leaves arise additional questions ranging from special aspects of ABA signaling to general principles of plant cell signaling organization.

Concerning guard cell of higher land plant stomata, which has "concentrated" sensory function and participates in integration of virtually whole plant metabolism, questions of signaling are of special interest. Further highly relevant physiological and biochemical experiments will require for revealing key points in signaling, like the nature of the cytoplasmic

factors which amplify and transduce ABA signal to anion channels behind commonly accepted $[Ca^{2+}]_{cyt}$. One of most potent candidate to this role may be a cellular phosphorylation/dephosphorylation mechanisms, which have quite a specificity and are poorly understood in plant cells yet.

Another "black box" in plant cell signaling and ion homeostasis represents the vacuole, which occupies up to 90% of plant cell volume and may contain up to …% of total ions. Presented in the literature data point to the participation of vacuoles in ion exchange processes, namely, H^+/Cl^- and H^+/Ca^{2+} exchange. These mechanisms may have direct relation to signaling and are of big interest, although accessing the function of intact plant vacuoles may represent big experimental difficulties.

The fact is intriguing, that in guard cells of isolated epidermis $[Ca^{2+}]_{cyt}$ increases are common during ABA action, while *in situ* registrations do not confirm them despite of obvious membrane response. Preliminary data suggest possible role for pH_{cyt} in ABA and some other stimuli transduction. Related to the vacuole activity the interconnection of Ca^{2+} and H^+ signaling, which is not studied in guard cells yet, may explain such a difference in behavior of intact and isolated guard cells. Breakage of Ca^{2+}/H^+ interconnection mechanism will remain a staircase with selectively broken odd or even sticks, which is still functional by some mean, but will represent doubtful instrument to be used.

Once selected the strategy of sitting life seemingly, plants evolutionary put themselves into a special, possibly simplified, or "льготные" conditions of the environmental information requirement. Naturally, plant organisms do not suffer from the idea of their location change within the living areal in search for the energy source. Thus plants do not select their environment and do not run into continuous flow of information related to geographical relocations like animals do. Such early evolutionary division on the principle of environmental information requirement may well not refuse that plant cell may utilize another than animal ways of information processing and have evolved corresponding specific organization of cell signaling machinery. Listed above experimental facts, including unimportance of $[Ca^{2+}]_{cyt}$ changes and commonly known second messengers in guard cell ABA signaling may represent support for such hypothesis.

LIST OF CITED LITERATURE

Ache P, Becker D, Ivashikina N, Dietrich P, Roelfsema MRG, Hedrich R. 2000. GORK, a delayed outward rectifier expressed in guard cells of *Arabidopsis thaliana*, is a K^+-selective, K^+-sensing ion channel. *FEBS Letters* **486**: 93–98.

Allan AC, Fricker DM, Ward JL, Beale MH, Trewavas AJ. 1994. Two transduction pathways mediate rapid effects of abcisic acid in *Commelina* guard cells. *Plant Cell* **6**: 1319-1328.

Allen GJ, Sanders D. 1994. Two voltage gated, calcium release channels co reside in the vacuolar membrane of broad bean guard cells. *Plant Cell* **6**: 685–694.

Allen GJ, Sanders D. 1996. Control of ionic currents in guard cell vacuoles by cytosolic and luminal calcium. *Plant Journal* **10**: 1055–1069.

Allen GJ, Muir SR, Sanders D. 1995. Release of Ca^{2+} from individual plant vacuoles by both InsP3 and cyclic ADP-ribose. *Science* **268**: 735–737.

Allen GJ, Amtmann A, Sanders D. 1998. Calcium-dependent and calcium-independent K^+ mobilization channels in *Vicia faba* guard cell vacuoles. *Journal of Experimental Botany* **49**: 305–318.

Allen GJ, Kuchitsu K, Chu SP, Murata Y, Schroeder JI. 1999a. Arabidopsis abi1-1 and abi2-1 phosphatase mutations reduce abscisic acid-induced cytosolic calcium rises in guard cells. *Plant Cell* **11**: 1785–1798.

Allen GJ, Kwak JM, Chu SP, Llopis J, Tsien RY, Harper JF, Schroeder JI. 1999b. Cameleon calcium indicator reports cytoplasmic calcium dynamics in *Arabidopsis* guard cells. *Plant Journal* **19**: 735–747.

Allen GJ, Chu SP, Schumacher K, Shimazaki CT, Vafeados D, Kemper A, Hawke SD, Tallman G, Tsien RY, Harper JF, Chory J, Schroeder JI. 2000. Alteration of stimulus-specific guard cell calcium oscillations and stomatal closing in *Arabidopsis* det3 mutant. *Science* **289**: 2338–2342.

Allen GJ, Chu SP, Harrington CL, Schumacher K, Hoffmann T, Tang YY, Grill E, Schroeder JI. 2001. A defined range of guard cell calcium oscillation parameters encodes stomatal movements. *Nature* **411**: 1053–1057.

Allen GJ, Murata Y, Chu SP, Nafisi M, Schroeder JI. 2002. Hypersensity of abscisic acid-induced cytosolic calcium increases in the *Arabidopsis* farnesyltransferase mutant *era1-2*. *Plant Cell* **14**: 1649–1662.

Anderson JA, Huprikar SS, Kochian LV, Lucas WJ, Gaber RF. 1992. Functional expression of a probable *Arabidopsis thaliana* potassium channel in *Saccharomyces cerevisiae*. *Proceedings of the National Academy of Sciences of USA* **89**: 3736–3740.

Anderson BE, Ward JM, Schroeder JI. 1994. Evidence for an extracellular reception site for abscisic acid in Commelina guard cells. *Plant Physiology* **104**: 1177–1183.

Armstrong F, Leung J, Grabov A, Brearley J, Giraudat J, Blatt MR. 1995. Sensitivity to abscisic acid of guard-cell K^+ channels is suppressed by abi1–1, a mutant Arabidopsis gene encoding a putative protein phosphatase. *Proceedings of the National Academy of Sciences of USA* **92**: 9520–9524.

Assmann SM. 1993 Signal transduction in guard cells. *Annual Reviews of Cell Biology* **9**: 345–375.

Assmann SM, Shimazaki KI. 1999. The multisensory guard cell. Stomatal responses to blue light and abscisic acid. *Plant Physiology* **119**: 809–815.

Assmann SM, Simoncini L, Schroeder JI. 1985. Blue light activates electrogenic ion pumping in guard cell protoplasts of *Vicia faba*. *Nature* **318**: 285–287.

Assmann SM, Snyder JA, Lee YRJ. 2000. ABA-deficient (aba1) and ABA-insensitive (abi1-1, abi2-1) mutants of *Arabidopsis* have a wild-type stomatal response to humidity. *Plant, Cell & Environment* **23**: 387–395.

Axelsen KB, Palmgren MG. 2001. Inventory of the superfamily of P-type Ion pumps in Arabidopsis. *Plant Physiology* **126**: 696–706.

Barbier-Brygoo H, Vinauger M, Colcombet J, Ephritikhine G, Frachisse J-M, Maurel C. 2000. Anion channels in higher plants: functional characterization, molecular structure and physiological role. *Biochim. Biophys. Acta* **1465**: 199–218.

Baum G, Long JC, Jenkins GI, Trewavas AJ. 1999. Stimulation of the blue light phototropic receptor NPH1 causes a transient increase in cytosolic Ca^{2+}. *Proceedings of the National Academy of Sciences of USA* **96**: 13554–13559.

Becker D, Zeilinger C, Lohse G, Depta H, Hedrich R. 1993. Identification and biochemical characterization of the plasma-membrane proton ATPase in guard cells of *Vicia faba* L. *Planta* **190**: 44–50.

Becker D, Geiger D, Dunkel M, Roller A, Bertl A, Latz A, Carpaneto A, Dietrich P, Roelfsema MRG, Völker C, Schmidt D, Müller-Röber B, Czempinski K, Hedrich R. 2004. AtTPK4, an *Arabidopsis* tandem-pore K^+ channel, poised to control the pollen membrane voltage in a pH- and Ca^{2+}-dependent manner. *Proceedings of the National Academy of Sciences of USA* **101**: 15621–15626.

Berkowitz G, Zhang X, Mercie R, Leng Q, Lawton M. 2000. Co-expression of calcium-dependent protein kinase with the inward rectified guard cell K^+ channel KAT1 alters current parameters in Xenopus laevis oocytes. *Plant and Cell Physiology* **41**: 785-790.

Birnbaum K, Shasha DE, Wang JY, Jung JW, Lambert GM, Galbraith DW, Benfey PN. 2003. A gene expression map of the Arabidopsis root. *Science* **302**: 1956–1960.

Blatt MR. 1987. Electrical characteristics of stomatal guard cells: the ionic basis of the membrane potential and the consequence of potassium chloride leakage from microelectrodes. *Planta* **170**: 272–287.

Blatt MR. 1988. Potassium-dependent, bipolar gating in K^+ channels of guard cells. *Journal of Membrane Biology* **102**: 235–246.

Blatt, M. R. 1990. Potassium channel currents in intact stomatal guard ceils: rapid enhancement by abscisic acid. *Planta* **180**: 445–455.

Blatt MR. 1992. K^+ channels of stomatal guard cells. Characteristics of the inward rectifier and its control by pH. *Journal of General Physiology* **99**: 615–644.

Blatt MR, Armstrong F. 1993. K^+ channels of stomatal guard cells: Abscisic-acid-evoked control of the outward rectifier mediated by cytoplasmic pH. *Planta* **191**: 330–341.

Blatt MR, Thiel G. 1994. K^+ channels of stomatal guard cells: bimodal control of the K^+ inward-rectifier evoked by auxin. *Plant Journal* **5**: 55–68.

Blatt MR, Thiel G, Trentham DR. 1990. Reversible inactivation of K^+ channels of Vicia stomatal guard cells following the photolysis of caged inositol 1,4,5-triphosphate. *Nature* **346**: 766–769.

Blatt MR, Grabov A, Brearley J, Hammond-Kosack K, Jones JDG. 1999. K^+ channels of Cf-9 transgenic tobacco guard cells as targets for *Cladosporium fulvum* Avr9 elicitor-dependent signal transduction. *Plant Journal* **19**: 453–462.

Blatt MR. 2000. Cellular signaling and volume control in stomatal movements in plants. *Annual Review of Cell and Developmental Biology* **16**: 221–241.

Bonza, M.C., Morandini, P., Luoni, L., Geisler, M., Palmgren, M.G., and De Michelis, M.I. 2000. At-ACA8 encodes a plasma membrane-localized calcium-ATPase of Arabidopsis with a calmodulin-binding domain at the N terminus. *Plant Physiology* **123**: 1495–1506.

Brearley J, Venis MA, Blatt MR. 1997. The effect of elevated CO_2 concentrations on K^+ and anion channels of *Vicia faba* L. guard cells. *Planta* **203**: 145–154.

Briggs WR, Christie JM. 2002. Phototropins 1 and 2: versatile plant blue-light receptors. *Trends in Plant Science* **7**: 204–210.

Carpaneto A, Cantù AM, Gambale F. Effects of cytoplasmic Mg^{2+} on slowly activating channels in isolated vacuoles of *Beta vulgaris*. *Planta*. **213**: 457-468.

Cellier F, Conejero G, Ricaud L, Doan TL, Lepetit M, Gosti F, Casse F. 2004. Characterization of AtCHX17, a member of the cation/H^+ exchangers, CHX family, from *Arabidopsis thaliana* suggests a role in K^+ homeostasis. *Plant Journal* **39**: 834–846.

Christie JM, Salomon M, Nozue K,Wada M, Briggs WR. 1999. LOV (light, oxygen, or voltage) domains of the blue light photoreceptor phototropin (nph1): Binding sites for the

chromophore flavin mononucleotide. *Proceedings of the National Academy of Sciences of USA* **96**: 8779–8783

Cosgrove DJ, Hedrich R. 1991. Stretch-activated chloride, potassium, and calcium channels coexisting in plasma membranes of guard cells of *Vicia faba* L. *Planta* **186**: 143–153.

Coursol S, Fan L-M, Le Stunff H, Spiegel S, Gilroy S, Assmann SM. 2003. Sphingolipid signalling in Arabidopsis guard cells involves heterotrimeric G proteins. *Nature* **423**: 651–654.

Cutler AJ and Krochko EJ. 1999. Formation and breakdown of ABA. *Trends in Plant Science* **4**: 472–478.

Czempinski K, Gaedeke N, Zimmermann S, Müller-Röber B. 1999. Molecular mechanisms and regulation of plant ion channels. *Journal of Experimental Botany* **50**: 955–966.

Czempinski K, Frachisse JM, Maurel C, Barbier-Brygoo H, Müller-Röber B. 2002. Vacuolar membrane localization of the *Arabidopsis* 'two-pore' K$^+$ channel KCO1. *Plant Journal* **29**: 809–820.

Davies JM, Hunt I, Sanders D. 1994. Vacuolar H$^+$-pumping ATPase variable transport coupling ratio controlled by pH. *Proceedings of the National Academy of Sciences of USA* **91**: 8547–8551.

De Angeli A, Thomine S, Frachisse JM, Ephritikhine G, Gambale F, Barbier-Brygoo H. Anion channels and transporters in plant cell membranes. *FEBS Letters* **581**: 2367-2374.

Demidchik V, Davenport RJ, Tester M. 2002. Nonselective cation channels in plants. *Annual Review of Plant Biology* **53**: 67–107.

DeSilva DLR, Hetherington AM, Mansfield TA. 1985a. Synergism between calcium ions and abscisic acid in preventing stomatal opening. *New Phytologist* **100**: 473–482.

DeSilva DLR, Cox RC, Hetherington AM, Mansfield TA. 1985b. Suggested involvement of calcium and calmodulin in the responses of stomata to abscisic acid. *New Phytologist* **101**: 555–563.

Diekmann W, Hedrich R, Raschke K, Robinson DG. 1993. Osmocytosis and vacuolar fragmentation in guard cell protoplasts: Their relevance to osmotically-induced volume changes in guard cells. *Journal of Experimental Botany* **44**: 1569–1577.

Dietrich P, Hedrich R. 1994. Interconversion of fast and slow gating modes of GCAC1, a guard cell anion channel. *Planta* **195**: 301–304.

Dietrich P, Hedrich R. 1998. Anions permeate and gate GCAC1, a voltage dependent anion channel. *Plant Journal* **16**: 479–487.

Dietrich P, Dreyer I, Wiesner P, Hedrich R. 1998. Cation sensitivity and kinetics of guard-cell potassium channels differ among species. *Planta* **205**: 277–287.

Dietrich P, Sanders D, Hedrich R. 2001. The role of ion channels in light-dependent stomatal opening. *Journal of Experimental Botany* **52**: 1959–1967.

Dolmetsch RE, Lewis RS, Goodnow CC, Healy JI. 1997. Differential activation of transcription factors induced by Ca2+ response amplitude and duration. *Nature* **386**: 855–858.

Dolmetsch RE, Xu K, Lewis RS. 1998. Calcium oscillations increase the efficiency and specificity of gene expression. *Nature* **392**: 933–936.

Drozdowicz YM, Rea PA. 2001. Vacuolar H^+ pyrophosphatases: from the evolutionary backwaters into the mainstream. *Trends in Plant Science* **6**: 206–211.

Esser JE, Liao Y-J, Schroeder JI. 1997. Characterization of ion channel modulator effects on ABA- and malate-induced stomatal movements: strong regulation by kinase and phosphatase inhibitors, and relative insensitivity to mastoparans. *Journal of Experimental Botany* **48**: 539–550.

Evans NH, McAinsh MR, Hetherington AM. 2001. Calcium oscillations in higher plants. *Current Opinion in Plant Biology* **4**: 415-420.

Felle H. 1988. Cytoplasmic free calcium in *Riccia* fluitans L. & *Zea mays* L. Interaction of Ca^{2+} and pH. *Planta* **176**: 248–255.

Felle H, Hanstein S, Steinmeyer R, Hedrich R. 2000. Dynamics of ionic activities in the apoplast of the sub-stomatal cavity of intact *Vicia faba* leaves during stomatal closure evoked by ABA and darkness. *Plant Journal* **24**: 297–304.

Fischer RA. 1968. Stomatal opening: Role of potassium uptake by guard cells. *Science* **160**: 784–785.

Franks PJ. 2003. Use of the pressure probe in studies of stomatal function. *Journal of Experimental Botany* **54**: 1495–1504.

Fuglsang AT, Borch J, Bych K, Jahn TP, Roepstorff P, Palmgren MG. 2003. The binding site for regulatory 14-3-3 protein in plant plasma membrane H^+-ATPase: Involvement of a region promoting phosphorylation-independent interaction in addition to the phosphorylation-dependent C-terminal end. *Journal of Biological Chemistry* **278**: 42266–42272.

Furuichi T, Cunningham KW, Muto S. 2001. A putative two pore channel AtTPC1 mediates Ca^{2+} flux in *Arabidopsis* leaf cells. *Plant and Cell Physiology* **42**: 900–905.

Gambale F, Kolb HA, Cantu AM, Hedrich R. 1994. The voltage-dependent H^+-ATPase of the sugar-beet vacuole is reversible. *European Biophysics Journal with Biophysics Letters* **22**: 399–403.

Gaxiola RA, Rao R, Sherman A, Grisafi P, Alper SL, Fink GR. 1999. The *Arabidopsis thaliana* proton transporters, AtNhx1 and Avp1, can function in cation detoxification in yeast. *Proceedings of the National Academy of Sciences of USA* **96**: 1480–1485.

Geelen D, Lurin C, Bouchez D, Frachisse JM, Lelievre F, Courtial B, Barbier-Brygoo H, Maurel C. 2000. Disruption of putative anion channel gene AtClC-a in *Arabidopsis* suggests a role in the regulation of nitrate content. *Plant Journal* **21**: 259–267.

Gilroy S, Read ND, Trewavas AJ. 1990. Elevation of cytoplasmic calcium by caged calcium or caged Inositol triphosphate initiates stomatal closure. *Nature* **346**: 769–771.

Gilroy S, Fricker MD, Read ND, Trewavas AJ. 1991. Role of calcium in signal transduction of *Commelina* guard cells. *Plant Cell* **3**: 333–344.

Goh CH, Oku T, Shimazaki K. 1995. Properties of proton-pumping in response to bluelight and fusicoccin in guard-cell protoplasts isolated from adaxial epidermis of *Vicia* leaves. *Plant Physiology* **109**: 187–194.

Goh CH, Kinoshita T, Oku T, Shimazaki K. 1996. Inhibition of blue light-dependent H$^+$ pumping by abscisic acid in *Vicia* guard cell protoplasts. *Plant Physiology* **111**: 433 –440.

Gosti F, Beaudoin N, Serizet C, Webb ARR, et al. 1999. ABI1 protein phosphatase 2C is a negative regulator of abscisic acid signaling. *Plant Cell* **11**: 1897–910.

Grabov A, Blatt MR. 1997. Parallel control of the inward-rectifier K$^+$ channel by cytosolic free Ca^{2+} and pH in *Vicia* guard cells. *Planta* **201**: 84–95.

Grabov A, Leung J, Giraudat J, Blatt MR. 1997. Alteration of anion channel kinetics in wild-type and abi1-1 transgenic *Nicotiana benthamiana* guard cells by abscisic acid. *Plant Journal* **12**: 203–213.

Grabov A, Blatt MR. 1998. Membrane voltage initiates Ca^{2+} waves and potentiates Ca^{2+} increases with abscisic acid in stomatal guard cells. *Proceedings of the National Academy of Science of USA* **95**: 4778 –4783.

Grabov A, Blatt MR. 1999. A steep dependence of inward-rectifying potassium channels on cytosolic free calcium concentration increase evoked by hyperpolarization in guard cells. *Plant Physiology* **119**: 277–287.

Grynkiewicz G, Poenie M, Tsien RY. 1985. A new generation of Ca^{2+} indicators with greatly improved fluorescence properties. *Journal of Biological Chemistry* **260:** 3440-3450.

Hamill, OP, Marty A, Neher E, Sakmann B, Sigworth FJ. 1981. European *Journal of Physiology* **391**: 85–100.

Hamilton DW, Hills A, Köhler B, Blatt MR. 2000. Ca^{2+} channels at the plasma membrane of stomatal guard cells are activated by hyperpolarization and abscisic acid. *Proceedings of the National Academy of Sciences of USA* **97**: 4967–4972.

Hamilton DW, Hills A, Blatt MR. 2001. Extracellular Ba^{2+} and voltage interact to gate Ca^{2+} channels at the plasma membrane of stomatal guard cells. *FEBS Letters* **491**: 99–103.

Han S, Tang R, Anderson LK, Woerner TE, Pei ZM. 2003. A cell surface receptor mediates extracellular Ca^{2+} sensing in guard cells. *Nature* **425**: 196–200.

Harmon AC, Gribskov M, Harper JF. 2000 CDPKs: a kinase for every Ca^{2+} signal? *Trends in Plant Sciences* **5**: 154–159.

Harper JF. 2001. Dissecting calcium oscillators in plant cells. *Trends in Plant Sciences* **6**: 395-397.

Hartung W, Sauter A, Hose E. 2002. Abscisic acid in the xylem: Where does it come from, where does it go to? *Journal of Experimental Botany* **53**: 27–32.

Heath OVS. 1959. Light and carbon dioxide in stomatal movements. *Encyclopedia of Plant Physiology* **17**: 415–464.

Hedrich R, Flügge UI, Fernandez JM. 1986. Patch-clamp studies of ion-transport in isolated plant vacuoles. *FEBS Letters* **204**: 228–232.

Hedrich R, Neher E. 1987. Cytoplasmic calcium regulates voltage dependent ion channels in plant vacuoles. *Nature* **329**: 833–836.

Hedrich R, Kurkdjian A, Guern J, Flügge UI. 1989. Comparative studies on the electrical-properties of the H^+ translocating ATPase and pyrophosphatase of the vacuolar-lysomal compartment. *EMBO Journal* **8**: 2835–2841.

Hedrich R, Marten I. 1993. Malate-induced feedback regulation of plasma membrane anion channels could provide a carbon dioxide sensor to guard cells. *EMBO Journal* **12**: 897–901.

Hedrich R, Busch H, Raschke K. 1990. Calcium ion and nucleotide dependent regulation of voltage dependent anion channels in the plasma membrane of guard cells. *EMBO Journal* **9**: 3889–3892.

Hedrich R, Marten I, Lohse G, Dietrich P, Winter H, Lohaus G, Heldt HW. 1994. Malate-sensitive anion channels enable guard cells to sense changes in the ambient CO_2 concentration. *Plant Journal* **6**: 741–748.

Hey SJ, Bacon A, Burnett E, Neill SJ 1997. Abscisic acid signal transduction in epidermal cells of Pisum sativum L. Argenteum: both dehydrin mRNA accumulation and stomatal sponses require protein phosphorylation and dephosphorylation. *Planta* **202**: 85–92.

Hong Y, Takano M, Liu CM, Gasch A, Chye ML, Chua NH. 1996 Expression of three members of the calcium-dependent protein kinase gene family in *Arabidopsis thaliana*. *Plant Molecular Biology* **30**: 1259–1275.

Hoshi T. 1995. Regulation of voltage-dependence of the KAT1 channel by intracellular factors. *Journal of General Physiology* **105**: 309–328.

Hosy E, Vavasseur A, Mouline K, Dreyer I, Gaymard F, Poree F, Boucherez J, Lebaudy A, Bouchez D, Véry AA, Simonneau T, Thibaud JB, Sentenac H. 2003. The

Arabidopsis outward K$^+$ channel GORK is involved in regulation of stomatal movements and plant transpiration. *Proceedings of the National Academy of Sciences of USA* **100**: 5549–5554.

Hosoi S, M. Iino, and K. Shimazaki. 1988. Outward-rectifying K$^+$ channels in stomatal guard cell protoplasts. *Plant and Cell Physiology* **29**: 907–911.

Hoth S, Dreyer I, Dietrich P, Becker D, Müller-Röber B, Hedrich R. 1997. Molecular basis of plant-specific acid activation of K$^+$ uptake channels. *Proceedings of the National Academy of Sciences of USA* **94**:4806–4810.

Hoth S, Hedrich R. 1999. Distinct molecular bases for pH sensitivity of the guard cell K$^+$ channels KST1 and KAT1. Journal of Biological Chemistry **274**: 11599–11603.

Hugouvieux V, Kwak JM, Schroeder JI. 2001. An mRNA cap binding protein, ABH1, modulates early abscisic acid signal transduction in *Arabidopsis*. *Cell* **106**: 477–487.

Hunt L, Mills JN, Pical C, Leckie CP, Aitken FL, et al. 2003. Phospholipase C is required for the control of stomatal aperture by ABA. *Plant Journal* **34**: 47–55.

Hwang I, Sze H, Harper JF. 2000. A calcium-dependent protein kinase can inhibit a calmodulin-stimulated Ca^{2+} pump (ACA2) located in the endoplasmic reticulum of *Arabidopsis*. *Proceedings of the National Academy of Sciences of USA* **97**: 6224–6229.

Iino M, Ogawa T, Zeiger E. 1985. Kinetic properties of the blue-light response of stomata. *Proceedings of the National Academy of Sciences of USA* **82**: 8019–8023.

Ilan N, Moran N, Schwartz A. 1995. The role of potassium channels in the temperature control of stomatal aperture. *Plant Physiology* **108**: 1161–1170.

Inada S, Ohgishi M, Mayama T, Okada K, Sakai T. 2004. RPT2 is a signal transducer involved in phototropic response and stomatal opening by association with phototropin 1 in *Arabidopsis thaliana*. *Plant Cell* **16**: 887–896.

Irving HR, Gehring CA, Parish RW. 1992. Changes in cytosolic pH and calcium of guard cells precede stomatal movements. *Proceedings of the National Academy of Sciences of USA* **89**: 1790–1794.

Ivashikina N, Hedrich R. 2005. K$^+$ currents through SV type vacuolar channels are sensitive to elevated luminal sodium levels. *Plant Journal* **41**: 606–614.

Jacob T, Ritchie S, Assmann SM, Gilroy S. 1999. Abscisic acid signal transduction in guard cells is mediated by phospholipase D activity. *Proceedings of the National Academy of Sciences of USA* **96**: 12192–12197.

Kaiser H, Kappen L. 2001. Stomatal oscillations at small apertures: indications for a fundamental insufficiency of stomatal feedback-control inherent in the stomatal turgor mechanism. *Journal of Experimental Botany* **52**: 1303–1313.

Keller BU, Hedrich R, Raschke K. 1989. Voltage-dependent anion channels in the plasma membrane of guard cells. *Nature* **341**: 450–453.

Kinoshita T, Nishimura M, Shimazaki K-I. 1995. Cytosolic concentration of Ca^{2+} regulates the plasma membrane H^+-ATPase in guard cells of fava bean. *Plant Cell* **7**: 1333–1342.

Kinoshita T, Shimazaki K. 1997. Involvement of calyculin A- and okadaic acid-sensitive protein phosphatase in the blue light response of stomatal guard cells. *Plant Cell Physiology* **38**:1281–1285.

Kinoshita T, Shimazaki K-I. 1999. Blue light activates the plasma membrane H^+-ATPase by phosphorylation of the C terminus in stomatal guard cells. *EMBO Journal* **18**: 5548–5558.

Kinoshita T, Doi M, Suetsugu N, Kagawa T, Wada M, Shimazaki KI. 2001. Phot1 and phot2 mediate blue light regulation of stomatal opening. *Nature* **414**: 656–660.

Kinoshita T, Emi T, Tominaga M, Sakamoto K, Shigenaga A, Doi M, Shimazaki KI. 2003. Blue-light- and phosphorylation-dependent binding of a 14-3-3 protein to phototropins in stomatal guard cells of broad bean. *Plant Physiology* **133**: 1453–1463.

Klein M, Cheng G, Chung M, Tallman G. 1996. Effects of turgor potentials of epidermal cells neighbouring guard cells on stomatal opening in detached leaf epidermis and intact leaflets of *Vicia faba* L. (faba bean). *Plant, Cell & Environment* **19**: 1399–1407.

Kluge C, Lahr J, Hanitzsch M, Bolte S, Golldack D, Dietz KJ. 2003. New insight into the structure and regulation of the plant vacuolar H^+-ATPase. *Journal of Bioenergetics and Biomembranes* **35**: 377–388.

Klüsener B, Young JJ, Murata Y, Allen GJ, Mori LC, Hugouvieux V, Schroeder JI. 2002. Convergence of calcium signalling pathways of pathogenic elicitors and abscisic acid in *Arabidopsis* guard cells. *Plant Physiology* **130**: 2152–2163.

Kolb HA, Marten I, Hedrich R. 1995. Hodgkin-Huxley analysis of a GCAC1 anion channel in the plasma membrane of guard cells. *Journal of Membrane Biology* **146**: 273 –282.

Köhler B, Blatt MR. 2002. Protein phosphorylation activates the guard cell Ca^{2+} channel and is a prerequisite for gating by abscisic acid. *Plant Journal* **32**: 185–194.

Koornneef M, Reuling G, and Karssen CM. 1984. The isolation and characterization of abscisic acid–insensitive mutants of *Arabidopsis thaliana. Physiologia Plantarum* **61**, 377–383.

Kuiper PJC. 1964. Dependence upon wavelength of stomatal movement in epidermal tissue of *Senecio odoris. Plant Physiology* **39**: 952–955.

Kwak JM, Murata Y, Baizabal-Aguirre VM, Merrill J, Wang M, Kemper A, Hawke SD, Tallman G, Schroeder JI. 2001. Dominant negative guard cell K^+ channel mutants re-

duce inward-rectifying K$^+$ currents and light-induced stomatal opening in *Arabidopsi*s. *Plant Physiology* **127**: 473–485.

Kwak JM, Moon JH, Murata Y, Kuchitsu K, Leonhardt N, DeLong A, Schroeder JI. 2002. Disruption of a guard cell-expressed protein phosphatase 2A regulatory subunit, RCN1, confers abscisic acid insensitivity in Arabidopsis. *Plant Cell* **14**: 2849-2861.

Kwak JM, Mori IC, Pei ZM, Leonhardt N, Torres MA, Dangl JL, Bloom RE, Bodde S, Jones JD, Schroeder JI. 2003. NADPH oxidase AtrbohD and AtrbohF genes function in ROS-dependent ABA signaling in *Arabidopsis*. *EMBO Journal* **22**: 2623-2633.

Langer K, Levchenko V, Fromm J, Geiger D, Steinmeyer R, Lautner S, Ache P, Hedrich R. 2004. The poplar K$^+$ channel KPT1 is associated with K$^+$ uptake during stomatal opening and bud development. *Plant Journal* **37**: 828–838.

Leckie CP, McAinsh MR, Allen GJ, Sanders D, Hetherington AM. 1998. Abscisic acid-induced stomatal closure mediated by cyclic ADP-ribose. *Proceedings of the National Academy of Sciences of USA* **95**: 15837–15842.

Lee HC. 1997. Mechanisms of calcium signaling by cyclic ADP-ribose and NAADP. *Physiological Reviews* **77**:1133–64

Lee YS, Choi YB, Shu S, Lee, J, Assmann SM, Joe CO, Kelleher JF and Crain RC. 1996. Abscisic acid-induced phosphinositide turn over in guard cell protoplasts of Vicia faba. *Plant Physiology* **110**: 987–996.

Lemtiri-Chlieh F, MacRobbie EAC. 1994. Role of calcium in the modulation of *Vicia* guard cell potassium channels by abscisic acid – a patch-clamp study. *Journal of Membrane Biology* **137**: 99–107.

Lemtiri-Chlieh F, MacRobbie EAC, Webb AAR, Manison NF, Brownlee C, Skepper JN, Chen J, Prestwich GD, Brearley CA. 2003. Inositol hexakisphosphate mobilizes an endomembrane store of calcium in guard cells. *Proceedings of the National Academy of Sciences of USA* **100**: 10091–10095.

Leube MP, Grill E, Amrhein N. 1998. ABI1 of Arabidopsis is a protein serine/threonine phosphatase highly regulated by the proton and magnesium ion concentration. *FEBS Letters* **424**: 100–104.

Leung J, Bouvier-Durand M, Morris P-C, Guerrier D, Chefdor F, Giraudat J. 1994. *Arabidopsis* ABA response gene ABI1 – features of a calcium-modulated protein phosphatase. *Science* **264**: 1448–1452.

Leung J, Merlot S, Giraudat J. 1997. The *Arabidopsis* abscisic acid-insensitive (ABI2) and ABI1 genes encode homologous protein phosphatases 2C involved in abscisic acid signal transduction. *Plant Cell* **9**: 759–771.

Levchenko V, Konrad KR, Dietrich P, Roelfsema MRG, Hedrich R. 2005. Cytosolic ABA activates guard cell anion channels without preceding Ca^{2+} signals. *Proceedings of the National Academy of Sciences of USA* **102**: 4203–4208.

Levchenko V, Guinot DR, Klein M, Roelfsema MRG, Hedrich R and Dietrich P. 2008 Stringent control of cytoplasmic Ca^{2+} in guard cells of intact plants compared to their counterparts in epidermal strips or guard cell protoplasts. *Protoplasma* **233**: 61-72.

Li J, Assmann SM. 1996. An abscisic acid-activated and calcium-independent protein kinase from guard cells of fava bean. *Plant Cell* **8**:2359–2368.

Li J, Lee Y-RJ, Assmann SM. 1998. Guard cells possess a calcium-dependent protein kinase that phosphorylates the KAT1 potassium channel. *Plant Physiol*ogy **116**: 785–795.

Li J, Wang XQ, Watson MB, Assmann SM. 2000. Regulation of abscisic acid-induced stomatal closure and anion channels by guard cell AAPK kinase. *Science* **287**: 300–303.

Li S, Assmann SM, Albert R. 2006 Predicting essential components of signal transduction networks: a dynamic model of guard cell abscisic acid signaling. *PLoS Biology* **4**: 1732–1748.

Linder B, Raschke K. 1992. A slow anion channel in guard cells, activating at large hyperpolarization, may be principal for stomatal closing. *FEBS Letters* **313**: 27–30.

Lino, B, Baizabal-Aguirre VM, de la Vara LEG. 1998. The plasma-membrane H^+-ATPase from beet root is inhibited by a calcium-dependent phosphorylation. *Planta* **204**: 352–359.

Lohse G, Hedrich R. 1992. Characterization of the plasma-membrane H^+-ATPase from *Vicia faba* guard cells. *Planta* **188**: 206–214.

Luan S, Li W, Rusnak F, Assmann SM, Schreiber SL. 1993. Immunosuppressants implicate protein phosphatase regulation of K^+ channels in guard cells. *Proceedings of the National Academy of Sciences of USA* **90**: 2202–2206.

MacRobbie EAC. 1981. Effect of ABA on 'isolated' guard cells of *Commelina communis* L. *Journal of experimental botany* **32**: 563–572.

MacRobbie EAC. 1987. Ionic relations of guard cells. In: Zeiger E, Farquhar GD, Cowan IR, eds. Stomatal Function. Stanford, CA, USA: Stanford University Press, 125–162.

MacRobbie EAC. 1995. ABA-induced ion efflux in stomatal guard cells: multiple actions of ABA inside and outside the cell. *Plant Journal* **7**: 565–576.

MacRobbie EAC. 1998. Signal transduction and ion channels in guard cells. *Philosophical Transactions of the Royal Society of London Series B Biological Sciences* **353**: 1475 –1488.

MacRobbie EAC. 2000. ABA activates multiple Ca^{2+} fluxes in stomatal guard cells, triggering vacuolar K^+ (Rb^+) release. *Proceedings of the National Academy of Sciences of USA* **97**: 12361–12368.

MacRobbie EAC. 2006. Control of volume and turgor in stomatal guard cells. *Journal of membrane biology* **210**: 131–142.

Maeshima M. 2000. Vacuolar H$^+$-pyrophosphatase. *Biochimica et Biophysica Acta – Biomembranes* **1465**: 37–51.

Marmagne A, Rouet MA, Ferro M, Rolland N, Alcon C, Joyard J, Garin J, Barbier-Brygoo H, Ephritikhine G. 2004. Identification of new intrinsic proteins in Arabidopsis plasma membrane proteome. *Molecular and Cellular Proteomics* **3**: 675 –691.

Marten I, Zeilinger C, Redhead C, Landry DW, Al-Awqati Q, Hedrich R. 1992. Identification and modulation of a voltage-dependent anion channel in the plasma membrane of guard cells by high-affinity ligands. *EMBO Journal* **11**: 3569 –3575.

Marten H, Hedrich R, Roelfsema MRG. Blue light inhibits guard cell plasma membrane anion channels in a phototropin-dependent manner. *Plant Journal* **50**: 29-39.

Marten H, Konrad K.R, Dietrich P, Roelfsema MRG, Hedrich R. 2007. Ca^{2+}-dependent and -independent abscisic acid activation of plasma membrane anion channels in guard cells of *Nicotiana tabacum. Plant Physiology* **143**: 28–37.

McAinsh MR, Brownlee C, Hetherington AM. 1990. Abscisic acid-induced elevation of guard cell cytosolic Ca^{2+} precedes stomatal closure. *Nature* **343**: 186–188.

McAinsh MR, Brownlee C, Hetherington AM. 1992. Visualizing Changes in Cytosolic-Free Ca^{2+} during the Response of Stomatal Guard Cells to Abscisic Acid. *Plant Cell* **4**:1113-1122.

McAinsh MR, Webb AAR, Staxen I, Taylor JE, Hetherington AM. 1995. Stimulus-induced oscillations in guard cell cytosolic free Ca^{2+}. *Plant Cell* **7**: 1207–1219.

Merlot S, Gosti F, Guerrier D, Vavasseur A, Giraudat J. 2001. The ABI1 and ABI2 protein phosphatases 2C act in a negative feedback regulatory loop of the abscisic acid signaling pathway. *Plant Journal* **25**: 1–10.

Merlot S, Mustilli AC, Genty B, North H, Lefebvre V, Sotta B, Vavasseur A, Giraudat J. 2002. Use of infrared thermal imaging to isolate Arabidopsis mutants defective in stomatal regulation. *Plant Journal* **30**: 601–609.

Meyer K, Leube MP, Grill E. 1994. A protein phosphatase 2C involved in ABA signal transduction in Arabidopsis thaliana. *Science* **264**:1452–1455.

Miediema H, Assmann SM. 1996. A membrane-delimited effect of internal pH on the K$^+$ outward rectifier of *Vicia faba* guard cells. *Journal of Membrane Biology* **154**: 227–237.

Mori IC, Muto S. 1997. Abscisic acid activates a 48-kilodalton protein kinase in guard cell protoplasts. *Plant Physiology* **113**: 833–840.

Mori IC, Murata Y, Yang Y, Munemasa S, Wang YF, Andreoli S, Tiriac H, Alonso JM, Harper JF, Ecker JR, Kwak JM, Schroeder JI. 2006. CDPKs CPK6 and CPK3 function in ABA regulation of guard cell S-type anion- and Ca^{2+}-permeable channels and stomatal closure. *PLoS Biol*. **4**: 1749–1762.

Mott KA and Buckley TN. 2000 Patchy stomatal conductance: emergent collective behaviour of stomata. *Trends in Plant Sciences* **5** 258 – 262.

Mustilli A-C, Merlot S, Vavasseur A, Fenzi F, Giraudat J. 2002 Arabidopsis OST1 protein kinase mediates the regulation of stomatal aperture by abscisic acid and acts upstream of reactive oxygen species production. *Plant Cell* **14**: 3089–3099.

Müller-Röber B, Ellenberg J, Provart N, Willmitzer L, Busch H, Becker D, Dietrich P, Hoth S, Hedrich R. 1995. Cloning and electrophysiological analysis of KST1, an inward rectifying K^+ channel expressed in potato guard cells. *EMBO Journal* **14**: 2409–2416.

Müller-Röber B, Ehrhardt T, Plesh G. 1998. Molecular features of stomatal guard cells. *Journal of Experimental Botany* **49**:293–304.

Nakamura RL, McKendree WL, Hirsch RE, Sedbrook JC, Gaber RF, Sussman MR. 1995. Expression of an *Arabidopsis* potassium channel gene in guard cells. *Plant Physiology* **109**: 371–374.

Navazio, L., Bewell, M.A., Siddiqua, A., Dickinson, G.D., Galione,A., and Sanders, D. 2000. Calcium release from the endoplasmic reticulum of higher plants elicited by the NADP metabolite nicotinic acid adenine dinucleotide phosphate. *Proceedings of the National Academy of Sciences of USA* **97**: 8693–8698.

Negi J, Matsuda O, Nagasawa T, Oba Y, Takahashi H, Kawai-Yamada M, Uchimiya H, Hashimoto M and Iba K. 2008. CO_2 regulator SLAC1 and its homologues are essential for anion homeostasis in plant cells. *Nature* **452**: 483 – 486.

Ng, C.K.Y., Carr, K., McAinsh, M.R., Powell, B., and Hetherington, A.M. 2001. Drought-induced guard cell signal transduction involves sphingosine-1-phosphate. *Nature* **410:** 596–598.

Ogunkanmi AB, Tucker DJ, Mansfield TA. 1973. An improved bioassay for abscisic acid and other antitranspirants. *New Phytologist* **72:** 277–282

Parmar PN, Brearley CA. 1995. Metabolism of 3- and 4-phosphorylated phosphatidylinositols in stomatal guard cells of *Commelina communis* L. *Plant Journal* **8**: 425–433.

Paterson NW, Weyers JDB and A'Brook R. 1988. The effect of pH on stomatal sensitivity to abscisic acid. *Plant, Cell and Environment* **11:** 83-89.

Pei Z-M, Ward JM, Harper JF, and Schroeder JI. 1996. A novel chloride channel in *Vicia faba* guard cell vacuoles activated by the serine/threonine kinase, CDPK. *EMBO Journal* **15**: 6564–6574

Pei Z-M, Kuchitsu K, Ward JM, Schwarz M, Schroeder JI. 1997. Differential abscisic acid regulation of guard cell slow anion channels in *Arabidopsis* wild-type and *abi1* and *abi2* mutants. *Plant Cell* **9**: 409–423.

Pei Z-M, Baizabal-Aguirre VM, Allen GJ, Schroeder JI. 1998. A transient outward-rectifying K^+ channel current down-regulated by cytosolic Ca^{2+} in *Arabidopsis thaliana* guard cells. *Proceedings of the National Academy of Sciences of USA* **95**: 6548–6553

Pei Z-M, Ward JM, Schroeder JI. 1999. Magnesium sensitizes slow vacuolar channels to physiological cytosolic calcium and inhibits fast vacuolar channels in fava bean guard cell vacuoles. *Plant Physiology* **121**: 977–986.

Pei Z-M, Murata Y, Benning G, Thomine S, Klüsener B, Allen GJ, Grill E, Schroeder JI. 2000. Calcium channels activated by hydrogen peroxide mediate abscisic acid signaling in guard cells. *Nature* **406**: 731–734.

Raschke K. 1975. Stomatal action. *Annual Review of Plant Physiology* **26**: 309–340.

Raschke K, Schnabl H. 1978. Availability of chloride affects the balance between potassium chloride and potassium malate in guard cells of *Vicia faba* L. *Plant Physiology* **62**: 84–87.

Raschke K, Shabahang M, Wolf R. 2003. The slow and the quick anion conductance in whole guard cells: their voltage-dependent alternation, and the modulation of their activities by abscisic acid and CO_2. *Planta* **217**: 639–650.

Roelfsema MRG, Hanstein S, Felle HH, Hedrich R. 2002. CO_2 provides an intermediate link in the red light response of guard cells. *Plant Journal* **32**: 65–75.

Roelfsema MRG. and Hedrich R. 2002. Studying guard cells in the intact plant: Modulation of stomatal movement by apoplastic factors. *New Phytologist* **153**: 425–431.

Roelfsema MRG. and Prins HBA. 1995. Effect of abscisic acid on stomatal opening in isolated epidermal strips of abi mutants of *Arabidopsis thaliana*. *Physiologia Plantarum* **95**: 373–378.

Roelfsema MRG, Prins HBA. 1997. Ion channels in guard cells of *Arabidopsis thaliana* (L.) *Heyn*h. *Planta* **202**: 18–27.

Roelfsema MRG, Staal M, Prins HBA. 1998. Blue light-induced apoplastic acidification of *Arabidopsis thaliana* guard cells: Inhibition by ABA is mediated through protein phosphatases. *Physiologia Plantarum* **103**: 466–474.

Roelfsema MRG, Steimeyer R, Staal M, Hedrich, R. 2001. Single guard cells recordings in intact plants: light induced hyperpolarization of the plasma membrane. *Plant Journal.* **26**, 1 – 13.

Roelfsema MRG, Levchenko V, Hedrich R. 2004. ABA depolarizes guard cells in intact plants, through a transient activation of R- and S-type anion channels. *Plant Journal* **37**: 578–588.

Roelfsema MRG. and Hedrich R. 2005. In the light of stomatal opening: new insights into 'the Watergate'. *New Phytologist* **167**: 665–691.

Roelfsema MRG, Konrad KR, Marten H, Psaras GK, Hartung W, Hedrich R. 2006. Guard cells in albino leaf patches do not respond to photosynthetically active radiation, but are sensitive to blue light, CO_2 and abscisic acid. *Plant, Cell and Environment* **29**: 1595–1605.

Romano LA, Jacob T, Gilroy S, Assmann SM. 2000. Increases in cytosolic Ca^{2+} are not required for abscisic acid-inhibition of inward K^+ currents in guard cells of *Vicia faba* L. *Planta* **211**: 209–217.

Rodriguez PL, Benning G, Grill E. 1998. ABI2, a second protein phosphatase 2C involved in abscisic acid signal transduction in *Arabidopsis*. *FEBS Letters* **421**: 185–90

Sahgal P, Martinez GV, Roberts C, Tallman G. 1994. Regeneration of plants from cultured guard cell protoplasts of *Nicotiana glauca* (Graham). *Plant Science* **97**: 199–208.

Saji S, Bathula S, Kubo A, Tamaoki M, Kanna M, Aono M, Nakajima N, Nakaji T, Takeda T, Asayama M and Saji H. 2008. Disruption of a Gene Encoding C4-Dicarboxylate Transporter-Like Protein Increases Ozone Sensitivity Through Deregulation of the Stomatal Response in *Arabidopsis thaliana. Plant Cell Physiology* **49**: 2–10.

Sanders D, Brownlee C, Harper JF. 1999. Communicating with calcium. *Plant Cell* 11: 691–706.

Sanders D, Pelloux J, Brownlee C, Harper JF. 2002. Calcium at the crossroads of signaling. *Plant Cell* **14**: S401–S417.

Schachtman DP, Schroeder JI, Lucas WJ, Anderson JA, Gaber RF. 1992. Expression of an inward-rectifying potassium channel by the *Arabidopsis* KAT1 cDNA. *Science* **258**: 1654–1658.

Scrase-Field SAMG and Knight MR. 2003. Calcium: just a chemical switch? *Current Opinion in Plant Biology* **6**: 500–506.

Sheen J. 1996. Ca^{2+}-dependent protein kinases and stress signal transduction in plants. Science **274**: 1900–1902.

Sheen J. 1998. Mutational analysis of protein phosphatase 2C involved in abscisic acid signal transduction in higher plants. *Proceedings of the National Academy of Sciences of USA* **95**: 975–80.

Schmidt C, Schroeder JI. 1994. Anion selectivity of slow anion channels in the plasma membrane of guard cells: Large nitrate permeability. *Plant Physiology* **106**: 383–391.

Schmidt C, Schelle I, Liao YJ, Schroeder JI. 1995. Strong regulation of slow anion channels and abscisic acid signaling in guard cells by phosphorylation and dephosphorylation events. *Proceedings of the National Academy of Sciences of USA* **92**: 9535–39

Schroeder JI, Raschke K, Neher E. 1987. Voltage dependence of K^+ channels in guard cell protoplasts. *Proceedings of the National Academy of Sciences of USA* **84**: 4108–4112.

Schroeder JI. 1988. K^+ transport properties of K^+ channels in the plasma membrane of *Vicia faba* guard cells. *Journal of General Physiology* **92**: 667– 683.

Schroeder JI, Hagiwara S. 1989. Cytosolic calcium regulates ion channels in the plasma membrane of *Vicia faba* guard cells. *Nature* **338**: 427–430.

Schroeder JI, Hagiwara S. 1990. Repetitive increases in cytosolic Ca^{2+} of guard cells by abscisic acid activation of nonselective Ca^{2+} permeable channels. *Proceedings of the National Academy of Sciences of USA* **87**: 9305–9309.

Schroeder JI, Keller BU. 1992. Two types of anion channel currents in guard cells with distinct voltage regulation. *Proceedings of the National Academy of Sciences of USA* **89**: 5025 – 5029.

Schroeder JI, Schmidt C, Sheaffer J. 1993. Identification of high-affinity slow anion channel blockers and evidence for stomatal regulation by slow anion channels in guard cells. *Plant Cell* **5**: 1831–1841.

Schroeder JI, Allen GJ, Hugouviex V, Kwak JM, Warren D. 2001. Guard cell signal transduction. *Annual Reviews of Plant Physiology and Plant Molecular Biology* **52**: 627 – 658.

Schulzlessdorf B, Hedrich R. 1995. Protons and calcium modulate SV-type channels in the vacuolar lysosomal compartment-channel interaction with calmodulin inhibitors. *Planta* **197**: 655–671.

Schulzlessdorf B, Lohse G, Hedrich R. 1996. GCAC1 recognizes the pH gradient across the plasma membrane: a pH-sensitive and ATP-dependent anion channel links guard cell membrane potential to acid and energy metabolism. *Plant Journal* **10**: 993–1004.

Schwarz M, Schroeder JI. 1998. Abscisic acid maintains S-type anion channel activity in ATP-depleted *Vicia faba* guard cells. *FEBS Letters* **428**: 177–182.

Schwartz A, Wu WH, Tucker EB, Assmann SM. 1994. Inhibition of inward K^+ channels and stomatal response by abscisic acid: An intracellular locus of phytohormone action. *Proceedings of the National Academy of Sciences of USA* **91**: 4019 – 4023.

Schwartz A, Ilan N, Schwarz M, Schaeffer J, Assmann SM, Schroeder JI. 1995. Anion channel blockers inhibit S-type anion channels and abscisic acid responses in guard cells. *Plant Physiology* **109**: 651– 658.

Serrano, R. 1988. Structure and function of proton translocating ATPase in plasma membranes of plants and fungi. *Biochimica et Biophysica Acta* **947**: 1-28.

Sharkey TD, Raschke K. 1981. Effect of light quality on stomatal opening in leaves of *Xanthium strumarium* L. *Plant Physiology* **68**: 1170–1174.

Shimazaki KI, Iino M, Zeiger E. 1986. Blue light-dependent proton extrusion by guard-cell protoplasts of *Vicia faba*. *Nature* **319**: 324–326.

Shimazaki KI, Doi M, Assmann SM, Kinoshita T. 2007 Light regulation of stomatal movement. *Annual review of plant biology* **58**: 219 – 247.

Sentenac H, Bonneaud N, Minet M, Lacroute F, Salmon JM, Gaymard F, Grignon C. 1992. Cloning and expression in yeast of a plant potassium-ion transport-system. *Science* **256**: 663 – 665.

Cheng S-H, Willmann MR, Chen H-C, Sheen JS. 2002. Calcium Signaling through Protein Kinases. The *Arabidopsis* Calcium-Dependent Protein Kinase Gene Family. *Plant Physiology* **129**: 469–485.

Stadler R, Büttner M, Ache P, Hedrich R, Ivashikina N, Melzer M, Shearson SM, Smith SM, Sauer N. 2003. Diurnal and light-regulated expression of AtSTP1 in guard cells of *Arabidopsis*. *Plant Physiology* **133**: 528–537.

Staxen I, Pical C, Montgomery LT, Gray JE, Hetherington AM, McAinsh MR. 1999. Abscisic acid induces oscillations in guard-cell cytosolic free calcium that involve phosphoinositide-specific phospholipase C. *Proceedings of the National Academy of Sciences of USA* **96**: 1779 –1784.

Stoelzle S, Kagawa T, Wada M, Hedrich R, Dietrich P. 2003. Blue light activates calcium-permeable channels in *Arabidopsis* mesophyll cells via the phototropin signaling pathway. *Proceedings of the National Academy of Sciences of USA* **100**: 1456–1461.

Sze H, Li X, Palmgren MG. 1999. Energization of plant cell membranes by H^+-pumping ATPases. Regulation and Biosynthesis. *Plant Cell* **11**: 677–689.

Sze H, Liang F, Hwang I, Curran AC, Harper JF. 2000. Diversity and regulation of plant Ca^{2+} pumps: Insights from expression in yeast. *Annual Review of Plant Physiology and Plant Molecular Biology* **51**: 433–462.

Szyroki A, Ivashikina N, Dietrich P, Roelfsema MRG, Ache P, Reintanz B, Deeken R, Godde M, Felle HH, Steinmeyer R, Palme K, Hedrich R. 2001. KAT1 is not essential for stomatal opening. *Proceedings of* the *National Academy of Sciences of USA* **98**: 2917–2921.

Talbott LD, Zeiger E. 1996. Central roles for potassium and sucrose in guard-cell osmoregulation. *Plant Physiology* **111**: 1051–1057.

Taylor AR, Assmann SM. 2001. Apparent absence of a redox requirement for blue light activation of pump current in broad bean guard cells. *Plant Physiology* **125**: 329–338.

Taylor JE, McAinsh MR. 2004. Signaling crosstalk in plants: Emerging issues. *Journal of Experimental Botany* **55**: 147–149.

Thiel G, Blatt MR. 1994. Phosphatase antagonist okadaic acid inhibits steady-state K^+ currents in guard cells of *Vicia faba*. *Plant Journal* **5**: 727–733.

Thiel G, MacRobbie EAC, Blatt MR. 1992. Membrane transport in stomatal guard cells: The importance of voltage control. Journal *of Membrane Biology* **126**: 1–18.

Trejo CL, Clephan AL, Davies WJ. 1995. How do stomata read abscisic acid signals? *Plant Physiology* **109**: 803–811.

Ward JM, Schroeder JI. 1994. Calcium-activated K^+ channels and calcium-induced calcium release by slow vacuolar ion channels in guard cell vacuoles implicated in the control of stomatal closure. *Plant Cell* **6**: 669–683.

Webb AA, Larman MG, Montgomery LT, Taylor JE, Hetherington AM. 2001. The role of calcium in ABA-induced gene expression and stomatal movements. *Plant Journal* **26**: 351–362.

Webb AA, McAinsh MR, Mansfield TA, Hetherington AM. 1996. Carbon dioxide induces increases in guard cell cytosolic free calcium. *Plant Journal* **9**: 287–304.

Wood NT, Allan AC, Haley A, Viry-Moussaid M and Trewavas AJ. 2000. The characterization of differential calcium signalling in tobacco guard cells. *Plant Journal* **24**, 335–344.

Yamazaki D, Yoshida S, Asami T, Kuchitsu K. 2003. Visualization of abscisic acid-perception sites on the plasma membrane of stomatal guard cells. *Plant Journal* **35**: 129–139.

Vahisalu T, Kollist H, Wang Y-F, Nishimura N, Chan W-Y, Valerio G, Lamminmäki A, Brosché M, Moldau H, Desikan R, Schroeder JI and Kangasjärvi J. 2008. SLAC1 is required for plant guard cell S-type anion channel function in stomatal signalling. *Nature* **452**: 487 – 491.

Venema K, Belver A, Marin-Manzano MC, Rodriguez-Rosales MP, Donaire JP. 2003. A novel intracellular K^+/H^+ antiporter related to Na^+/H^+ antiporters is important for K^+ ion homeostasis in plants. *Journal of Biological Chemistry 278*: 22453–22459.

Véry AA, Gaymard F, Bosseux C, Sentenac H, Thibaud JB. 1995 Expression of a cloned plant K^+ channel in *Xenopus* oocytes: analysis of macroscopic currents. *Plant Journal* **7**: 321–332.

Véry, AA, Robinson MF, Mansfield TA, Sanders D. 1998. Guard cell cation channels are involved in Na^+-induced stomatal closure in a halophyte. *Plant Journal* **14**, 509–522.

Véry AA, Sentenac H. 2002. Cation channels in the *Arabidopsis* plasma membrane. *Trends in Plant Science* **7**: 168–175.

LIST OF PUBLICATIONS

1. **Roelfsema MRG, Levchenko V, Hedrich R.** 2004. ABA depolarizes guard cells in intact plants, through a transient activation of R- and S-type anion channels. *Plant Journal* **37**: 578 – 588.

2. **Langer K, Levchenko V, Fromm J, Geiger D, Steinmeyer R, Lautner S, Ache P, Hedrich R.** 2004. The poplar K^+ channel KPT1 is associated with K^+ uptake during stomatal opening and bud development. *Plant Journal* **37**: 828 – 838.

3. **Levchenko V, Konrad KR, Dietrich P, Roelfsema MRG, Hedrich R.** 2005. Cytosolic ABA activates guard cell anion channels without preceding Ca^{2+} signals. *Proceedings of the National Academy of Sciences of USA* **102**: 4203 – 4208.

4. **Carpaneto A, Ivashikina N, Levchenko V, Krol E, Jeworutzki E, Zhu J-K, Hedrich R.** 2007. Cold transiently activates calcium-permeable channels in *Arabidopsis* mesophyll cells. *Plant Physiology* **143**: 487 – 494.

5. **Levchenko V, Guinot DR, Klein M, Roelfsema MRG, Hedrich R, Dietrich P.** 2008. Stringent control of cytoplasmic Ca^{2+} in guard cells of intact plants compared to their counterparts in epidermal strips or guard cell protoplasts. *Protoplasma* **233**: 61–72.

Personal data

Name	Victor Levchenko
Nationality	Republic of Belarus
Birthday	3 February 1978
Birthplace	Pruzhany, Republic of Belarus
Marital status	Divorcee

Education

January 2002 - August 2005	Ph.D. Student, Laboratory of Molecular Plant Physiology and Biophysics, Bavarian Julius-von-Sachs Institute of Biological Sciences, Julius-Maximilians University of Würzburg.
November 2000 - January 2002	Ph. D. Student, Laboratory of Photoregulation of Cell Processes, Institute of Photobiology, National Academy of Sciences of Belarus, Minsk, Belarus.
September 1995- July 2000	Undergraduate Student, Biological Faculty, Belarusian State University, Minsk, Belarus. Five-year High Education Diploma in Biology and Chemistry with a First-Class Honours.
September 1986 – June 1995	Secondary School №2, Pruzhany, Brest Region, Belarus

Research experience

January 2008 - Present	Laboratory of Plant Cell Physiology, Biological Faculty, Belarusian State University, Minsk, Belarus. **Project** "Cellular signaling in higher plant root cells upon pathogen fungal attack by *Fizarium*"
January 2002 - August 2005	Laboratory of Molecular Plant Physiology and Biophysics, Bavarian Julius-von-Sachs Institute of Biological Sciences, Julius-Maximilians University of Würzburg. ***Thesis*** "Studies of Ca^{2+}-signaling and Cl^--conductance changes in response to abscisic acid, voltage changes and cold, in the plasma membrane guard cells"
November 2000 - January 2002	Laboratory of Photoregulation of Cell Processes, Institute

of Photobiology, National Academy of Sciences of Belarus, Minsk, Belarus. ***Project*** "Cyclic nucleotide-induced changes in levels of cytoplasmic Ca2+ activity in plant cells"

Poster presentation

Levchenko V. Roelfsema MRG. and Hedrich R. PP 4-5: Studying guard cell responses to abscisic acid within intact leaves. 13-th International Workshop on Plant Membrane Biology. 6-10 July 2004 Montpellier, France

ERKLÄRUNG

Hiermit erkläre ich, dass ich die vorliegende Dissertation in allen Teilen selbst angefertigt und keine anderen als die angegebenen Quellen und Hilfsmittel verwendet habe.

Ich habe die Dissertation weder in gleicher noch in ähnlicher Form in anderen Prüfungsverfahren vorgelegt.

Ich erkläre weiterhin, dass ich bislang noch keine weiteren akademischen Grade erworben oder zu erwerben versucht habe.

Minsk, 2009   ....